



Technische Universität München
Department für Biowissenschaftliche Grundlagen

Development and application of trace analysis for emerging organic pollutants in surface water

Dominik Deyerling

Vollständiger Abdruck der von der Fakultät Wissenschaftszentrum Weihenstephan für Ernährung, Landnutzung und Umwelt der Technischen Universität München zur Erlangung des akademischen Grades eines

Doktors der Naturwissenschaften

genehmigten Dissertation.

Vorsitzender: Univ.-Prof. Dr.-Ing. Heiko Briesen
Prüfer der Dissertation: 1. apl. Prof. Dr. rer. nat. Dr. agr. habil. Karl-Werner Schramm
2. Univ.-Prof. Dr. rer. nat. habil. Thomas Letzel

Die Dissertation wurde am 17.06.2015 bei der Technischen Universität München eingereicht und durch die Fakultät Wissenschaftszentrum Weihenstephan für Ernährung, Landnutzung und Umwelt am 24.10.2015 angenommen.

Preface

The doctoral thesis which is presented here is the result of work conducted from February 2012 until April 2015 within the research group Molecular EXposomics (MEX) of the German Research Center for Environmental Health and was funded as part of the Yangtze Project by the German Federal Ministry for Education and Research.

Primarily, I like to thank Prof. Dr. Karl-Werner Schramm for giving me the opportunity to prepare this thesis under his supervision. His support for an independent working atmosphere offered me the possibility to conduct individual experimental work which helped to solve issues during instrumental method development. Moreover, I appreciated the participation in numerous national and international scientific congresses and meetings for deepening my knowledge as well as for gaining experience in the presentation of scientific results. Finally, his experience in the field of environmental analysis was always beneficial to judge and interpret own scientific findings.

Furthermore, I particularly appreciated the support from Dr. Gerd Pfister during the orientation time at the measurement instrument. Especially the assistance regarding technical issues was welcome throughout this work.

Additionally, I want to offer my sincere thanks to Dr. Jingxian Wang for the fruitful discussions of scientific results and her support during the environmental sampling campaign at the Three Gorges Dam in China in 2012. Particularly, I like to thank our Chinese cooperation partners within the Yangtze Project Dr. Yonghong Bi and Dr. Chengrong Peng from the Institute of Hydrobiology of the Chinese Academy of Sciences for the extended support during the environmental sampling campaign in the Three Gorges Reservoir in 2012 and 2013. Without the help of our Chinese cooperation partners, both sampling campaigns would not have been possible.

Furthermore, I want to acknowledge the contribution of our German cooperation partners within the Yangtze Project. Thanks to Wei Hu for his support in topographic mapping and his contribution to the modeling of discharges of the Yangtze River. I also appreciated the help of Prof. Dr. Bernhard Westrich concerning the description of the Yangtze discharge model. Moreover, my thanks go to Anja Wolf, Katrin Bieger, Tilman Floehr, Andreas Holbach, Felix Stumpf, Ye Yuan, Dr. Björn Scholz-Starke, Irene Kranzioch and all other participants of the Yangtze Project for the productive meetings and the interesting thoughts about the impoundment of the Yangtze River.

Besides, I want to highlight the contribution of my working colleagues within the research group MEX. My thanks go to Felix Antritter for the support during several sampling campaigns and during laboratory work. Silke Bernhöft helped particularly during orientation and throughout

the laboratory work of this thesis. Theresa Maria Rock contributed samples and standard solutions for the analysis of catecholamines. Norbert Fischer introduced me to one of our sampling sites in the Alps. Moreover, I like to thank Joachim Nagler for the positive working atmosphere and the proofreading of this thesis. Thanks also to Bernhard Henkelmann for the management of orders, laboratory supply and proofreading of several manuscripts. Additionally, I appreciated the scientific advice and productive talks with Dr. Marchela Pandelova, Dr. Walkiria Levy, Dr. Meri De Angelis and Cedrique Temoka. Moreover, I enjoyed the exchange with our visiting scientists and doctoral fellows Dr. Zhenlan Xu, Dr. John Mumbo, Jacques Ehret, Dr. Rajesh Rathore, Dr. Burak Karacık, Atilla Yilmaz, Valentina Zingarelli and Nali Xu.

Alongside scientific exchange, I particularly enjoyed professional and private discussions with all members of the working group, including those I could not mention here. Specifically, I want to send my thanks to Josie Kunze, Dr. Daniela Rascher and Dr. Martin Rieger and Claudia Corsten for providing me many times new motivation during daily routine.

My thanks are also directed to Beate Gruber, George Dragan, Sebastian Wohlfahrt, Michael Fischer, Janos Varga, Markus Oster, Matthias Fuchs, Benedikt Weggler, Vesta Kohlmeier, Geza Kocsis and all other members of the research group Comprehensive Molecular Analytics for the great working atmosphere and the social activities.

Thanks to my good friends Christian Franik and Christian Wichmann for the extensive proofreading. Without your suggestions, this thesis would not exist in the current version.

Finally, I like to thank my brother Johannes Deyerling for providing high-quality photography and my whole family for the continuous support throughout my studies and during this doctoral thesis. My warmest thanks go to my girlfriend Claudia for providing me essential mental support during the critical phases of this work.

List of Publications

At the time of completion of this thesis, parts of this work have already been published in professional journals or are in preparation for submission:

D. Deyerling, J. Wang, W. Hu, B. Westrich, C. Peng, Y. Bi, B. Henkelmann, K.-W. Schramm, PAH distribution and mass fluxes in the Three Gorges Reservoir after impoundment of the Three Gorges Dam, *Science of the Total Environment*, 491-492 (2014) 123-130

DOI: 10.1016/j.scitotenv.2014.03.076.

D. Deyerling, J. Wang, Y. Bi, C. Peng, G. Pfister, B. Henkelmann, K.-W. Schramm, Depth profile of persistent and emerging organic pollutants upstream of the Three Gorges Dam gathered in 2012/13, *Environmental Science and Pollution Research*, in press

DOI: 10.1007/s11356-015-5805-8

D. Deyerling, K.-W. Schramm, Integrated targeted and semantic non-targeted analysis of water sample extracts with micro-scale LC-MS, *MethodsX*, 2 (2015) 399-408

DOI: 10.1016/j.mex.2015.10.002

Kurzfassung

Wasserlösliche organische Rückstände wie Pharmazeutika, polare Pestizide und Perfluoralkylsäuren (PFAAs) sind von zunehmendem Belang für die Umwelt. Unmetabolisierte pharmazeutische Rückstände aus dem menschlichen Gebrauch und der Behandlung von Viehbestand werden durch die klassische Abwasserbehandlung nur teilweise beseitigt und gelangen folglich in erheblichen Mengen in Oberflächengewässer. Die Beeinträchtigung einer empfindlichen Fischart konnte bereits auf die Spurenkonzentration von Pharmazeutika im Wasser zurückgeführt werden. PFAAs sind Chemikalien die wegen ihrer einzigartigen Eigenschaften weitverbreitet sind. Üblicherweise werden sie als schmutzabweisende Agenzien in Textilien und Teppichen, in der Behandlung von Lebensmittelverpackungen und in der Herstellung von Polymeren verwendet. Nach ihrer Freisetzung in die Umwelt sind diese persistent und können sich in der Nahrungskette anreichern. In Oberflächengewässern finden sich organische Rückstände wie Pharmazeutika und PFAAs wegen der hohen Verdünnungsfaktoren üblicherweise nur in niedrigen Konzentrationen. Die vorliegende Arbeit berichtet über die Entwicklung einer analytischen Methode für die Bestimmung von Spurenkonzentrationen aufkommender organischer Schadstoffe in Oberflächenwasser und deren Anwendung bei der Umweltprobenahme des Flusses Jangtse in China.

Eine Isotopenverdünnungsanalyse wurde mittels Ultrahochleistungsflüssigchromatographie und Quadrupol-Flugzeit-Massenspektrometrie realisiert. Dafür wurde die Eignung unterschiedlicher Flusskonfigurationen des chromatographischen Systems im Nano- und Mikro-Maßstab für die Analyse von mittelpolaren bis polaren Substanzen untersucht. Außerdem wurden optimierte Betriebsparameter für die Elektrospray-Ionenquelle im Nano- und Standard-Maßstab bestimmt. Dabei konnten die besten Ergebnisse mit einem Betrieb im Mikro-Maßstab und der Standard-Elektrospray Ionenquelle erzielt werden. Trotzdem ermöglichten verbesserte Betriebsparameter der Nano-Electrospray Ionenquelle deren stabilen Betrieb über längere Zeiträume hinweg. Der Vergleich von spezialisierten Betriebsarten des Massenspektrometers führte zur Entwicklung einer hybriden Betriebsmethode, welche alle generierten Ionen gleichzeitig fragmentiert, wodurch die Vorteile der Flugzeitdetektion mit denen der kollisionsinduzierten Dissoziation verbunden werden konnten. Somit konnte die Empfindlichkeit des Instruments bei gleichzeitigem Erhalt eines hohen Grades an Rauschunterdrückung maximiert werden. Unter Berücksichtigung der ermittelten Leistungsfähigkeit des Messgerätes wurden mehrere Pharmazeutika, polare Pestizide und PFAAs für die Analyse ausgewählt. Messgerätkalibrierungen für die Quantifizierung konnten mit einer angemessenen Linearität, Empfindlichkeit und Reproduzierbarkeit im Nano- und Mikro-Maßstab erstellt werden. Trotzdem zeigten die Ergebnisse für

quantitative Aufgaben einen reproduzierbareren und geeigneteren Betrieb mit der Flusskonfiguration im Mikro-Maßstab.

Außer der Entwicklung einer instrumentellen Messmethode wurde ein aktives Wasserprobensystem entworfen, das die Anreicherung von großen Wasservolumina erlaubte, um Spurenkonzentrationen organischer Rückstände in Oberflächenwasser detektieren zu können. Dazu wurden selbstgepackte Glaskartuschen mit Polymerharz verwendet um bis zu 300 L Wasser vor Ort mit Hilfe einer batteriebetriebenen Schlauchpumpe anzureichern. Das Probensystem wurde für eine Umweltprobekampagne des Flusses Jangtse im Jahr 2013 verwendet. Der Probenahmestandort war etwas stromaufwärts der Drei-Schluchten-Talsperre gelegen. Dabei wurden Wasserproben in 11, 31 und 50 m Wassertiefe genommen. Für die Analyse der Proben wurde eine geeignete laborative Extraktions- und Aufreinigungsmethode, basierend auf Festphasenextraktion (SPE), entwickelt. Die Leistung der Extraktions- und Aufreinigungsmethode wurde anhand von Laborversuchen mit anschließender Analyse durch die entwickelte instrumentelle Methode bewertet. Die Untersuchung zeigte erhebliche Signalunterdrückung in Labor- und Umweltproben durch analytischen Hintergrund welcher nicht ausreichend durch die SPE überwunden werden konnte. Weiterhin war die Retentionsfähigkeit der Probekartuschen für polare Analyten begrenzt. Dennoch erlaubten die Umweltproben des Flusses Jangtse die weitere Charakterisierung der Fähigkeiten des Probensystems und die qualitative Diskussion der Verteilung der Analyten mit der Wassertiefe.

Schließlich wurde ein Arbeitsablauf für die Non-Target-Analyse eingeführt und auf die hochaufgelösten Massenspektrometriedaten angewendet, die während der Analyse von Umweltproben gesammelt worden sind. Einige Treffer konnten in den Probenextrakten identifiziert sowie deren Detektionswahrscheinlichkeit diskutiert werden. Durch die Unabhängigkeit des entwickelten Arbeitsablaufes vom Probenursprung kann dieser als Werkzeug für die Entdeckung von Stoffen durch die Nachbearbeitung bereits aufgezeichneter Massenspektrometriedaten dienen.

Abstract

Water soluble organic residues like active pharmaceutical ingredients, polar pesticides and perfluorinated alkyl acids (PFAAs) are of growing environmental concern. Unmetabolized pharmaceutical residues from human consumption and the treatment of livestock are only partly removed in classic wastewater treatment and thus enter surface water in considerable amounts. Adverse effects on a sensitive fish species could already be attributed to trace amounts of pharmaceuticals in water. PFAAs are chemicals which are widely used due to their unique properties. Typically, they are used as stain repellents in textiles and carpets, the treatment of food packagings and for polymer production. Once released into the environment they are persistent and can bioaccumulate in the food chain. In surface water, organic residues like pharmaceuticals and PFAAs are usually found at low concentrations due to high dilution factors. The work presented reports on the development of an analytical method for the determination of trace amounts of selected emerging organic pollutants in surface water and its application in environmental sampling of the Yangtze River in China.

An isotope dilution analysis was realized with ultra high-performance liquid chromatography coupled to a quadrupole time-of-flight hybrid mass spectrometer. Therefore, the applicability of different fluidic configurations of the chromatographic system in nano- and micro-scale were evaluated for the analysis of medium to polar residues. Besides, optimized operation conditions for nano-scale and standard-scale electrospray ion sources were determined. Thereby, the best results for targeted analysis could be achieved with micro-scale separation and the application of a standard-scale ion source. Nevertheless, improved operational parameters for nano-scale electrospray allowed its stable operation during prolonged time windows. The comparison of different specialized mass spectrometric experiments lead to the development of a hybrid operation mode for the fragmentation of all ions at the same time with which the benefits of time-of-flight detection and collision induced dissociation could be combined. Thus, instrument sensitivity could be maximized while maintaining a high degree of background reduction. After consideration of the determined instrument capabilities, several pharmaceuticals, polar pesticides and PFAAs were chosen for analysis. Instrumental calibrations for quantitative measurements were established with reasonable linearity, sensitivity and reproducibility for both nano-scale and micro-scale chromatography setups. Nevertheless, the results indicated a more reproducible and convenient operation with the micro-fluidic configuration for quantitative analytical tasks.

Besides instrumental method development, an active water sampling technique was designed which allowed the enrichment of high volumes of water in order to detect trace amounts of

VIII

organic residues in surface water. Self-packed glass cartridges with polymeric resin were used to enrich volumes of up to 300 L on-site with the help of a battery-driven peristaltic pump. The sampling system was used for an environmental sampling campaign of the Yangtze River in 2013. The sampling site was located slightly upstream of the Three Gorges Dam and water samples were taken in 11, 31 and 50 m water depth. For sample analysis, a suitable laboratory extraction and cleanup method based on solid-phase extraction (SPE) was developed. The extraction and cleanup performance was assessed in a laboratory recovery study with the established instrumental method. The investigation indicated considerable signal suppression in laboratory and environmental samples by analytical background which could not be sufficiently resolved by the SPE cleanup. Furthermore, the retention capabilities of the sampling cartridges for the polar analytes was limited. Nevertheless, environmental samples from the Yangtze River allowed further characterization of the capabilities of the sampling system and qualitative discussion of analyte distribution with water depth.

Finally, a workflow for non-target screening was introduced and applied on the high resolution mass spectrometric data gathered during environmental sample analysis. Several suspects in the sample extracts could be identified and their detection plausibility was discussed. With the developed workflow being independent from the sample origin, it can be used as tool for the discovery of compounds by post-processing of already recorded mass spectrometric data.

Contents

1. Introduction	1
1.1. The impoundment of the Yangtze River	1
1.2. Persistent and emerging organic pollutants	4
1.2.1. Perfluorinated compounds	5
1.2.2. Pharmaceutical residues	8
1.3. Regulations of organic pollutants in the European Union	11
2. Theoretical background	12
2.1. Liquid chromatography	12
2.1.1. Reversed-phase chromatography	16
2.1.2. Retention Time Index	18
2.2. Quadrupole time-of-flight mass spectrometry	19
2.3. Electrospray ionization	24
2.4. Solid-phase extraction	26
2.5. Analysis of catecholamines with LC-MS	28
2.6. Applications of LC-MS in the analysis of emerging organic pollutants in water	29
3. Scope of work	31
4. Experimental part	33
4.1. Reagents and chemicals	33
4.2. Preparation of standard stock solutions	34
4.3. Analytical instrumentation	36
4.3.1. Liquid chromatography system	36
4.3.2. Mass spectrometric detection system	38
4.4. Experimental parameters for instrumental measurement	40
4.5. Instrument calibration	41
4.5.1. Calibration standards for perfluorinated compounds	42
4.5.2. Calibration standards for pharmaceuticals and polar pesticides	43
4.6. Derivatization of catecholamines	44
4.7. Evaluation of solid-phase extraction cartridges	44
4.8. Evaluation of syringe filters	46
4.9. Active water sampling system	46
4.10. Laboratory performance evaluation of large volume water sampling	48
4.11. Environmental sampling and analysis of the Yangtze River	50

4.12. Workflow for directed non-target screening	52
5. Results and Discussion	54
5.1. Chromatographic method development	54
5.1.1. Nano-scale chromatography with trap column	54
5.1.1.1. Evaluation of trapping parameters	54
5.1.1.2. Trapping and gradient elution with pharmaceuticals and polar pesticides	56
5.1.1.3. Trapping and gradient elution with perfluorinated compounds	59
5.1.2. Nano-scale chromatography with direct injection	60
5.1.2.1. Gradient elution with pharmaceuticals and polar pesticides .	60
5.1.2.2. Gradient elution with perfluorinated compounds	63
5.1.3. Micro-scale chromatography with direct injection	65
5.1.4. Applicability of the fluidic configurations for calibration and quantifi- cation	67
5.2. Mass spectrometric method development	69
5.2.1. Operation of the nano-electrospray interface	69
5.2.2. Operation of the standard electrospray interface	72
5.2.3. Operation of the Q-TOF mass spectrometer	74
5.3. Instrumental calibration and linearity	80
5.3.1. Nano-scale chromatography with direct injection	80
5.3.2. Micro-scale chromatography with direct injection	83
5.3.3. Applicability of the instrumental calibrations for quantification	85
5.4. Laboratory recovery experiments	86
5.4.1. Selection of a solid-phase extraction chemistry	86
5.4.2. Syringe filter evaluation	89
5.4.3. Performance evaluation of large volume water sampling	91
5.5. Evaluation of large volume sampling with samples from the Yangtze River . . .	97
5.6. Inclusion of non-target analysis into the presented method	101
6. Conclusion and Outlook	107
7. Appendix	110
List of figures	110
List of tables	115
Bibliography	116

List of Abbreviations

<i>m/z</i>	mass-to-charge ratio
AC	alternating current
ADC	analog-to-digital converter
AIF	all ion fragmentation
API	atmospheric pressure ionization
AQC	6-aminoquinolyl-N-hydroxysuccinimidyl carbamate
ASM	auxiliary solvent manager
BSM	binary solvent manager
CID	collision induced dissociation
CRM	charged residue model
DC	direct current
DDT	dichlorodiphenyltrichloroethane
DEET	<i>N,N</i> -diethyl- <i>m</i> -toluamide
DI	direct injection
DPT	dual-pump trapping
ECF	electrochemical fluorination
EQS	environmental quality standards
ESI	electrospray ionization
EU	European Union
FTOH	fluorotelomer alcohol
GHP	GH Polypro membrane
HETP	height equivalent of a theoretical plate
HPLC	high-performance liquid chromatography

XII

HRMS	high resolution mass spectrometry
i. d.	inner diameter
IDL	instrumental detection limit
IEM	ion evaporation model
LC	liquid chromatography
LLE	liquid-liquid extraction
LOQ	limit of quantification
MALDI	matrix-assisted laser desorption/ionization
MCP	microchannel plate
MDL	method detection limit
MRM	multiple reaction monitoring
MS	mass spectrometry / mass spectrometer
NOEC	no-observed adverse effect concentration
NSAID	nonsteroidal anti-inflammatory drug
OCP	organochlorine pesticide
ODS	octadecylsilane
PAH	polycyclic aromatic hydrocarbon
PCB	polychlorinated biphenyl
PCCD	polychlorinated dibenzo-p-dioxin
PCDF	polychlorinated dibenzofuran
PFAA	perfluorinated alkyl acid
PFAS	perfluoroalkylsulfonate
PFC	perfluorinated compound
PFCA	perfluoroalkylcarboxylic acid

XIII

PFOS	perfluorooctane sulfonic acid / perfluorooctanesulfonate
POP	persistent organic pollutant
POSF	perfluorooctane sulfonyl fluoride
PS-DVB	polystyrene divinylbenzene
PTFE	polytetrafluoroethylene
Q-TOF	quadrupole time-of-flight
r.f.	radio frequency
RC	regenerated cellulose
RPC	reversed-phase chromatography
RSD	relative standard deviation
RTI	retention time index
SM	sample manager
SPE	solid-phase extraction
SPMD	semi-permeable membrane device
TDC	time-to-digital converter
TGD	Three Gorges Dam
TGP	Three Gorges Project
TGR	Three Gorges Reservoir
TIC	total ion current
TOF-MS	time-of-flight mass spectrometer
UHPLC	ultra high-performance liquid chromatography
VO	virtual organism
WHO	World Health Organization

1. Introduction

Substances referred to as pollutants are compounds or mixtures that may have negative effects on ecosystems, live animals or material goods [1]. This wide definition, however, classifies a large number of chemicals as possible pollutants. In contrast, environmental pollutants are defined as substances that may harm live animals and humans [1]. The input of these kind of chemicals from anthropogenic sources should be kept as low as possible as one goal of environmental protection. Therefore, the monitoring of substances in the environment becomes mandatory to gain information on the origin, fate, distribution and behavior of chemical compounds in the environment. This environmental monitoring may become a demanding task as the investigation of various compound classes in different matrices like air, water, soil and sediment requires specially adapted analytical methods. Environmental pollutants may be grouped into chemicals of inorganic and organic nature. Both groups of chemicals are dispersed among the various matrices. Organic pollutants may enter the aquatic environment directly by disposal of industrial effluents or domestic sewage. Besides, organics from agriculture may be washed out into surface waters by rain or floods. Finally, wet deposition of organic compounds adsorbed to aerosol particles may be a source for organic pollutants into surface waters.

1.1. The impoundment of the Yangtze River

The Yangtze River (Chinese: Changjiang) is with its length of 6,300 km the longest river in Asia and the third-longest river worldwide. The river exhibits a total catchment area of 1,810,000 km² and the annual water discharge at Yichang varied over the past 100 years between 5,000 and 40,000 m³ s⁻¹ (see Fig. 1) [3, 4]. The maximum discharge levels are reached during the rainy summer months in which also a considerable transport of suspended matter is observable [4]. The Upper Yangtze Reaches with a length of 4,300 km spanning from the Geladandong Mountains down to Yichang can be divided into two sections: the Upstream Three Gorges Reservoir from the Qinghai-Tibetan Plateau to Chongqing (3,640 km) and the Three Gorges Reservoir (TGR) from Chongqing to Yichang (660 km) [5]. The latter one counted 16.749 million people as inhabitants in 2010 of which 12.136 million and 4.613 million were rural and urban inhabitants, respectively [6]. The TGR is located within a subtropical monsoon climate zone (Köppen Cfa) with an annual rainfall higher than 1100 mm (see Fig. 2). This moderate climate zone is distinguished by a maximum annual temperature above 22 °C and at least four months with a mean temperature above 10 °C. Furthermore, a significant precipitation is apparent in all seasons [1]. With the approval of the construction plans by the National People's Congress in 1992, the Yangtze River was impounded at Sandouping (near Yichang) by the

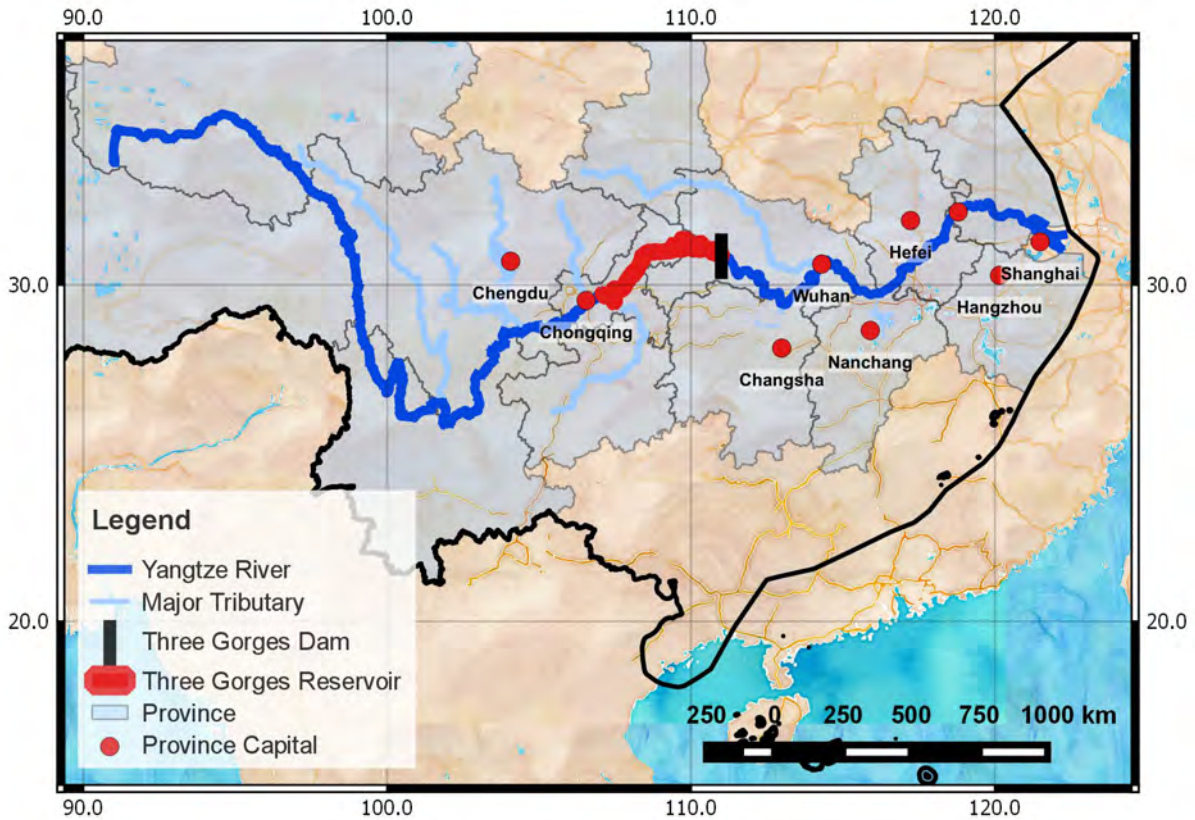


Fig. 1: Map of the Yangtze River drainage basin with highlighted major tributaries as well as related provinces with their capitals (© OpenStreetMap contributors [2])

construction of the Three Gorges Dam (TGD) which was completed in 2008/2009 [4, 6, 7, 8]. The dam was built for extended flood control, safeguarding the water supply, improving ship navigation and production of hydroelectric power [4]. With its length of 2,335 m and height of 181 m, it is China's largest dam and additionally one of the largest dams worldwide [5]. In 2010, the dam reached its designed maximum impoundment level of 175 m and was able to store 26.4 billion m^3 of accumulated flood water within TGR. In parallel, the Three Gorges Power Plant passed full-operation tests of the installed capacity of 22,500 MW [6]. The regulation of the water flow of the Yangtze River at Yichang invokes a fluctuation of the water level within the TGR of up to 30 m [4]. The stored water from the rainy summer months is released from January to May in order to reduce the impoundment level to 145 m and to assure water supply downstream of the TGD [4]. With water scarcity being a growing issue in China, especially the Yangtze River serves as important drinking water source for 186 cities [4, 9]. Moreover, increased flow velocity during dry months is intended for flushing accumulated sediment during the water storage phase [4]. Nevertheless, this is a challenging task as the Yangtze River transports 951.3 billion m^3 yearly runoff which is 52 % of the total yearly runoff in China [10]. Besides the beneficial effects of the TGD, there are, however, emerging socio-economic and

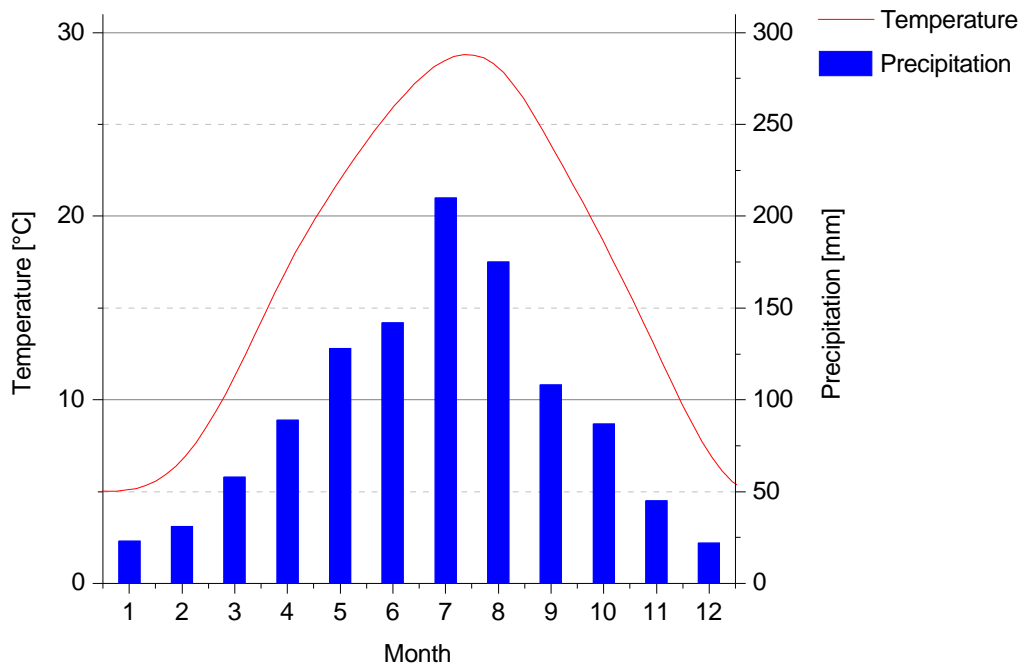


Fig. 2: Climate diagram of the city Yichang located in proximity to the Three Gorges Dam in Hubei Province, China (data obtained from [11])

environmental consequences which have to be faced [5, 12, 13, 14]. The considerable socio-economic impact of the TGD construction can be mainly attributed to the necessary resettlement of over 1.3 million people due to the flooding of huge areas of land in the reservoir area. Moreover, resettlement for the Three Gorges Project (TGP) has been typically involuntary at an inadequate compensation [15]. Besides, the flooding causes a severe loss of farmlands and infrastructure which in turn negatively affects the communities living within the reservoir zone [12, 15]. Impacts on the environment may arise from the dissolution of minerals and agrochemicals from the flooded farmlands. The decreased flow velocity within the reservoir and the increased residence time and water depth created a new hub for transformational changes of emitted pollutants [16]. Furthermore, the impoundment results in indirect consequences from pollution sources which have already been identified in a river regarded as one of the most polluted ones worldwide [16, 17]. Within the TGR, increased navigation and transportation attributes to the emission of considerable amounts of oil containing wastewater from ships (481,300 t in 2010) [6]. Moreover, the reservoir has to deal with the introduction of high volumes of urban sewage (615 million t in 2010) and the introduction of untreated wastewater can still be observed (25 million t in 2010) [6]. Urban sewage adds up with industrial effluent from mainly the metropolitan centers Chongqing, Changshou, Fuling and Wangzhou (220 million t in 2010) which may impose severe environmental threats if no specialized treatment is conducted [6].

Promoted by the humid climate, pollutants within the TGR become highly diluted within the large waterbody leading in fact to low abundances of these substances in surface water [5, 14, 18]. When taking the whole water body into account, however, these low concentrations of the single substances correspond to high total mass fluxes within the river and the reservoir [5, 14, 16, 18, 19]. Therefore, specialized analytical tools are needed allowing the detection and quantification of substances with concentrations in the ng L^{-1} and pg L^{-1} -scale in order to identify environmental threats despite the high analyte dilution.

1.2. Persistent and emerging organic pollutants

An example for organic environmental pollutants which are typically monitored in different matrices is the group of persistent organic pollutants (POPs). Once released into the environment, these compounds show resistance to biodegradation and tend to bioaccumulate in the food chain. Exposure to these chemicals may induce acute toxic effects on live animals and humans as well as chronic toxic effects due to long-time exposure [20]. Besides, some POPs are known to be carcinogenic or at least known to act as possible human carcinogens. Due to their extended lifetime in the environment, these compounds can undergo long-range transports and reach remote areas like the Antarctic [20, 21]. Guidelines for the limitation of production, intentional and unintentional release of POPs into the environment have been declared by the Stockholm Convention of the United Nations Environment Programme (UNEP) [20] since 2004. The Convention agreed on the elimination of production for most of the regulated substances. Among them are organochlorine pesticides (OCPs) and polychlorinated biphenyls (PCBs). The production and use of other compounds like the insecticide dichlorodiphenyltrichloroethane (DDT) and the surfactant perfluorooctane sulfonic acid (PFOS) have been restricted to certain applications [20]. Unintentionally produced POPs like polychlorinated dibenzo-p-dioxins (PCDDs) and polychlorinated dibenzofurans (PCDFs), which are among the most cancer-causing chemicals known, can be formed during combustion processes like waste incineration and are also addressed by the Stockholm Convention supporting measures for the reduction of their release into the environment [20].

Nevertheless, there are other organic trace compounds which are commonly not referred to as POPs but still exhibit POP-like properties, posing possible threats to environmental and human health. Polycyclic aromatic hydrocarbons (PAHs) are naturally found in the environment but may also originate from anthropogenic sources [22]. Most of the atmospheric PAHs are formed and released from incomplete combustion processes like the burning of fossil and non-fossil fuels from car and truck engines, fuel burning energy power plants, domestic heating and incineration [22]. Volcanic activities and forest fires may serve as natural PAH proxies [23].

Some isomers are known for possible carcinogenic and mutagenic activity by the formation of DNA adducts [24]. Moreover, animal models indicated carcinogenicity, genotoxicity, immunotoxicity and teratogenicity of PAHs [25]. Due to their aromatic ring structure, PAHs can readily adsorb onto the surface of carbonaceous particles and thus be widely spread in the environment [23]. Besides, the affinity of PAHs towards particles was directly related with the carcinogenic potency of diesel soot [26].

1.2.1. Perfluorinated compounds

Organic chemicals in which all hydrogen atoms have been replaced by fluorine are commonly referred to as perfluorinated compounds (PFCs). Although substances containing one or multiple fluorine atoms are naturally produced by higher plants and certain microorganisms like fungi, PFCs (except trifluoroacetic acid) can be attributed to anthropogenic origin only [27, 28]. Key compounds for investigation of this substance class are the linear perfluorinated alkyl acids (PFAAs), perfluorooctanoic acid (PFOA) and perfluorooctane sulfonic acid (PFOS) and their corresponding salts perfluorooctanoate and perfluorooctanesulfonate (see Fig. 3). The large scale production of PFCs has its origin in the discovery of the process for the electrochemical fluorination (ECF) of organic molecules. The process was discovered by Joseph H. Simons at the State College of Pennsylvania (USA) sponsored by the 3M corporation in the 1930s and published after World War II in 1949 in the Journal of the Electrochemical Society [29, 30]. Nevertheless, for the production of promising PFCs in an efficient yield for industrial appliances, further research was needed in the 3M research laboratories [31]. At this early stage, the introduction of functional groups into perfluorinated alkyl chains proposed major problems. Furthermore, analytical techniques were limited and the identification of reaction products was a challenging task [31]. According to Simons, ECF is carried out by dissolving a substrate for fluorination in anhydrous hydrogen fluoride within an electrolysis cell with iron cathode and nickel anode. The reaction is started by applying voltages between 5 and 6 V to the cell. Critical for the reaction is the solubility of the fluorination substrate in hydrogen fluoride. However, partly soluble substrates can still be accessed by stirring a suspension [32]. Early reactions at the 3M laboratories with butyric acid lead to excess production of oxygen difluoride and low recoveries of C_3F_8 . However, this issue could be solved by using butyric anhydride as fluorination substrate. The reaction then produced perfluorobutyramide in recoverable yields which could finally be transformed to the corresponding perfluorocarboxyl acid by synthetic chemistry [31]. In general, ECF of linear compounds yields linear and branched isomers as well as some impurities [33].

PFCs are also accessible via telomerization yielding mostly linear products with an even number

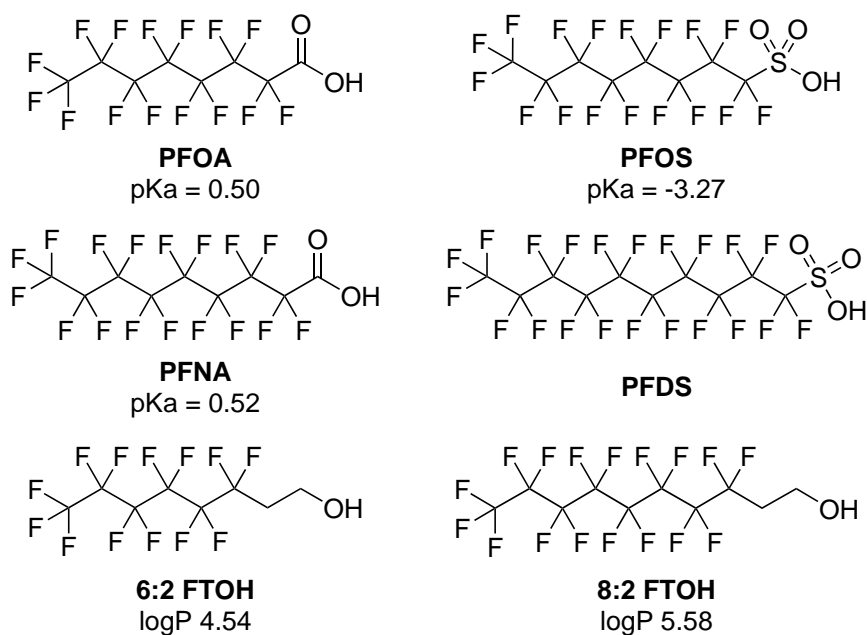


Fig. 3: Molecular structures of typically produced and investigated perfluorinated compounds (pKa-values obtained from [34]; logP-values of FTOHs from [35])

of carbon atoms. Additionally, this technique offers the production of fluorotelomer alcohols (FTOHs) which are used for the production of fluoropolymers [1]. During telomerization, perfluoroethylene is polymerized in a radical reaction with the aid of iodine in iodine pentafluoride. The resulting perfluoroalkylchains are brought to reaction with ethylene resulting in perfluoroalkylethyl iodides in which the iodine can be replaced by a hydroxy group to yield FTOHs. Highly pure PFCAs can then be obtained by oxidizing of the resulting FTOHs [1].

The commercialization of the production lead to the broad application of PFCs, especially of PFAAs like PFOS and PFOA. Due to the strength of the chemical bond between carbon and fluorine, they exhibit resistance to acids and bases, oxidizing agents, photolysis and heat [1]. Thus they are virtually immune to chemical and biodegradation. PFAAs work as specialized repellents for oil and water at the same time and are consequently suitable for the modification of surfaces in textiles (like Gore-Tex[®]), carpets (like Scotchgard[®]), paper and packaging materials for food [1]. Furthermore, PFAAs are utilized for the reduction of surface tension in cosmetics, pesticides, cleaning agents, aqueous fire fighting foams and as processing aids in galvanization and as emulsifier in the production of fluoropolymers like Teflon[®] [1, 36, 37, 38, 39]. The worldwide broad field of application of PFCs lead to high total production numbers. The historical production of perfluorooctane sulfonyl fluoride (POSF) was estimated to be 122,500 t between 1970 and 2002 [33]. The global production and use of PFCAs during 1951 and 2004 was estimated to be between 4400 and 8000 t [40]. In 2002, the main manufacturer of PFCs (3M) chose to phase out production of POSF related products and PFOA. Additionally, POSF

and PFOS became restricted in use by the Stockholm Convention in 2009 [20] (see also section 1.3.).

Due to their chemical properties, the highly stable PFCs behave persistent in the environment meaning once released, they do not degrade and thus may tend to bioaccumulate in plants or in the food chain which may impose environmental threats or even danger to humans. Without proper means to remove these persistent compounds from environmental matrices, it is mandatory to limit emission as far as possible. PFCs have already been detected widespread in the environment. They appear to be ubiquitous residing in air, soil, sediment and water [27, 28, 39, 40, 41, 42]. Volatile PFCs like FTOHs can undergo long-range transport and even reach remote areas like the Antarctic which are far away from any possible anthropogenic source [43, 44, 45]. FTOHs are typically detected in house dust samples and thus invoke a certain exposure source especially for humans [46, 47]. Maybe most alerting is the fact that PFCs, due to their ubiquitous appearance, can routinely be detected in human blood serum [48, 49]. Input of PFCs into the environment can be attributed to direct and indirect sources. Typically, PFC manufacturing plants can be regarded as point sources. As an example for direct emission, the production of PFCs at the company 3M requires over 600 intermediate manufacturing steps which include venting and washing steps leading to PFC contaminated air, water and solid residues. With technically demanding and expensive after-treatment systems, it was possible to reduce PFC-emissions to air and water by up to 50 % which means that still a considerable PFC amount is released into the environment during manufacture [33]. Aqueous fire fighting foams may serve as example for historic direct PFC input into the environment. Being used by the military and at airports worldwide, PFC-containing formulations have been used routinely in fire fighting exercises causing direct PFC contamination of soil and water [50]. The emission of PFCA from this source was estimated to be between 5 and 10 t yearly from 1965 to 1974 [40]. PFC losses of products like PFC-containing textiles, carpets, paper and packaging are suspected to contribute up to 85 % of the total indirect PFC emissions [33]. In general, PFCs are also emitted through wastewater treatment plants in which the oxidative milieu can increase the burden of PFCAs by oxidizing FTOHs [42, 51, 52]. Moreover, association of PFCs with particles may lead to an accumulation in sewage sludge [42, 51, 53]. In Arnsberg (Germany), illegal deposition of PFC-containing waste contaminated the sewage sludge of the associated wastewater treatment plant. Local farmers administered the sewage sludge routinely as special fertilizer to their fields. In that way, the nearby river Möhne, serving as drinking water reservoir for the small city Arnsberg, was contaminated by large amounts of PFCAs washed out from the fields into the reservoir. Finally, this lead to elevated PFC levels in the local drinking water supply and to an increased exposure of the local inhabitants to PFOA and PFOS which resulted

in elevated levels of these chemicals in their blood sera [53, 54].

Within the human body, PFOA seems to exhibit an exceptional long half-life of more than 4 years which was estimated from levels determined in blood serum from workers in the PFC industry and from the incident in Arnsberg [53]. Investigations of PFOA residence in rats, dogs and monkeys, however, showed clearance within only a few days [55]. Consequently, results from the animal model might not be applicable for humans directly [53]. Meanwhile adverse effects on human health are still under investigation and it is tried to estimate the risk potential for humans from animal models as well as from epidemiological studies [55]. In a study from 2009, however, results indicated adverse effects of PFOA and PFOS on the fertility of women [53, 56].

1.2.2. Pharmaceutical residues

The abundance of pharmaceuticals in the aquatic environment which can also be seen as part of emerging organic pollutants drew more and more attention during recent years although first investigations in Germany had already been conducted in the 1970s [57]. However, only in recent years, the progress in liquid chromatography and mass spectrometry allowed the routine monitoring of various organic residues in water samples at low environmental concentrations [58, 59]. The increasing application and high prescription numbers of pharmaceuticals for human health and livestock lead to an increasing burden of these substances in rivers, lakes and reservoirs in developed [60, 61] as well as in developing countries like China [62, 63]. In Germany, the consumption of pharmaceuticals with environmental relevance according to the Federal Environment Agency grew by 20 % within ten years from 6,200 t to 8,120 t in 2012. Thereby, more than half of this amount can be attributed to only 16 active pharmaceutical ingredients. The most prescribed pharmaceuticals intended for human use are nonsteroidal anti-inflammatory drugs, antiasthmatics and psychopharmaceuticals [64]. Furthermore, intensive livestock farming requires the broad application of pharmaceuticals. Thus, livestock farming used 1600 t of antibiotic pharmaceuticals in Germany in 2011 [65]. Additionally, for the treatment of livestock, hormones and anti-inflammatory pharmaceuticals for local application are needed [66].

Fig. 4 illustrates the input paths of pharmaceutical residues into the environment. Typically, pharmaceuticals are brought into the environment by human consumption and the treatment of livestock as large fractions of the pharmaceutical active ingredients are excreted unmetabolized [57]. Besides, inappropriate disposal of pharmaceuticals may also contribute to the burden of these substances in wastewater. The classic wastewater treatment conducted with domestic sewage including flocculation, sedimentation and active sludge treatment is not capable to

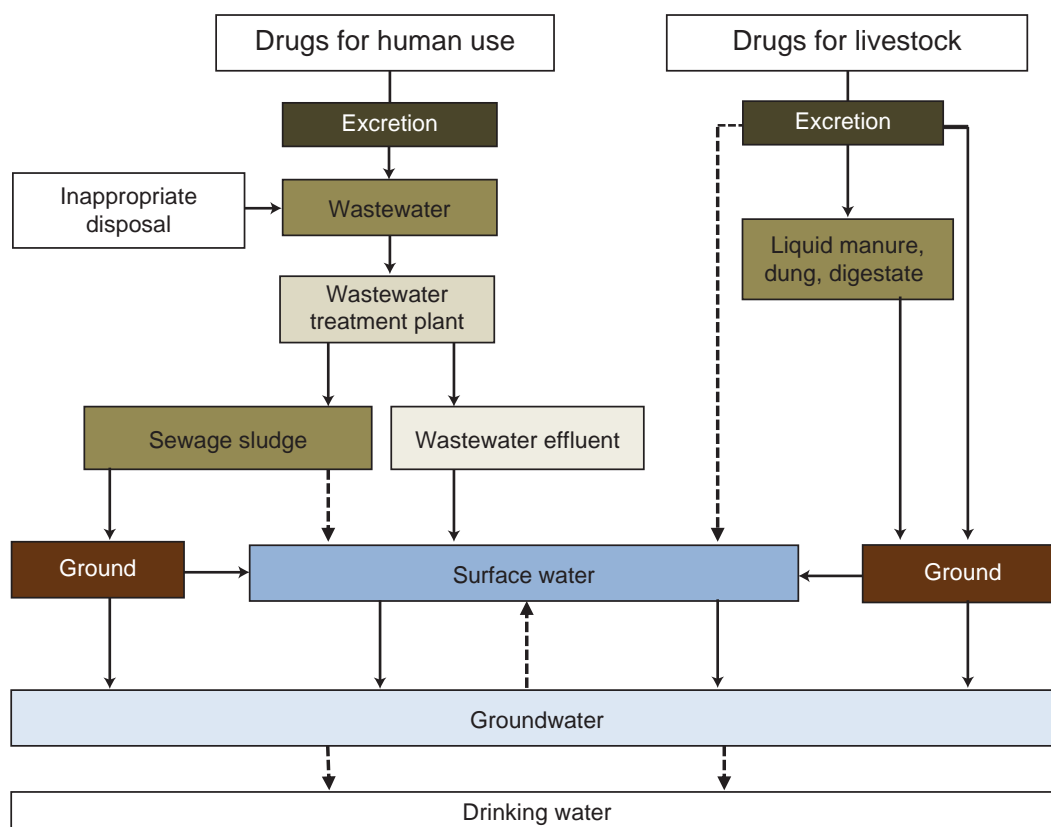


Fig. 4: Main paths of emission of pharmaceuticals intended for human use and livestock into the environment (according to [64])

reach total elimination of pharmaceutical residues [63, 64]. Thus, effluents from wastewater treatment plants (WWTPs) contain considerable amounts of pharmaceutical active compounds which enter surface water directly. In addition to wastewater effluents, pharmaceuticals reside in sewage sludge, too [64, 67]. In Germany, domestic sewage sludge, liquid manure and dung from livestock farming are applied on crop fields as special fertilizer and in landscaping projects (800,000 t in 2012) [64, 68]. Once applied, soluble organic residues may also enter surface water by washing out or migrate to groundwater from which drinking water production might be affected as a last consequence (see Fig. 4).

Pharmaceutical classes typically detected in surface water in a developed country like Germany are iodized X-ray contrast agents, anticonvulsants, analgesics, antibiotics, beta blocker, lipid lowering agents and synthetic hormones [64, 67]. Some individual substances are regularly detected in concentrations above $1 \mu\text{g L}^{-1}$ in surface waters [64]. Due to dilution effects, however, the main bulk of pharmaceutical residues is detected below $0.1 \mu\text{g L}^{-1}$ [64, 67].

Within the environment, pharmaceuticals may influence the metabolism of plants and animals according to their mode of action. However, direct effects of exposure which could be traced back to a single pharmaceutical residue are rare due to the high dilution and usually low concen-

tration apparent in the environment. As one example may serve the declining vulture population in Pakistan which was brought into connection with the analgesic diclofenac. The direct exposure of the vulture population by eating livestock animals treated with the pharmaceutical lead to renal failure and visceral gout [69]. Chronic exposure to low concentrations of pharmaceuticals is the more common case. The potent synthetic hormone 17α -ethinyl estradiol used in birth-control pills was observed to lead to feminization of the fish species fathead minnow (*Pimephales promelas*) by chronic exposure to only 5 to 6 ng L⁻¹. Consequently, a decline of population within a 7-year experiment could be observed [70]. Within another study, the overall no-observed adverse effect concentration (NOEC) in fathead minnow was determined to be as low as 1 ng L⁻¹ [71]. Besides hormones, effects from chronic exposure to other residues have also been investigated. In a laboratory study, exposure of rainbow trout (*Oncorhynchus mykiss*) and carp (*Cyprinus carpio*) to four different pharmaceuticals (one anticonvulsant, one analgesic, one beta blocker, one lipid-lowering agent) revealed ultrastructural effects on liver, kidney and gills at environmental relevant concentrations of 1 to 2 µg L⁻¹ after 28 days of exposure. The effects varied according to the pharmaceutical residue and the investigated organ but for three of the 4 investigated residues, effects could already be observed at a concentration of 1 µg L⁻¹ [72]. Antibiotics represent another group of highly potent pharmaceutical residues which propose a certain environmental threat. Sulfonamide antibiotics were observed to have phytotoxic effects and influence on soil respiration. The effects varied according to the plant species and the single antibiotic substances [73]. Sulfonamide antibiotics appear to be taken up by willow and maize and reside mainly in the roots. At environmental concentrations, these antibiotics affected root growth negatively and impaired plant performance and biomass production at exceptionally high concentrations [74]. Within a practical study, antibiotics were administered to piglets in order to gain specifically contaminated liquid manure which was administered to test fields. After growing crops and field salad on the test fields, the antibiotics could be detected mainly in the roots but additionally within the corn of wheat which was suggested as possible entrance of antibiotics into food [75]. Although antibiotics may invoke adverse effects on plants and especially crop plants growing on fields fertilized with liquid manure, due to their nature, they also promote a certain selective pressure on the complex microbial community in arable soils. A significant increase of resistance genes against sulfonamide antibiotics was found in soils two months after they had been treated with antibiotic-containing liquid manure [76]. This is particularly alerting as these genes being usually located on self-transferable or mobilizable plasmids capable of transferring this ability throughout the microbial community [77, 78]. Consequently, the application of liquid manure has to be taken into consideration as a contributing factor to the development of infectious diseases from multi-resistant

bacteria [76, 79]. With many different pharmaceutical residues being mixed within the environment, toxicological effects from the compound mixture can differ from the exposure to single substances alone. This mixture toxicity can be evaluated using bioassays in combination with chemical analysis [80, 81, 82]. Where the chemical analysis can describe the abundance of known chemicals, bioassays can give hints to mixture toxicity or indicate that there are chemicals not yet covered by targeted analysis which cause a certain adverse effect [80]. Therefore, bioassays in combination with chemical analysis can be used as a tool for the early identification of evolving environmental threats from pharmaceutical residues.

Due to the pronounced entry of pharmaceutical residues through wastewater, more advanced wastewater treatment techniques like membrane filtration, ozonation and activated carbon adsorption are under evaluation [83, 84] or even applied (e. g. Switzerland: advanced treatment in large and medium sized wastewater treatment plants financed by an extra duty of the inhabitants) [85]. Furthermore, environmental risk assessment studies are now included in the approval process of new pharmaceutical active ingredients.

1.3. Regulations of organic pollutants in the European Union

The guidance from the Stockholm Convention regarding the elimination and restriction of POPs as well as monitoring approaches for emerging organic pollutants are reflected in directives from the European Union (EU) which have to be translated into domestic legislation by the member states. The EU water framework directive, set up in 2000, was established to preserve and achieve a respectable water quality of all water bodies. Therefore, the directive defines certain quality endpoints covering biological, hydromorphological, physico-chemical and chemical endpoints. Moreover, a list of priority substances was released which covered already most of the POPs that were listed in 2001 in the Stockholm Convention [86]. Limit values called environmental quality standards (EQS) were introduced in 2008 for 33 priority substances [20, 87]. In case of exceeding these EQS, the respective member state has to implement measures to reduce the burden of the respective substance in the aquatic environment [85].

Regarding pharmaceutical residues in water, the EU introduced mandatory studies on the environmental impact of new pharmaceutical active compounds as part of the approval process in 2004. Nevertheless, the results from the environmental assessment may not affect market authorization of new pharmaceuticals in any case [88]. The directive aimed to achieve a significant improvement of the knowledge on environmental toxicity of new pharmaceutical compounds although this guidance is not applicable to pharmaceuticals that have been approved already [85]. Since 2013, the list of priority substances was expanded by 12 compounds and some EQS-values were reduced. Additionally, pharmaceutical residues were addressed for the first time by

introducing guidance to the European Commission to set up a watch list with a maximum of 10 substances that will have to be monitored throughout the EU [89]. Up until now, however, the EU does not force any mandatory measures from the member states that would have to be undertaken to lower the burden of pharmaceuticals in surface water.

Special focus is drawn on the quality of water intended for human consumption. The EU established a drinking water directive in 1980 which was renewed in 1998. In contrast to the water framework directive, the guidance for drinking water is more strict and introduces guiding and limiting levels for inorganic and organic residues [90, 91]. It was acted with caution as the allowed levels were set up to 20 times lower than the guidance from the World Health Organization (WHO) [91, 92]. Moreover, in terms of organic pollutants, the directive sets parameters predominantly for groups of compounds rather than for single substances. In comparison to the 1980s, the current drinking water directive does not further regulate the analytic monitoring tools but sets boundaries for trueness, accuracy and limit of detection the applied detection method has to achieve [91]. Consequently, single laboratories involved in the monitoring of drinking water are free to apply alternative measurement techniques as long as they achieve sufficient analytical quality. Restricted from drinking water is a whole group of organic pesticides, a selection of four PAHs and some lower molecular organic compounds [91]. In Germany, the EU drinking water directive was translated into national law by the drinking water regulation in 2001 which has been revised several times since its release where its current status was determined in August 2013 [93]. But even since 1975 Germany regulated drinking water quality [94]. The levels stated in the current German drinking water regulation are equal to most of the values set in the EU drinking water directive or are lower for a few parameters. All in all, the legislation in the EU for the protection of the aquatic environment exhibits high precaution for threats from already identified organic pollutants. Moreover, future threats from emerging organic pollutant are being assessed to propose solutions for emerging threats. Nevertheless, the continuous industrial development increases the number of organic chemicals released to the environment which will always necessitate the adaption of legislation to new identified chemical pollutants.

2. Theoretical background

2.1. Liquid chromatography

Liquid chromatography (LC) is a common approach to achieve separation of a mixture of compounds which is of analytical interest. Even more important in environmental analysis, however,

is the separation of the analytes from matrix compounds which may already be partly realized with a suitable laboratory cleanup. The importance of matrix separation depends on the analytical detection technique which is coupled with the chromatography. Nevertheless, most available detection techniques are not able to detect a mixture of compounds at the same time. The working principle of LC is based on the different separation of compounds between two distinct phases. Thus, chromatography can be seen as infinitely repeated separation experiments between a stationary and a mobile phase resulting in a continuously operated separation. In liquid chromatography, the stationary phase is usually a column with immobilized surface-active material in small-particle form or less common a porous monolith [95]. The mobile phase in case of reversed-phase chromatography usually is a mixture of organic solvent and pure water. For chromatography, a compound mixture is administered in a small volume on the top of the column and forced through the column by the liquid flow of the mobile phase. During the passage through the column, each analyte interacts with the mobile and the stationary phase which is characteristic for each compound according to its distribution coefficient K_X :

$$K_X = \frac{c_{stat}}{c_{mob}} \quad (2.1)$$

where c_{stat} and c_{mob} are the concentrations of the compound X in the stationary and the mobile phase, respectively. Due to the different values of K and the continuously operated partition between the two phases, the compound mixture becomes separated. Compounds with higher affinity to the stationary phase and corresponding higher K -value elute later from the column than compounds with lower affinity and smaller K -value. In this context, the longer a compound needs for elution the higher its retention on the chromatographic column is. The diffusion processes during liquid chromatography are well described by the van Deemter equation:

$$H = A + \frac{B}{u} + C \cdot u \quad (2.2)$$

where H is the height equivalent of a theoretical plate (HETP), u is the flow velocity of the mobile phase and A , B and C are diffusional terms that cause band broadening and the typical Gaussian peak shape. Term A is caused by the different pathway the compounds can take through the tightly packed stationary particles of the column (see Fig. 5). This pathway may be fortunate by chance which leads to a fast passage through the column or may be less fortunate yielding to a longer pass-through time. The effect of this process called Eddy diffusion may be smaller the more the particles in the column are evenly sized [95].

Natural diffusion of the sample occurs in all three dimensions. Diffusion in or against the direction of the mobile phase flow contributes to band broadening (see Fig. 6) and is described

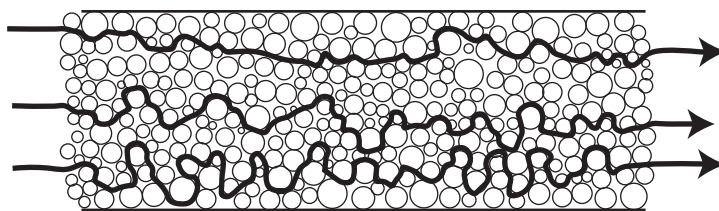


Fig. 5: Illustration of possible fortunate and unfortunate pathways through the packed column (Eddy diffusion) according to [95]; a narrow size distribution of the column bed helps to reduce this effect

as term B in equation 2.2 [95]. Longitudinal diffusion is indirect proportional to the flow velocity. Consequently, higher flow rates diminish the effect of longitudinal diffusion on band broadening. Additional influence factors on term B are viscosity and temperature of the mobile phase.

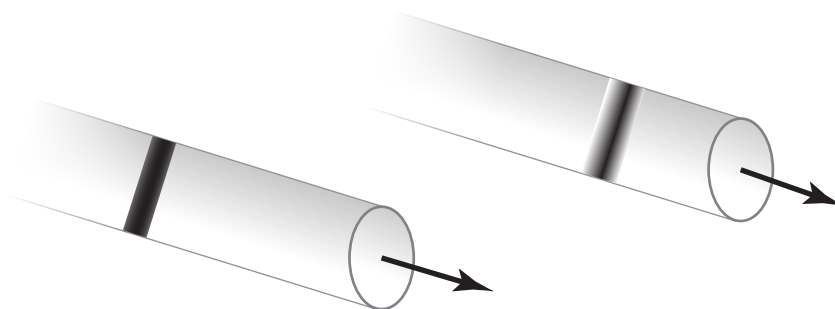


Fig. 6: Band broadening due to diffusion in and against the direction of the linear flow in the chromatographic column (longitudinal diffusion); faster elution yields a reduction of this effect

The third term C of the van Deemter equation describes the mass transfer between the mobile and the stationary phase and thus the different adsorption behavior and residence time of the analyte molecules on the surface and in the pores of the stationary phase particles. The impact of term C on band broadening is direct proportional to flow velocity as the analytes attached to the stationary phase gain a higher amount of the linear distance to the analyte band in a given time window than at lower u . This effect can be reduced by using smaller stationary particles or particles with a thin, porous surface layer [95]. High flow rates necessary for a fast separation and a short analysis time, however, reduce the chromatographic separation performance.

In order to achieve the best separation of compounds in LC, H has to be minimized according to the HETP-concept yielding the maximum number of theoretical plates N for a given column length. Each theoretical plate can be seen as a column segment in which a full equilibration of the partition of a compound between mobile and stationary phase is reached. Fig. 8 illustrates the van Deemter curve plotting H against the linear flow velocity u . Obviously, the separation

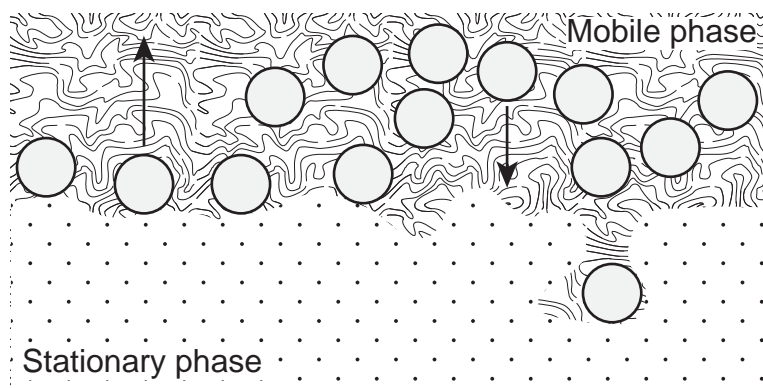


Fig. 7: Mass transfer between mobile and stationary phase according to [95]; higher linear flow velocity leads to higher spatial differences between adsorbed and free analyte molecules and consequently to band broadening

performance of a LC-instrument will be optimal at the flow rate u_{opt} . Depending on the complexity of the analytical task, separation performance can be sacrificed for a shorter analysis time and higher sample throughput.

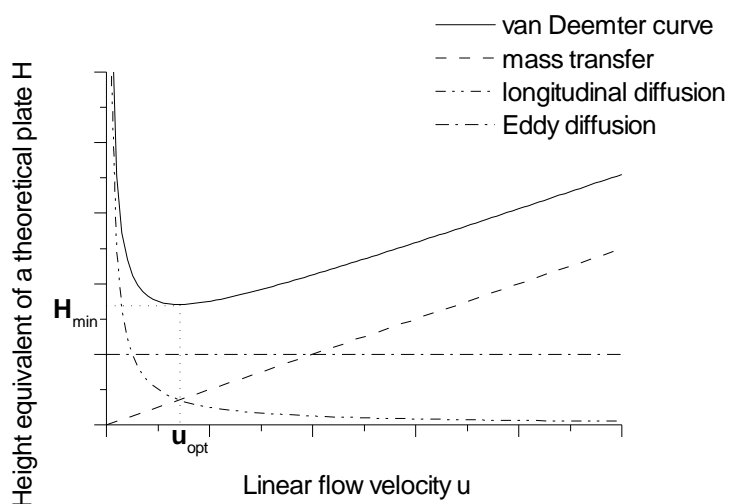


Fig. 8: Exemplary plot of the van Deemter curve with its components plotted as dotted lines; LC separation performance optimizes at the linear flow rate u_{opt} with H_{min}

The analytical results of LC coupled with a suitable detection system are displayed in a chromatogram plotting the signal intensity against the time starting with the time of sample injection on the head of the column. Typical analyte signals arrive at the detector as Gaussian shaped peaks with a peak maximum at a characteristic retention time t_R which can be used for qualitative analysis. Besides, the chromatogram yields quantitative information (peak area and peak height) as well as information on the quality of the separation. From the peak width ω or the peak width at half-height $\omega_{1/2}$, the number of theoretical plates N can be calculated:

$$N = 16 \cdot \left(\frac{t_R}{\omega} \right)^2 = 5.54 \cdot \left(\frac{t_R}{\omega_{1/2}} \right)^2 \quad (2.3)$$

At the same time, knowing N , H is defined as:

$$H = \frac{L}{N} \quad (2.4)$$

where L is the length of the chromatographic column. The quality of the separation of two neighboring peaks is expressed by the resolution R . Two peaks are separated to baseline if $R > 1.5$:

$$R = 2 \cdot \frac{t_{R2} - t_{R1}}{\omega_1 + \omega_2} = 1.18 \cdot \frac{t_{R2} - t_{R1}}{\omega_{1/2_1} + \omega_{1/2_2}} \quad (2.5)$$

Technical advances since the establishment of classical column chromatography in the 1900s by Tswett [96] led to the development of computer controlled high-performance liquid chromatography (HPLC) which finds broad application in modern analytics. Progress in the generation of stationary phases with narrow size distributions and smaller particles led to a large gain in chromatographic resolution over the past decades [96]. At the same time, the back pressure generated by columns with spherical particles smaller than 10 μm in diameter results in operational pressures above 130 bar [96]. Since 2004, progress in the design of columns and the construction of high pressure pumps lead to the application of particles with a diameter smaller than 2 μm whereas reliability and operability of the instruments remained comparable to HPLC [97]. Further reduction of particle size required pumps providing 600 to 1000 bar but also reduced the sample runtime for routine analysis to under 10 min. Therefore, sub-2-micron chromatography is usually referred to as ultra high-performance liquid chromatography (UHPLC) [97].

2.1.1. Reversed-phase chromatography

The chemical nature of the stationary phase in a chromatography column has to be adjusted to the separation task. A large variety of column chemistries have been made commercially available and widened the field of application of HPLC from the analysis of small organic molecules over applications for biomolecules up to ion chromatography and many more [95, 96]. One common column material are surface modified silica particles. Silica itself consists of silicon atoms bridged in three dimensions by oxygen atoms. Silica supported materials are most widely used in chromatography due to their outstanding properties making them suitable for various applications like size exclusion and ion exchange [98]. The material can form irregular gels or

spherical particles in dependence on the production process such as the hydrolysis of sodium silicate or the polycondensation of polyethoxysiloxane with subsequent dehydration [95]. The reactive hydroxy-groups at the surface of the material allow chemical bonding to modify the surface permanently and thus enable numerous stationary phases [95, 98]. For the analysis of aqueous solutions with small organic molecules, biomolecules, pharmaceutical active ingredients or food extracts, silica modified with octadecylsilane (ODS), named C-18 chemistry, found wide distribution [99]. Therefore, the reactive hydroxy groups of porous silica react with the highly hydrophobic chloro(dimethyl)octadecylsilane. This results in an hydrophobized silica surface which corresponds to reversion of the silica surface property which is usually highly polar. Fig. 9 illustrates the surface of a silica particle modified with ODS. A fence-like structure is formed by ODS on the particle surface. Additionally, free hydroxy groups, that have not reacted with ODS due to steric reasons, can be treated with trimethylchlorosilane in order to reduce the number of free silanol groups that may have adverse effects on analyte retention as they can act as active centers for ion exchange or polar interaction [95]. Most C-18 columns are stable over a pH-range from 3 to 8. Basic conditions lead to the dissolution of the silica support whereas low pH leads to siloxane bond hydrolysis [100].

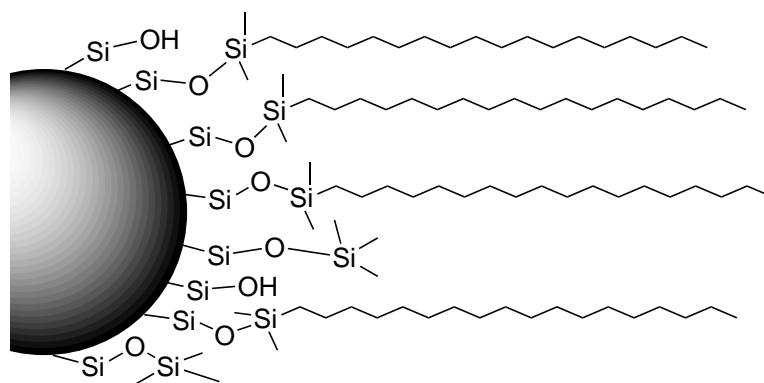


Fig. 9: Model structure of a silica particle surface modified with octadecylsilane (ODS) and end-capped with trimethylchlorosilane (C-18 column chemistry); the alkyl chains form a dynamic lattice fence-like structure

C-18 chromatography columns require organic solvents with high polarity for the elution of retained compounds. This combination of column material and solvent system is commonly known as reversed-phase chromatography (RPC). The retention mechanism of C-18-phases can be regarded as partition between an amorphous bulk liquid hydrocarbon layer and the mobile phase. Nevertheless, the actual retention mechanism in reversed-phase chromatography is far more complex. More accurate is the assumption that partition and adsorption are the driving forces for retention at the same time [99]. Water, which is one of the strongest elution media in other chromatographic applications, cannot penetrate the hydrophobic analyte binding carbon

layer and thus is the weakest eluting solvent in RPC [95]. Consequently, highly polar water miscible organic solvents like methanol or acetonitrile are used for elution as they can penetrate the hydrophobic layer. The retention on C-18 columns increases with the hydrophobicity of the analytes, bonding density of alkyl chains and the degree of end-capping [95]. Highly retentive C-18 columns are needed for the separation of polar compounds that have only weak interaction with the stationary phase. Retention of polar compounds in RPC can be further increased by distinct silanol activity leading to hydrogen bond acceptor or cation exchange activity in acidic or basic environment, respectively [101].

Typically, elution in RPC is carried out with a linear gradient between an aqueous mobile phase (solvent A) and an organic mobile phase (solvent B) rather than with a fixed solvent mixture (isocratic elution). Binary gradient pump equipment allows the adjustment of solvent composition at the start and the end of the separation as well as the gradient steepness. The continuous increase of organic solvent during separation reduces chromatographic issues like peak tailing and reduces the peak width. At the same time, RPC methods with gradient elution can be used for various analytes without gradient optimization in many cases [102].

2.1.2. Retention Time Index

As already mentioned in section 2.1., the retention time t_R reveals qualitative information which can be used for the identification of unknown substances or the validation of already known substances. The retention time, however, strongly depends on the conditions of the chromatographic system including dead volume, column chemistry, separation temperature and solvents. Therefore, the normalization of retention time is necessary in order to apply it as a characteristic parameter in databases which can be used in turn for compound identification. In gas chromatography, the Kováts retention index was introduced in the 1950s and normalized the retention time to n-alkanes eluting before and after the corresponding substance [103]. In RPC, however, due to the rather complex influence factors on analyte retention (see section 2.1.1.), various approaches and models exist for the normalization of retention time in order to make it available as characteristic criterion [104, 105, 106]. Additionally, the introduction of LC coupled mass spectrometry as detector for liquid chromatography gave access to the exact mass of eluting analytes which is enough information for doubtless compound information for many applications. Consequently, the efforts for establishing a universally applicable parameter for the complex retention in RPC lost importance.

Nevertheless, for upcoming approaches with non-target analysis any further qualitative information on unknown signals is welcome. For non-ionic analytes, the retention-time index (RTI) reveals a possibility to predict the retention time on a chromatography system based on the

octanol-water partition coefficient (K_{OW} or P -value) [107, 108]. If quantitative analysis is carried out at the same time for multiple compounds, the application of RTI does not require any further calibration data as the retention information of the calibration standards is sufficient. The RTI is basically a normalization of the $\log P$ -values of the investigated analytes on a linear scale from 50 to 150. Therefore, the first and last eluting compound are assigned to an RTI-value of 50 and 150, respectively. According to the normalization, the RTI-value of a compound which is eluting in between the first and last eluting compound can be calculated:

$$RTI_i = (\log P_i - \log P_{i-1}) \cdot \left[\frac{150 - 50}{\log P_{max} - \log P_{min}} \right] + RTI_{i-1} \quad (2.6)$$

where the index i indicates the compounds in eluting order, $\log P_{max}$ and $\log P_{min}$ are the maximum and minimum values of the partition coefficient within the calibration, respectively (which are usually the first and last eluting compounds in RPC). In RPC applications with non-ionic analytes, the RTI-value is linearly correlated with retention time. The correlation quality depends on the structural similarity of the analyzed compounds [102]. Consequently, the RTI sets up a correlation between retention time of unknown signals and their corresponding $\log P$ -value. In combination with high resolution mass spectrometry, the measured exact mass and $\log P$ -value of unknown compounds are available at the same time for database related compound identification.

2.2. Quadrupol time-of-flight mass spectrometry

Since the 1950s, mass spectrometry (MS) evolved into an essential analytical technique that found wide application in chemistry, biochemistry, pharmaceutical science and medicine as well as in related disciplines [109]. The performance of mass spectrometers has been increased and today commercially available high resolution mass spectrometry (HRMS) allows for the calculation of sum formulae of the detected ions from their measured mass deficiency. The time-of-flight mass spectrometer (TOF-MS) is one example for a mass analyzer with HRMS capabilities. The basic working principle of this type of instrument is the fact that ions with different mass-to-charge ratio (m/z) need different time to travel through a field-free drift space. This working principle, however, dictates that TOF-measurements have to be carried out discontinuously. Therefore, the application of TOF-MS was limited since its commercialization in the mid 1950s [109]. In the 1980s, the development of TOF detection was forced again due to the development of the pulsed ionization technique matrix-assisted laser desorption/ionization (MALDI) [109]. Furthermore, the subsequent introduction of TOF-MS with orthogonal acceleration allowed the coupling with ionization techniques that produce constant ion beams like

electrospray ionization [110].

The relationship between the time-of-flight and m/z results from considering that the energy uptake E_{el} of an ion with the mass m_i and the charge of z elementary charges e travelling through the potential U . E_{el} corresponds to the kinetic energy E_{kin} of the translatory motion:

$$E_{el} = e \cdot z \cdot U = \frac{1}{2} \cdot m \cdot v^2 = E_{kin} \quad (2.7)$$

Consequently, the velocity of the ion is defined as:

$$v = \sqrt{\frac{2 \cdot e \cdot z \cdot U}{m_i}} \quad (2.8)$$

The TOF-MS can be seen as a time measurement instrument that determines the drift time t of an ion for the distance s :

$$t = \frac{s}{v} = \frac{s}{\sqrt{\frac{2 \cdot e \cdot z \cdot U}{m_i}}} \quad (2.9)$$

After transformation of equation 2.9, m/z can be determined with the time-of-flight and the instrument parameters U and s :

$$\frac{m_i}{z} = \frac{2 \cdot e U t^2}{s^2} \quad (2.10)$$

In TOF-MS instruments with orthogonal acceleration, ion packets are injected from a constant ion beam by a pulsed electric field (pusher) with a frequency of several kilohertz (kHz). The field-free drift space in most modern TOF analyzers is designed with either a single or double reflection stage (ion mirror) due to different reasons. At first, the size of the instrument compartment can be reduced due to the doubling of the drift space back and forth within one tube. Secondly, the mass resolution improves due to the increased flight distance. The direct dependence of the flight time t and the drift space s according to equation 2.9 leads to a longer time window between the impact of ions with different m/z on the detector. Therefore, the electronics can resolve ions with smaller differences in their m/z -value. The most important advantage from at least a single ion reflection stage within a TOF-tube is the compensation of initial energy and spatial spread of the ions at the state of extraction from the constant ion beam by the pusher [109, 110]. Briefly, the ions pushed into the TOF tube dive into the ion mirror with different depths according to their kinetic energy. Ions with higher kinetic energy stay longer within the retarding field than ions with lower energy which leads to a time-of-flight correction that tremendously increases TOF mass resolution [109]. Additionally, the ion mirror leads to focusing of the ion beam which projects different initial ion positions onto a

two-dimensional detection plane [111]. For the ion detection in TOF-MS instruments, very fast electronics are needed to reach high mass resolution. Ion packets with only slightly different m/z -values arrive in very short time intervals at the detector. Additionally, the pusher works with kHz-frequencies resulting in the recording of several thousand MS spectra per second. Typically, a time-to-digital converter (TDC) with a detector like a microchannel plate (MCP) is fast enough for this application. The TDC is basically a pulse counting device that is used to count the ion signals converted by the MCP into a measurable electronic pulse. TDCs cannot, however, determine signal intensity. Therefore, the signal intensity is gathered in TDC-detector combinations with the addition of several thousand spectra. Due to the fact that a TDC has a characteristic counting dead time in which it is unable to register another count, high ion currents lead to a saturation of TDC-detector combinations in which the signal is not proportional to the ion flux any more [109]. Within saturation, the mass peak intensity is suppressed and the centroid is shifted towards lower m/z -values. For that reason, TOF instruments with TDC usually apply mathematical dead time correction which helps to extend the dynamic range by a factor of about 10 [110]. In latest instruments, this issue is reduced by using 8-bit analog-to-digital converters (ADCs) that digitize the detector signal with a rate of up to 4 GHz onto a 0-255 numeric scale (in contrast to 0-1 when using a TDC) [109].

TOF-MS instruments are nowadays usually combined with quadrupole mass analyzers to perform tandem MS experiments that combine collision induced dissociation (CID) of ions with HRMS detection of the produced fragments for substance identification and structural investigations. The resulting hybrid quadrupole time-of-flight MS (Q-TOF) evolved to the commercially most successful hybrid instrument [109]. Quadrupoles usually consist of four square mounted cylindrical rods which function as electrodes. The rods of the quadrupole are operated with a direct and an alternating current (DC and AC) at the same time directing ions which are entering the quadrupole parallel to its rods in the center into a spiral trajectory. Only ions with a certain m/z -value are able to pass the quadrupole for a given ratio of AC/DC voltages [109]. Besides, quadrupoles can be operated with AC-only which turns them into radio frequency (r.f.) ion optics that transfer the whole ion beam. The same principle is exploited with r.f.-hexa- and octapoles which are commonly used for ion transport and collision cells. Quadrupoles and Multipoles in r.f.-only mode allow ion transfer within the instruments at relatively high pressures between 10^{-3} to 10^{-2} mbar with high efficiency.

Fig. 10 illustrates a typical setup of a Q-TOF MS. At the entrance of the instrument, the ion beam is focused and collisionally cooled by a multipole in r.f.-only operation. Subsequently, a quadrupole mass analyzer transfers either the whole ion beam (r.f.-only mode) or a specific m/z into a collision cell (quadrupole or multipole). The collision cell, operated with collision

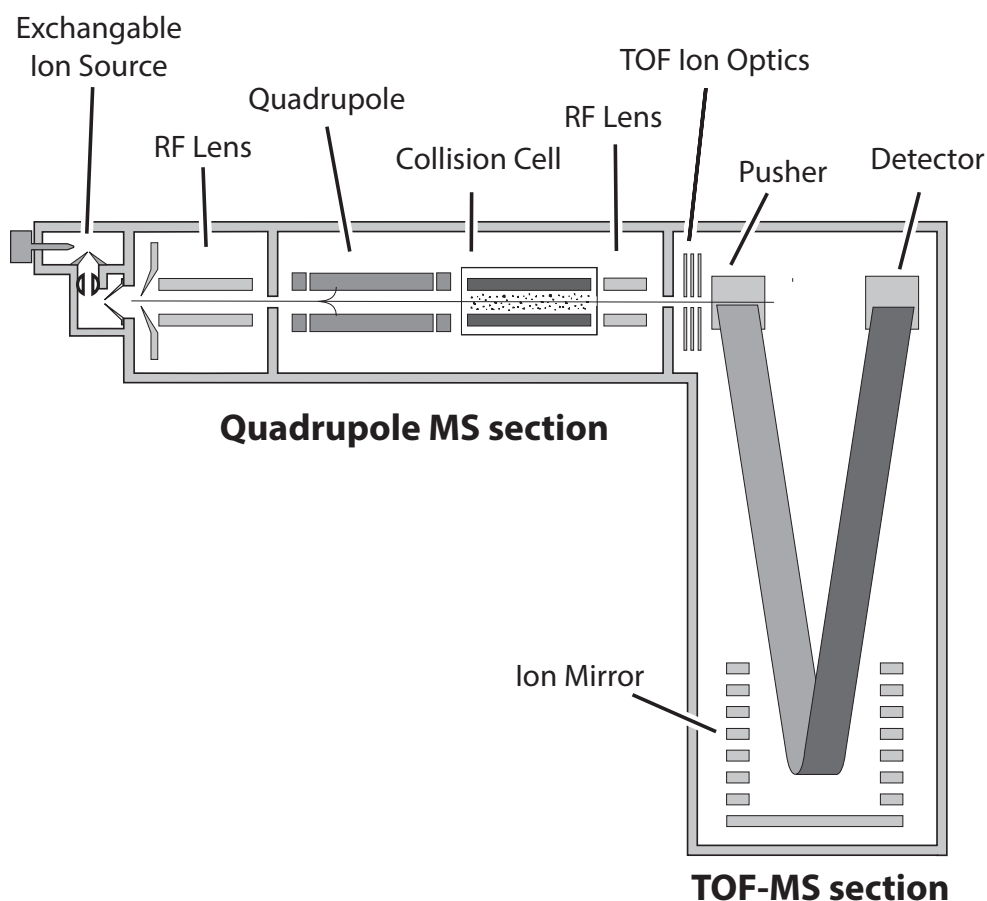


Fig. 10: Illustration of a typical internal layout of a Q-TOF mass spectrometer; ions are transferred by multipoles in r.f.-only mode; the pusher transforms the continuous ion beam into pulsed ion packets that can be measured in the field-free drift-space of the TOF tube (according to [112])

gas at low collision energies, helps to further confine the ion beam by collisional cooling which improves sensitivity and mass resolution. Additionally, with higher collision energy set, ions undergo CID within the collision cell and all generated fragments can be detected with high resolution in the TOF analyzer. Another multipole serves as transfer lens which guides the beam to the ion optics at the entrance of TOF drift space where the pusher is located. The pusher transfers ion packets into an accelerator column that raises the kinetic energy of the ions to several keV before they enter the field-free drift space [110]. After one stage of reflection the ions arrive at the detector and the resulting electronic pulse is recognized by the electronics. There are typically three types of MS experiments that are carried out with Q-TOF instruments:

- **TOF-MS mode:** The quadrupole MS is set to ion transmission (r.f.-only), the collision energy is kept low to avoid ion fractionation and molecular ions are detected in the TOF-MS. In order to increase the quadrupole transmission window, the r.f.-voltage is

often modulated (stepped or ramped) during acquisition. Nevertheless, extensive modulation leads to decreased signal intensity [110]. This mode is suitable for standard injections in method development or non-target analysis. For quantification, however, ion fractionation may help to reduce background.

- **Product ion scan:** A precursor ion is filtered by the quadrupole MS and fragmented with elevated collision energy in the collision cell. Subsequently, all resulting fragment ions are detected with the TOF-MS. Product ion spectra are useful for compound identification with MS databases as well as quantification of known compounds based on their specific fragmentation products.
- **Precursor ion scan:** The quadrupole MS is operated like in TOF-MS mode (wide mass transmission window, r.f.-only) and fractionation of all incoming ions is yielded with elevated collision energy while the TOF-MS spectra are under surveillance for specific ion fragments. If ion fragments of interest are found, the collision energy is lowered to identify the corresponding precursor ion. The identification of phospho- and glycopeptides, peptides, proteins and lipids are typical applications for this type of MS experiment [110].

In principle, it is possible to transfer common MS/MS experiments known from triple quadrupole instruments (instruments in which a quadrupole is used instead of a TOF analyzer) to Q-TOF instruments. There are, however, differences in detection sensitivity and analytical possibilities that evolve from the capabilities of the TOF analyzer. In product ion scan mode, the TOF analyzer can detect fragmentation products over a wide m/z -range with high mass resolution without negative influence on sensitivity. Therefore, especially compound identification processes are beneficial on Q-TOF instruments. In contrast, triple quadrupole instruments have to scan the analyzing quadrupole with the sensitivity being dependent on the monitored mass window as well as on the desired mass resolution. For quantification purposes, however, these instruments benefit from monitoring only selected fragment ions that have previously been chosen for analysis. This mode of operation called multiple reaction monitoring (MRM), increases the sensitivity of triple quadrupole instruments for quantification noticeably above the one achieved by Q-TOF instruments [110]. Additionally, taking into account that the dynamic range of detection of Q-TOF instruments may be limited due to issues that evolve from the detector-electronics assembly (as previously discussed), this type of MS should not be applied for rather simple quantification experiments in the first place. Still, the versatility of these hybrid MS instruments regarding qualitative and quantitative analysis helps to compensate shortcomings not at last due to economic reasons.

2.3. Electrospray ionization

The coupling of liquid chromatography with mass spectrometry requires a technique that continuously transforms a liquid flow from atmospheric pressure into a steady ion beam in vacuum. Ionization techniques achieving this transfer are called atmospheric pressure ionization techniques (API). Electrospray ionization (ESI) as one representative for API-techniques evolved from a development process that involved different approaches for solvent evaporation, ionization and transfer from atmospheric pressure to high vacuum [109]. The final success and broad application of ESI is based on its capability for the soft ionization of mid-polar to ionic organics over a m/z -range up to 3000 Da in routine and several 10,000 Da in special cases [109]. API techniques require a high-performance differential pumped vacuum system at the inlet of the mass spectrometer. Over the years, advanced engineered designs have become commercially available increasing robustness, ion transmission, ionization softness and pumping efficiency. Nevertheless, shared properties of all ESI sources are the electrostatic nebulizing of the liquid flow at atmospheric pressure, a heating system for solvent vaporization, supersonic expansion within the first pumping stage and high-performance differential pumping systems [109].

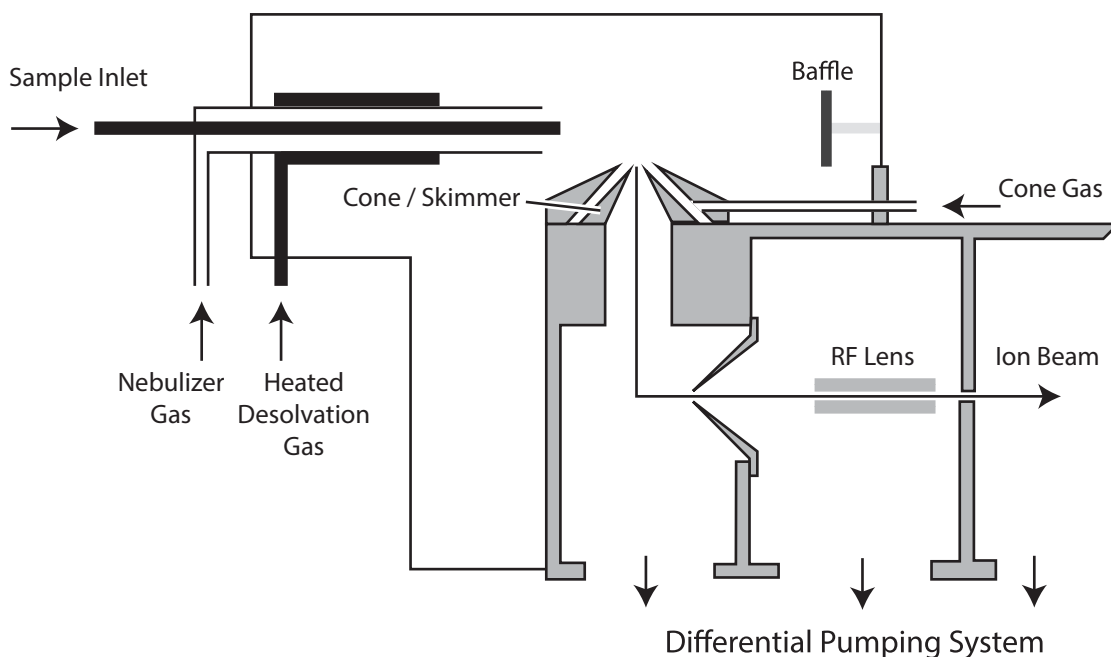


Fig. 11: Illustration of a electro spray ion source with Z-spray layout; the spray is pneumatically stabilized allowing regular liquid flows between $4\text{-}200\ \mu\text{L min}^{-1}$ and up to $1\ \text{mL min}^{-1}$ in megaflow operation; differential pumping achieved with rotary and turbomolecular pumps (according to [112])

Fig. 11 illustrates a typical layout of a standard-sized ESI interface. The liquid flow from either LC or syringe pump is connected via a capillary tubing to a stainless steel capillary. When the

liquid reaches the end of the capillary, it forms an electrostatic spray due to a voltage of 3-4 kV between the capillary and the entrance of the mass spectrometer. Additionally, the nebulization is further assisted and pneumatically stabilized by a stream of nebulizer gas (usually nitrogen) that increases analyte flow and reduces surface tension of the solvents used [109]. The evaporation of solvent is further supported by a heated stream of nitrogen (desolvation gas) which is introduced as curtain around the electrospray. Typically, the spray is not directed towards the entrance of the mass spectrometer but in 45 or 90 degree angle. A fraction of the free ions is transferred by a cone shaped electrode (skimmer) into the mass spectrometer where the ion beam is focused by ion optics into the quadrupole mass analyzer. At the sample cone, a sheath gas in reverse flow orientation can be introduced for protection against contamination as well as to reduce ion cluster formation. Differential pumping is carried out by using a rotary pump in first stage and several turbomolecular pumps to establish high vacuum.

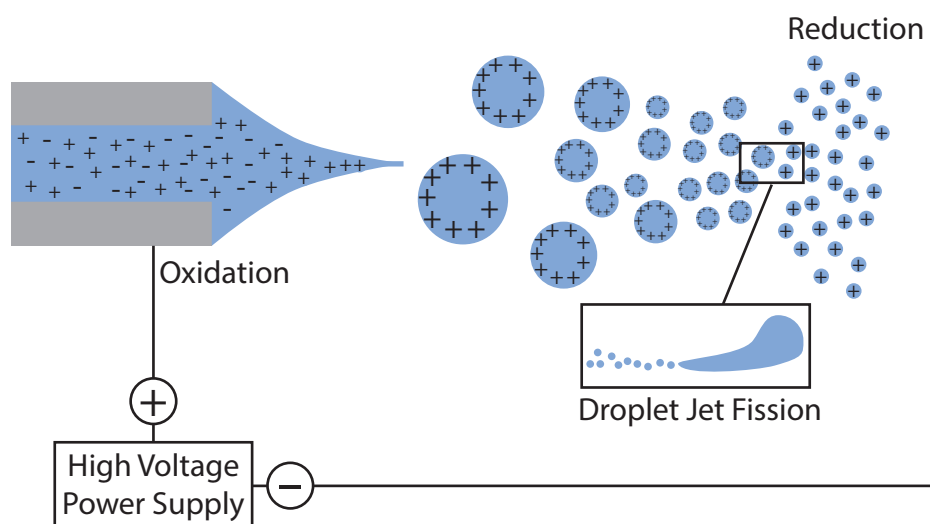


Fig. 12: Schematic representation of electrospray formation within an ESI interface; the high voltage leads to a deformation of the ionic liquid into a Taylor cone; the resulting droplets shrink due to solvent evaporation and finally release free ions

ESI operation requires that analyte ions are already abundant within the liquid flow as the interface does not actively produce ions [109]. The electrospray at the tip of the ESI interface needle is formed due to the electrostatic forces being higher than the surface tension. A fine liquid jet is formed in the direction of the counter electrode. This liquid jet, however, is not stable but collapses forming many small droplets that drift apart due to the Coulomb repulsion. Further solvent evaporation of the small droplets leads to an increase of charge until the Rayleigh-Limit is reached [113]. Originally, it was thought that droplet fission occurs above this limit in the manner of Coulomb explosions [109]. More recent investigations, however, introduced the concept of droplet jet fission which describes a deformation of the liquid droplets due to their movement

and the release of smaller microdroplets that carry high amounts of charge (see Fig. 12). There are different models with which the complete desolvation of ions may be explained [114, 115]. Moreover, the developed models for the release of free ions are still under discussion [116]. Ions from large molecules may be released according to the charged residue model (CRM). The model assumes that after a droplet fission cascade, a droplet remains that only contains one analyte ion. Remaining charges within such a droplet like protons are transferred to the analyte ion upon total desolvation. Therefore, the CRM more likely explains the ionization of macromolecules like proteins that can carry multiple charges. The abundance of only one charge within the residual solvent droplet appears obviously unlikely and thus the formation of singly charged molecular ions of small molecules. Nevertheless, the CRM does not imply that the formation of singly charged molecular ions is not possible [109]. The ion evaporation model (IEM) explains the formation of free ions by ion evaporation from the surface of very small microdroplets (<10 nm) [116]. The model is supported by the observation that the number of charges of a molecule is proportional to its proportion on the surface of the microdroplet. Consequently, analyte molecules emitted from smaller microdroplets with higher charge density carry more charges than molecules from larger droplets with lower charge density. Additionally, planar molecules carry in mean more charges than small compact molecules [109]. Independent whether the CRM and IEM describe the true mechanism of ion formation in ESI, CRM seems to be more suitable for large molecules whereas IEM seems to fit better for small molecules [109].

2.4. Solid-phase extraction

For the sensitive detection of analytes in environmental as well as in biological matrices, a suitable sample cleanup procedure is mandatory for the removal of distracting matrix compounds from the original sample. Although LC and MS exhibit already powerful capabilities for compound separation from analytical background, sample cleanup procedures remain mandatory up until now for most matrices to yield highly sensitive and reliable detection. Solid-phase extraction (SPE) became popular during the 1990s and found broad application mainly in the analysis of aqueous environmental and biological samples [117]. Especially for the extraction of medium to highly polar substances from aqueous solutions, SPE was found to be more suitable than liquid-liquid extraction (LLE) with organic solvents. Additionally, it was possible to replace LLE for some applications by SPE which is beneficial for the reduction of organic solvent consumption in analysis due to environmental and economic reasons [117].

Typical SPE-applications are carried out with disposable cartridges (see Fig. 13) filled with dedicated stationary phases that are selected according to the analytical task. Similar to chromato-



Fig. 13: Different types of disposable cartridges for solid-phase extraction (SPE) (Picture: Johannes Deyerling)

graphic applications, samples are percolated through a usually pre-conditioned SPE-cartridge. The stationary phase for SPE is chosen for either the trapping of matrix compounds onto the cartridge and the free elution of the target compounds or the retention of analytes in the cartridge and the passage of the analyte matrix. Consequently, the analytes can be found in the eluate in the former case or on the SPE cartridge in the latter case which requires an additional selective elution step. In most SPE applications, the sorbent is designed to selectively enrich the target compounds which makes it possible to include a further washing step before the selective elution of analytes. The SPE-cleanup can be carried out offline as sample pre-treatment prior to analysis on an LC-instrument or online in direct connection to a chromatographic system which is attractive for the routine analysis of a large number of samples [117].

The working principle of SPE is similar to chromatography which has already been described in section 2.1. Indeed, many SPE applications involve the principles of RPC for enrichment of analytes from aqueous samples [117]. SPE can thereby be seen as frontal chromatography during the enrichment step of compounds from an aqueous solution as well as during an optional washing step. In contrast, displacement chromatography is carried out during selective compound elution [117]. Due to the short column length in the SPE-cartridge, the “chromatographic column” only exhibits a very small plate number, thus the cartridges are usually not suitable for either compound separation nor fractionation. However, with the goal of SPE being the separation of target compounds from the sample matrix, the limited plate number is not a quality criteria. On the contrary, recent development of SPE stationary phases tries to yield a high retention of a whole spectrum of analytes, increasing the versatility of the corresponding phase. In that context, polar modified polystyrene divinylbenzene (PS-DVB) evolved as a

promising SPE sorbent for the reliable retention of medium to polar analytes that can be either neutral or ionic. Sorbent beds like PS-DVB may not reach the requirements for application in chromatography columns but SPE can benefit from their special selectivities [117].

The most important characteristics for the application of SPE in environmental analysis is the breakthrough volume of analytes. This parameter determines the maximum possible aqueous sample size that can be used and consequently the maximum achievable enrichment factor. Therefore, the sorbent selectivity as well as the size of the SPE cartridge have to be adjusted to reach the requirements of the analytical task. Method development to determine a suitable SPE protocol, however, has to be carried out in many cases by a time consuming empirical process. Nevertheless, information on the chemical and physical properties like polarity of the target compounds assists with the preselection of promising SPE chemistries as well as with the identification of starting points for the development of an elution protocol. Within certain boundaries, the retention on hydrophobic SPE cartridges may be estimated from the logP-value similar like described in section 2.1.2. Still, the retention estimation can only yield rough hints and cannot replace empirical method optimization completely [117].

2.5. Analysis of catecholamines with LC-MS

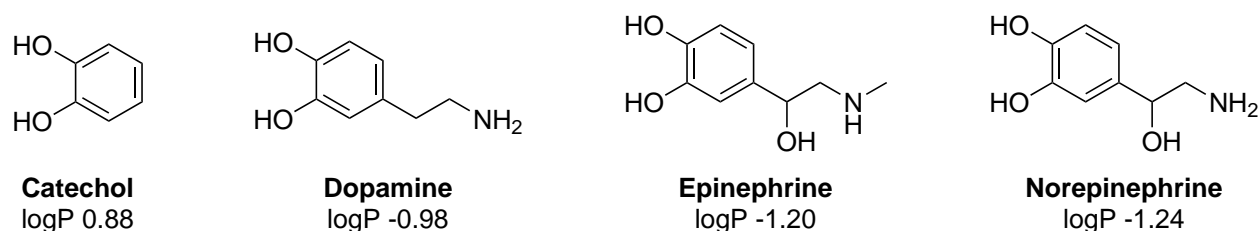


Fig. 14: Molecular structures of catechol and the catecholamines dopamine, epinephrine and norepinephrine (logP-values from PHYSPROP database [118])

Catecholamines are essential neurotransmitters and hormones in mammals. Chemically, they are classified as monoamines and share the catechol as a structural motive. Their most important representatives are dopamine, epinephrine and norepinephrine (see Fig. 14). They act as neuro-modulators in the central nervous system and are involved in the stress response from psychological and environmental stressors. Catecholamines prepare for physical activity like the fight-or-flight response increasing heart rate, blood pressure and blood glucose levels [1]. Therefore, they act as important biomarkers for neuroendocrine and cardiovascular disorder, have been linked to schizophrenia and Parkinson's disease and are found in larger amounts in patients with catecholamine-synthesizing tumours with life-threatening consequences. [119, 120, 121]. The analysis of catecholamines in biological matrices is predominantly carried out using RPC

in combination with an electrochemical detector [119, 122, 123]. Some methods also involve fluorescence detection [119, 124]. Nevertheless, the application of MS detection for the determination of catecholamines is less common. In order to achieve a reasonable retention of these highly polar analytes on C-18 column chemistries, ion pair reagents are routinely employed. Many ionpair reagents, however, form involatile residues and thus are not available for ionization in ESI [123]. In recent years, the application of suitable volatile ion pair reagents or the employment of special column chemistries which achieve good retention of catecholamines made MS detection available for this group of analytes [125, 126, 127, 128].

2.6. Applications of LC-MS in the analysis of emerging organic pollutants in water

The analysis of water soluble organic residues today is usually carried out with LC coupled with an ESI interface to a MS for detection. With the universal detection capabilities of mass spectrometry, modern LC-MS analysis methods are able to cover the detection of a wide range organic residues covering besides PFCs and pharmaceutical residues also residues from personal care products and polar pesticides [58, 59, 61, 129, 130, 131, 132, 133, 134, 135]. Therefore, the targets of these water analysis methods are sometimes also referred to as organic micro-contaminants or micro-pollutants [58, 61].

Analyte enrichment in water samples is usually carried out by SPE with a suitable chemistry adjusted to the target compounds [129, 130]. Depending on the sample origin, some methods also include the filtration of the water sample prior enrichment [130]. The SPE itself can be carried out manually in the laboratory or as online-SPE directly coupled to the LC-MS system. In the latter case, sample analysis nearly becomes fully automatized with optional sample filtration and the addition of internal standards being the only manual step within the whole analytical process [61].

Analytical methods for the detection of organic micro-pollutants in water typically reach a limit of quantification (LOQ) in the $\mu\text{g L}^{-1}$ or higher ng L^{-1} -range. *Wode et al.* presented a LC-MS method for the detection of 72 micropollutants in water involving online-SPE with 1 mL sample size and reached a LOQ between 10 and 380 ng L^{-1} in drinking water, surface water and wastewater effluent [61]. *Nödler et al.* reached LOQs between 1.2 and 160 ng L^{-1} by enriching 500 mL of water sample (river water or seawater) by manual offline SPE prior instrumental LC-MS analysis [58]. *Vanderford et al.* developed a method for the quantification of pharmaceutical residues in treated wastewater and surface water and yielded LOQs between 0.25 and 1 ng L^{-1} by SPE enrichment of 500 mL in an automated offline SPE system [59]. For the determination of PFCs in seawater, *Theobald et al.* established a particular sensitive method involving the enrichment of 9 L water sample on a SPE cartridge with a custom designed auto-

matic sampling system. In combination with LC-MS detection, LOQs between 3 and 41 pg L^{-1} were achieved [136, 137].

The numerous developed detection and quantification methods differ essentially in the optimization for certain water matrices and the selection of micro-pollutants [58, 59, 61, 137]. According to the analytical task, the selection of analytes and their matrix vary. There is no universal method as the total number of known micro-contaminants and their chemical properties would be too manifold for detection in a single analytical run. Besides analyte selection, quality assurance limits the total number of investigated analytes within one single method. Most LC-MS methods employ isotopically labelled standard substances which are added to the water sample prior extraction and analysis as internal standards (IS). These standard substances are used to correct the analytical result for extraction recovery and matrix effects. The artificially labeled compounds behave chemically equal to the native substances but can be discriminated by MS. Multi-residue analytical techniques require the purchase of many isotopically labeled equivalents which raises the costs of a single analysis. Alternatively, several native compounds can also be corrected with the signal of one single isotopically labeled substance with similar retention time depending on whether a certain analytical error is acceptable [61].

Although water as medium for analysis appears to exhibit a less complex matrix in comparison to soil and biological samples, the analysis of organic residues in water has to face issues due to matrix effects. With modern LC-MS instruments allowing nearly the total separation of analyte signals from background, matrix effects appear to be less present in analytic results at a first glance. Signal suppression and signal enhancement, however, routinely occur during LC-MS analysis of environmental samples caused by coeluting substances which disturb the ionization processes in the ESI interfaces but are usually not visible within the acquired mass spectra [138]. There are typically two methods for the assessment of matrix effects in LC-MS. The first is the comparison of a standard signal of a spiked extracted sample with the signal of the standards in a pure solution. Alternatively, a solution of a known compound is infused after the chromatographic column generating a constant signal which varies according to signal enhancement or suppression during an analytical injection [138]. In analytical method development, matrix effects are usually considered by the signal correction with internal standards or standard addition. *Stüber and Reemtsma* compared the results achieved with standard addition in environmental analysis of naphthalene sulfonates with external calibration and external calibration in environmental matrix. Yielding a deviation below 25 % with external calibration in environmental matrix, they suggested that for some analytical approaches, external calibration might be applicable but advised periodical reference measurements by means of standard addition in order to account for a varying matrix [139]. Another alternative for the reduction of

matrix effects in LC-MS is the reduction of flow rate and the downscaling of the LC and the ESI source. With standard-sized equipment, *Kloepfer et al.* achieved a reduction of matrix effects by 45 to 60 % by post-column flow splitting, corresponding to a reduction of the analytical flow from 200-500 $\mu\text{L min}^{-1}$ down to 20-100 $\mu\text{L min}^{-1}$ [140].

A further reduction of chromatography scale leads to micro and nano-chromatography which requires special chromatographic equipment and ESI sources. Nano-LC-MS is commonly applied in the analysis of complex protein mixtures and biological samples in proteomics approaches [141, 142, 143]. In general, highest sensitivity, peak capacity and low sample consumption are the result of the instrumental downscaling process. However, these achievements are at the expense of injection runtime (up to several hours per injection) and instrument robustness [142, 144]. Therefore, applications of nano-LC-MS in environmental analysis are rare [145, 146]. Nevertheless, also environmental analysis could benefit from a reduction of matrix effects during analysis. *Schmidt et al.* showed that matrix effects are practically absent at flow rates below 20 nL min^{-1} . However, commercially available nano-LC systems are usually operated at 200 to 500 nL min^{-1} at which still a certain matrix effect has to be expected [147].

3. Scope of work

The main part of the presented work incorporated the development of a novel analytical method for the enrichment and determination of polar organic residues in surface water. The method development encompassed the design of a water sampling system and its application in the field, the development of a suitable laboratory cleanup as well as the establishment of a quantification method on an existing nano-UHPLC-MS instrument. Furthermore, the established method should be involved in environmental sampling of the Yangtze River near the Three Gorges Dam (China).

At first, the measurement and detection capabilities of the UHPLC-MS instrument had to be evaluated against reliability of analyte detection and quantification. Typical strengths and shortcomings of the analytical instrument had to be identified and consequences on the possibilities for the application of the instrument in the analytical method had to be evaluated. Therefore, instrumental method development for derivatized catecholamines should serve as model application for the evaluation of instrumental capabilities. Based on these findings, a chromatographic and mass spectrometric method for a selected group of polar residues partly recognized as emerging organic pollutants should be developed. The analytes should be proposed based on the identified capabilities of the UHPLC-MS instrument.

Besides targeted analysis, a combined approach including a limited non-target analysis should be developed to post-process the datasets acquired during the measurement of field data. Therefore, a workflow should be developed based on passive samplers which have been previously deployed at the small river Selke in Meisdorf (Germany) which in turn was suitable to serve as universal tool for the analysis of previously acquired samples.

In parallel, a water sampling technique had to be developed allowing the enrichment of high volumes of surface water directly at the sampling location. The generated water samples should serve for method verification as well as for environmental monitoring at the same time. High enrichment factors were found to be necessary to reduce the method detection limit in a concentration range in which residues of emerging organic pollutants are expected in water bodies like the Yangtze River with high dilution and low charge. Therefore, solid-phase extraction in a large scale was thought to meet the requirements for the analytical task. Due to commercial solid-phase extraction being only available for small sample volumes at high costs, an economic and effective alternative with self-packed sampling cartridges had to be found.

Finally, another topic of this work was the optimization of extraction and cleanup parameters for the generated samples in order to yield a sample quality that was sufficient to allow reliable analyte detection and quantification. This task entailed the determination of a suitable extraction solvent and the adjustment of SPE parameters to yield maximum analyte recovery and to minimize matrix effects.

4. Experimental part

4.1. Reagents and chemicals

Organic solvents for laboratory work (methanol, acetonitrile and acetone) were purchased in analytical grade from Promochem (Wesel, Germany). Organic solvents for UHPLC analysis and the preparation of standard solutions (methanol and acetonitrile) were obtained in UHPLC-grade (0.2 μm -filtered) from the same company. Formic acid, used as organic modifier in the mobile phase, was purchased in UHPLC-grade also from Promochem. Ultrapure water was generated fresh on the day of use with a water purification system consisting of a RiOs reverse osmosis unit with Progard 1 silver cartridge and a Milli-Q Gradient unit with Quantum EX Ultrapure Organex cartridge and Q-Guard 1, both from Merck Millipore (Darmstadt, Germany). Prior to use in UHPLC appliances the freshly generated ultrapure water was distilled in a subboiling distillation apparatus (Maassen GmbH, Germany) as further precautionary cleanup step, removing any particulates that may have been emitted from the ultrapure water system for prolonging the lifetime of nano-ESI emitters.

Crystalline sodium sulfate was purchased in analytical grade from Promochem (Wesel, Germany). Polymeric resins Amberlite XAD7HP and XAD16N as well as Supelpak-2 (precleaned XAD-2) were obtained from Sigma-Aldrich (Steinheim, Germany). Ammonium formate, used as organic modifier for the mobile phases, was obtained in MS grade from Sigma-Aldrich. Polypropylene solid-phase extraction cartridges packed with 500 mg polar modified polystyrene-divinylbenzene copolymer Chromabond HR-X were obtained from Macherey-Nagel (Dueren, Germany). Glass wool was also obtained from Sigma-Aldrich and heat-treated at 400 °C.

Acetaminophen (paracetamol), atenolol, diclofenac sodium, ibuprofen, naproxen and sulfamethoxazole were purchased as pure solid native standards from Dr. Ehrenstorfer (Augsburg, Germany, now part of the LGC group, Teddington, UK), atrazine, simazin and linuron were obtained from Riedl-de Haën (Seelze, Germany) and carbamazepine from Sigma-Aldrich (Steinheim, Germany). Most isotopically labeled equivalents were obtained dissolved in 1 mL of organic solvent: acetaminophen-D4 (100 ng μL^{-1} in methanol, Cerilliant, Sigma-Aldrich), Caffeine- $^{13}\text{C}_3$ (1000 ng μL^{-1} in methanol, Sigma-Aldrich) sulfamethoxazole-D4 (100 ng μL^{-1} in acetonitrile, Dr. Ehrenstorfer), atrazine-D5 (100 ng μL^{-1} in acetone, Dr. Ehrenstorfer), simazin-D5 (100 ng μL^{-1} in acetone Dr. Ehrenstorfer) and linuron-D6 (100 ng μL^{-1} in acetone, Dr. Ehrenstorfer). Upon first usage, the liquid standard solutions were transferred into CERTAN capillary bottles (Supelco, Sigma-Aldrich, Steinheim, Germany). Diclofenac-D4, naproxen-D3 and carbamazepine-D10 were obtained as solid substances from Santa Cruz Biotechnology (Dallas, USA), ibuprofen-D3 was purchased solid from Sigma-Aldrich. The standard sub-

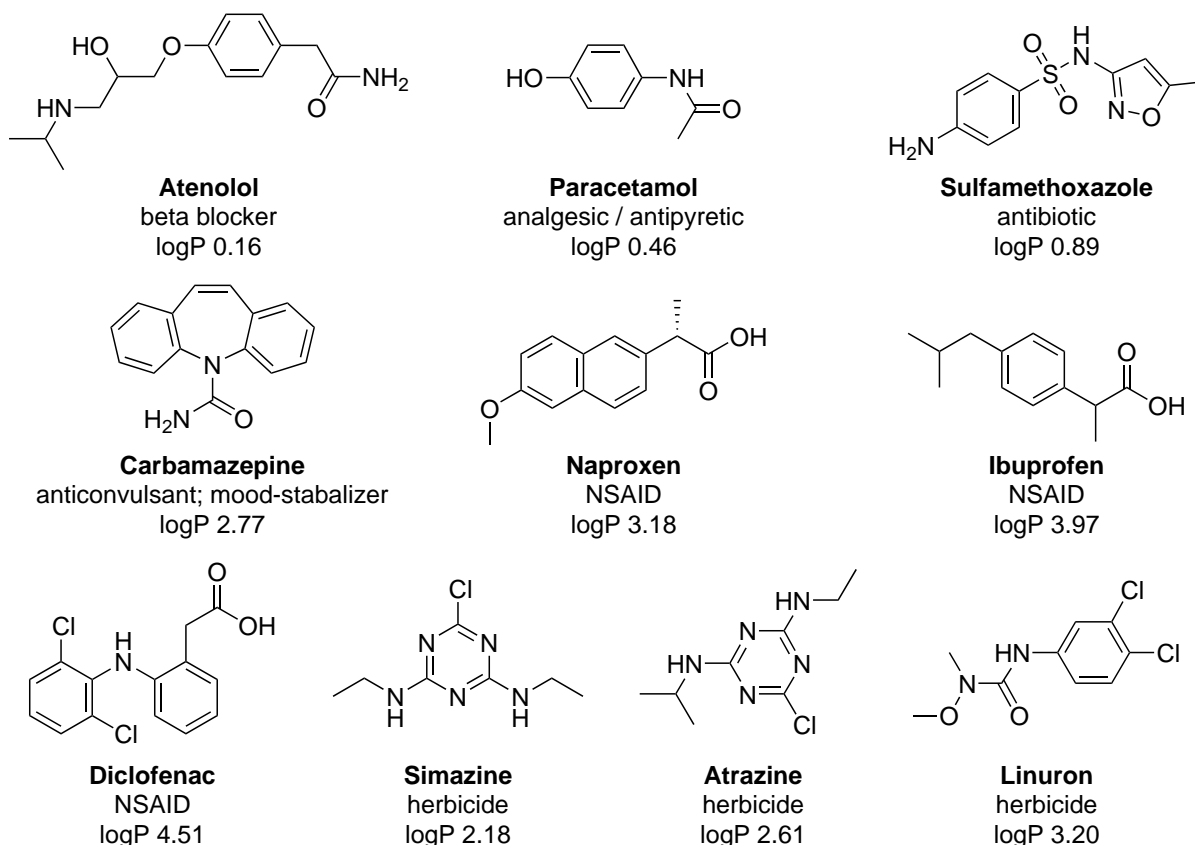


Fig. 15: Molecular structures of the investigated pharmaceutical residues and pesticides, their application and their log *P*-value (experimental values from PHYSPROP database [118]); NSAID = Nonsteroidal anti-inflammatory drug

stances and solutions were stored either at 4 °C in the fridge or at -20 °C in the freezer according to the advice of the manufacturers.

For the analysis of perfluorinated compounds (PFCs) standards were obtained from Wellington Laboratories (Guelph, Canada). A standard mixture containing native perfluoroalkylcarboxylic acids (PFCAs) and native perfluoroalkylsulfonates (PFASs) was used for tuning and calibration purposes. Table 4.1 lists the PFCs contained by the mixture at a concentration of 2 ng μL^{-1} in methanol. A mass labeled PFC-mixture with a concentration of 2 ng μL^{-1} in methanol, that contained all labeled PFCs listed in Table 4.1, was used as internal standard for PFC-analysis. The PFC standard solutions were transferred to CERTAN capillary bottles upon first usage and stored at 4 °C in the fridge.

4.2. Preparation of standard stock solutions

For the preparation of stock solutions from solid substances, a precision balance SBC 21 from SCALTEC Instruments GmbH (Göttingen, Germany) was used. Individual standard solutions for tuning purposes were generated by solving 1 mg of each compound in a volume of 10 mL

Table 4.1: List of PFCs contained within the native standard mixture and the mass labelled mixture

Compound	Acronym	Mass labelled standard
Perfluorobutanoic acid	PFBA	Perfluoro-[1,2,3,4- ¹³ C ₄]butanoic acid
Perfluoropentanoic acid	PFPeA	
Perfluorohexanoic acid	PFHxA	Perfluoro-[1,2- ¹³ C ₂]hexanoic acid
Perfluoroheptanoic acid	PFHpA	
Perfluorooctanoic acid	PFOA	Perfluoro-[1,2,3,4- ¹³ C ₄]octanoic acid
Perfluorononanoic acid	PFNA	Perfluoro-[1,2,3,4,5- ¹³ C ₅]nonanoic acid
Perfluorodecanoic acid	PFDA	Perfluoro-[1,2- ¹³ C ₂]decanoic acid
Perfluoroundecanoic acid	PFUDA	Perfluoro-[1,2- ¹³ C ₂]undecanoic acid
Perfluorododecanoic acid	PFDoA	Perfluoro-[1,2- ¹³ C ₂]dodecanoic acid
Perfluorotridecanoic acid	PFTTrDA	
Perfluorotetradecanoic acid	PFTeDA	
Perfluorohexadecanoic acid	PFHxDA	
Perfluorooctadecanoic acid	PFODA	
Potassium perfluoro-1-butanesulfonate	PFBS	Sodium perfluoro-1- hexane[¹⁸ O ₂]sulfonate
Sodium perfluoro-1-hexanesulfonate	PFHxS	
Sodium perfluoro-1-octanesulfonate	PFOS	Sodium perfluoro-1- [1,2,3,4- ¹³ C ₄]octanesulfonate
Sodium perfluoro-1-decanesulfonate	PFDS	

acetonitrile yielding a concentration of 100 ng μL^{-1} . A native stock solution for calibration purposes was prepared by solving 10 mg of each standard substance into a volume of 100 mL using a volumetric flask. Consequently, each compound in the multi-analyte stock solution had a concentration of 100 ng μL^{-1} . All prepared stock solutions were kept in the dark at 4 °C in a fridge. Prior to use, stock solutions were equilibrated to room temperature for at least 30 minutes.

The solid mass labelled standards carbamazepine-D10, diclofenac-D4 and naproxen-D3 which have been delivered in aliquots of 1 mg were individually dissolved in methanol and quantitatively transferred to a 10 mL volumetric flask yielding a standard concentration of 100 ng μL^{-1} . A stock solution of ibuprofen-D3 (shipped as 50 mg aliquot) was prepared analog to the preparation of the native stock solution, solving 10 mg in 100 mL acetonitrile using a volumetric flask yielding a final concentration of 100 ng μL^{-1} .

4.3. Analytical instrumentation

4.3.1. Liquid chromatography system

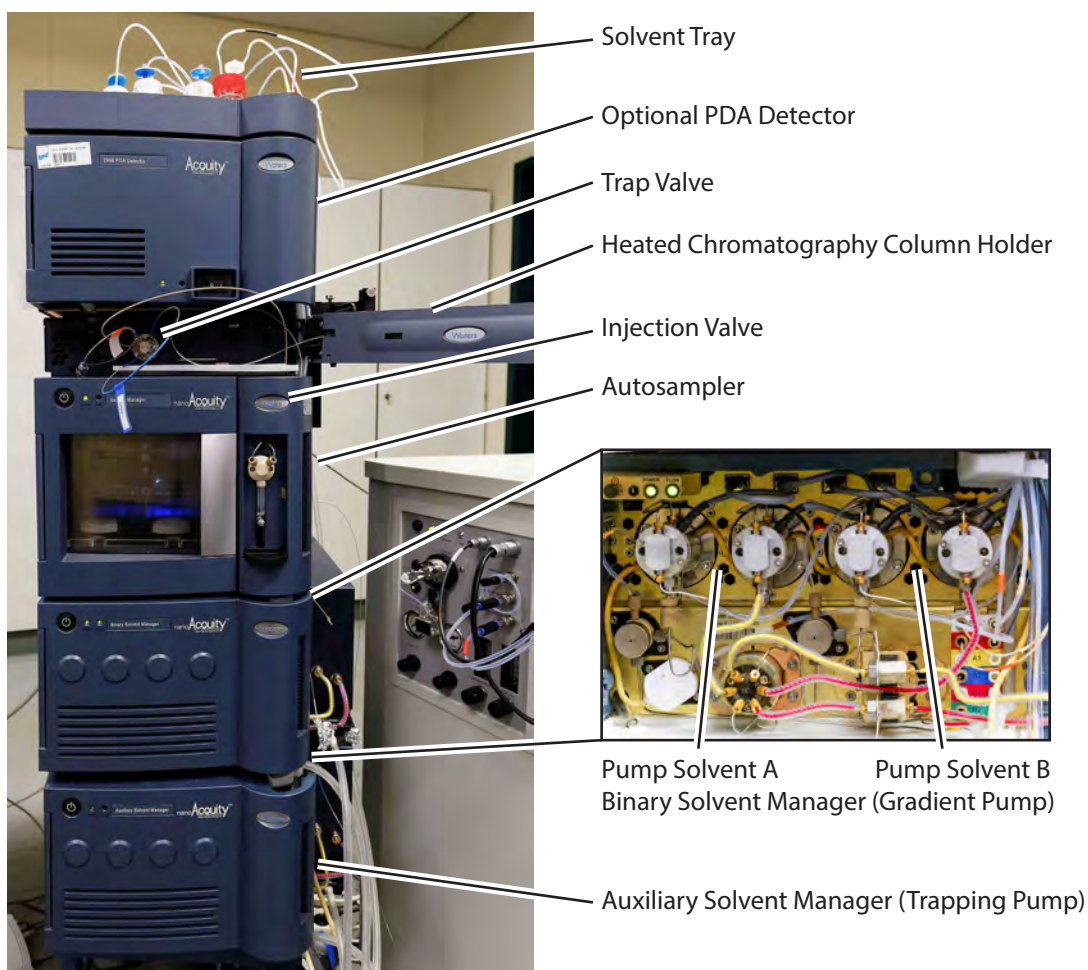


Fig. 16: Ultra high-performance liquid chromatography system Waters nanoAcquity UPLC (Picture: Johannes Deyerling)

Compound separation was carried out on a nanoAcquity UHPLC system (Waters Corporation, Milford, USA) shown in Fig. 16. The liquid chromatography system uses a binary gradient pump (binary solvent manager, BSM) which is designed to supply precise analytical gradients (with aqueous and organic solvents) without flow-splitting between $0.20 - 5.00 \mu\text{L min}^{-1}$. Therefore, it is possible to carry out separations in nano- and micro-scale. The gradient pump, transfer tubes and capillary separation columns can withstand pressures of up to 10,000 psi (690 bar) which is necessary for UHPLC separations. Additionally, a pump with two separate solvent lines (auxiliary solvent manager, ASM) and a pressure rating up to 5000 psi (345 bar) is available to supply solvent flow for sample preconcentration on a trapping-column and lock-spray applications. Both pumps need additional solvent supply (seal wash solvent, usually water

with up to 10 % acetonitrile) for washing the pump seals providing the removal of precipitates and lubrication. Injections are carried out with an autosampler (sample manager, SM) featuring a conditioned sample compartment, a sample loop of 2 or 5 μL volume and an up to 60 $^{\circ}\text{C}$ heatable column holder. The autosampler is capable of injecting full loop volumes as well as variable volumes between 10 and 90 % of the installed sample loop volume. After each injection, the autosampler needle is washed with strong wash solvent (usually pure acetonitrile, default consumption 300 μL per injection) and subsequently with weak wash solvent (usually highly aqueous, default consumption 900 μL per injection). The weak wash solvent is also used during partial loop injections to fill the remaining loop volume and has therefore to be adjusted to the starting gradient of the separation.

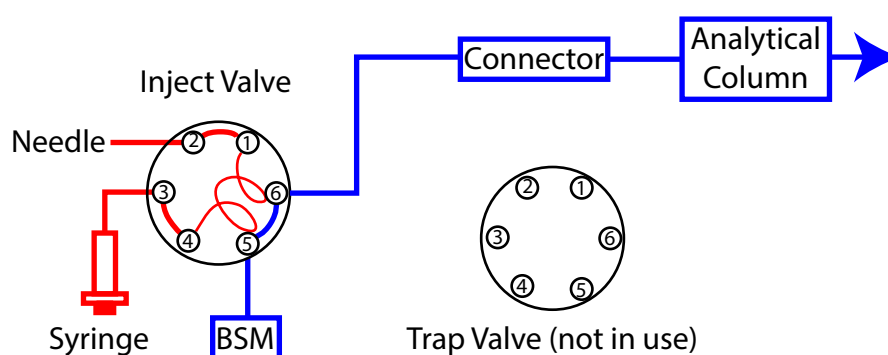


Fig. 17: Fluidic configuration for direct injection; the illustrated injection valve state fits compound elution or loading of the sample loop

The UHPLC-system can be operated with capillary analytical columns (column bed in fused silica capillary, 75 to 150 μm i. d.) or micro-scale analytical columns (column bed in stainless steel housing, 300 μm i. d.). Capillary column chromatography, also referred to as nano-scale liquid chromatography, is carried out with flow rates between 0.20 and 1.20 $\mu\text{L min}^{-1}$ whereas micro-scale LC is usually operated between 4.00 and 5.00 $\mu\text{L min}^{-1}$. During the presented study, two column dimensions in nano-scale (0.75 μm i. d. x 150 mm) and micro-scale (300 μm i. d. x 150 mm) were used, both with the same C-18 column chemistry (HSS-T3, 1.8 μm particle size, Waters) specifically suitable for a reasonable retention of highly polar substances. The nano-scale column was operated at a flow rate between 0.25 and 0.30 $\mu\text{L min}^{-1}$ whereas the micro-scale column was run at 4.00 $\mu\text{L min}^{-1}$.

The LC system was used with two different fluidic configurations. In direct injection configuration (DI), the system is operated with the BSM as single pump and only the inject valve is occupied (see Fig. 17). Sample injection in this configuration is carried out by switching the inject valve from the state illustrated in Fig. 17 to connect ports 4/5 and 1/6, respectively. Subse-

quently, the sample is flushed onto the analytical column with the analytical gradient. To avoid excessive system volume during analysis, the inject valve is switched back after the flushing of the sample loop is thought to be finished, disconnecting the loop from the fluidic path. This configuration, however, results in long sample loading times for nano-scale separations (e. g. 8 min with 2 μL -loop at 0.25 $\mu\text{L min}^{-1}$).

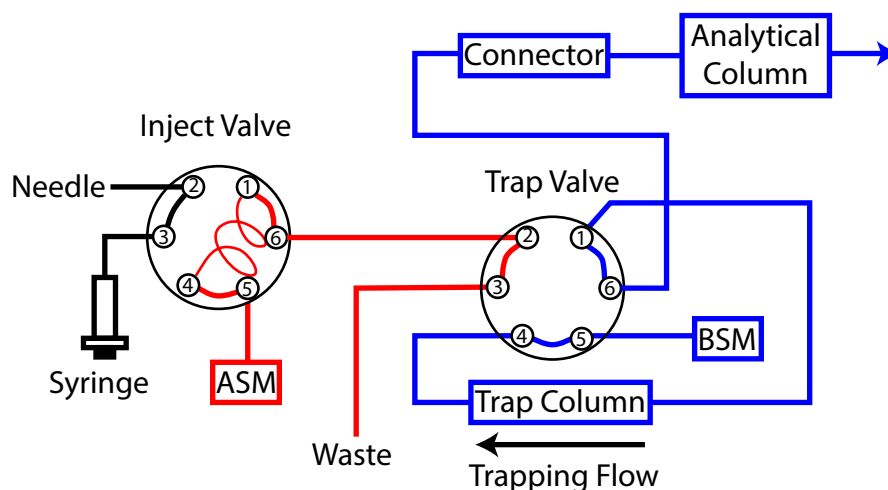


Fig. 18: Fluidic configuration for dual-pump trapping with reverse flushing of the trap column: the indicated valve state fits for elution of pre-concentrated compounds from the trap column to the analytical column

Alternatively, the LC system was operated in dual-pump trapping configuration (DTP). Therefore, the sample is pre-concentrated and pre-cleaned on a separate trap column from which the sample is subsequently eluted onto the analytical column for separation (see Fig. 18). During the time of the study, only a single C-18 trap column dimension and chemistry was commercially available (Symmetry C-18, 180 μm i. d. x 20 mm, 5 μm particle size, Waters). Using DPT configuration, the ASM delivers an isocratic trapping flow usually with a flow rate between 4 and 5 $\mu\text{L min}^{-1}$ thus clearly reducing the sample loading time in nano-scale operation. During trapping, the BSM continuously flushes the (capillary) analytical column with mobile phase. By switching the trap valve to the state illustrated in Fig. 18, the BSM elutes the pre-concentrated sample onto the analytical column for separation. Whether the sample is forward or reverse flushed from the trap column can be decided by inversion of the connection on ports 1 and 4 on the trap valve.

4.3.2. Mass spectrometric detection system

The UHPLC-system was coupled to a hybrid quadrupole time-of-flight mass spectrometer Q-TOF2 (Waters-Micromass, Manchester, UK) for the detection of analytes. The internal setup and the basic working principle of the MS have already been explained in section 2.2. The

MS was operated in TOF-MS mode for tuning, method development and non-target analysis whereas the product ion scan mode was used for background reduction during quantification and further compound identification in non-target runs.

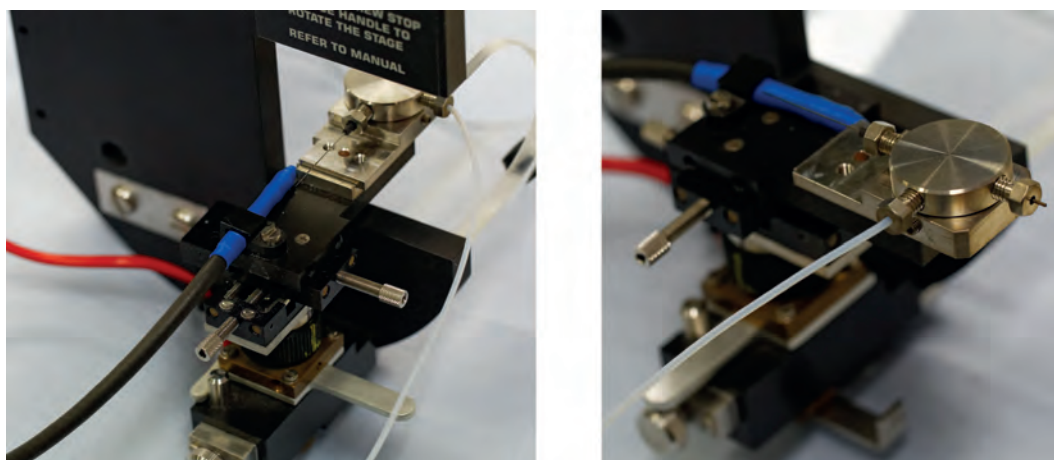


Fig. 19: Picture of the nano-electrospray interface (dismounted) with three axis manipulator in operating position (left) and service position (right) (Picture: Johannes Deyerling)

The MS instrument can be equipped with two different ESI sources in Z-spray configuration applicable for different flow-ranges. Micro-scale separations with a flow rate between 4 and 5 $\mu\text{L min}^{-1}$ require the standard ESI interface using pneumatic stabilization as illustrated in Fig. 11. Ion beam stabilization at an analytical flow rate of 4 $\mu\text{L min}^{-1}$ was achieved with a capillary voltage of 2.5 kV, a desolvation gas flow of 200 L h^{-1} heated to 120 $^{\circ}\text{C}$, a cone gas flow of 50 L h^{-1} and a slightly opened nebulizer flow. Nano-scale separations require a special nano-ESI source which consists of a precise three-axis manipulator (see Fig. 19) for the placement of the emitter position towards the sample cone of the MS. Additionally, the interface features an integrated microscope for visual control of the nano-ESI operation. The microscope picture is monitored using a microscope camera (Moticam 1000, 1.3 Megapixel, Xiamen, China) attached to the control PC of the LC-MS instrument. A grommet at the bottom of the nano-ESI interface allows the introduction of a microscope light source (KL 1500 LCD, Schott, Mainz, Germany) to increase the visibility of the nanospray. Fused silica emitters with distal conductive coating, 20 μm i. d. tapered towards 10 μm i. d. at the tip and 7 cm length (PicoTip FS360-20-10D, New Objective, Woburn, USA) were cut at the distal end with a capillary column cutter with rotating diamond blade (Hewlett-Packard, Palo Alto, USA) and connected to the outlet of the capillary column with a zero dead volume connector (PicoClear, New Objective). The special capillary connector is clear in design and allows leak tight connections by compression of an elastomer core. Alternatively, a MicroTight zero dead volume connector (IDEX Health & Science, Oak Harbor, USA) was applied. For the investigation of possible

leakages of the micro-fluidic connections, a magnification lens was available (Lenscope Magnifier, Bausch & Lomb, Rochester, USA). An ion beam was achieved at a capillary voltage around 1.8 kV with either no further pneumatic stabilization or with a nanoflow-gas adjusted at around 7 psi (0.50 bar). New and used emitters were also investigated by light microscopy (DM IRBE, Leica Microsystems, Wetzlar, Germany).

The mass calibration of the MS was carried out predominantly by direct infusion of 0.1 % phosphoric acid in 50:50 acetonitrile:water (v:v) with a syringe pump (Pump 11, Harvard Apparatus, Holliston, USA) at a flow rate of 4 $\mu\text{L min}^{-1}$ with the standard ESI source. The nano-ESI source was found inapplicable for the connection to the syringe pump resulting in instable spray formation and short emitter lifetime. Therefore, MS calibrations during nano-ESI operation were carried out by remounting the standard ESI source for infusion of the calibration solution. During method development, weekly MS calibrations were sufficient for the identification of the known target compounds. Sufficiently high mass accuracy for the analysis of environmental samples was achieved by repeating the MS calibration procedure on a daily basis.

4.4. Experimental parameters for instrumental measurement

Gradient elution required the preparation of an aqueous and an organic mobile phase which are referred to as solvent A and B, respectively. For work with positive ionization, 0.1 % formic acid in subboiled ultrapure water was used as solvent A and 0.1 % formic acid in acetonitrile was used as solvent B. Best results for negative ionization were achieved using 1 mM ammonium formate and 1 mM formic acid as organic modifiers in subboiled ultrapure water for solvent A and in acetonitrile for solvent B. In fluidic configurations with analyte trapping, a mixture of the corresponding mobile phases A:B 99:1 (v:v) was used as trapping solvent. All mobile phases were prepared in 100 mL reservoirs. The solvents were degassed prior to usage by administering vacuum to the reservoir while treating with ultrasonic for 5 min. The aqueous mobile phase A was replaced routinely on a weekly basis in order to keep the background signal low. The temperature of the chromatographic separation column was kept constant at 30 °C throughout all chromatography runs.

For the evaluation of the separation performance of the LC system as well as for the optimization of the analytical gradient, dilutions of the standard stock solutions had to be prepared. The dilutions of the stock solutions were carried out in mobile phase to assure full compatibility when injected for analysis. According to analysis in positive or negative ionization mode, the standards were diluted in the corresponding mobile phases A and B for positive or negative ionization, respectively.

Samples from laboratory test extractions as well as environmental samples had to be reconsti-

tuted in a corresponding mixture of mobile phase A and B. Therefore, a sample aliquot was evaporated under a gentle stream of nitrogen at 40 °C to near dryness in a 1.5 mL polypropylene tube (Sarstedt, Nümbrecht, Germany) and subsequently reconstituted in the desired mobile phase mixture. Prior to the transfer to a heat-treated snap seal sample vial with optional heat-treated 300 µL glass insert (both from Sigma-Aldrich, Steinheim, Germany), samples were centrifuged for 30 min at 4 °C at 14,000 x g with an ultracentrifuge (Heraeus Multifuge 3SR Plus, Thermo-Fisher, Boston, USA) to avoid any introduction of particles into the chromatography system.

4.5. Instrument calibration

Dilutions of the standard stock solutions had to be prepared to investigate the linearity of the system response and to calibrate the system for quantification experiments. In general, calibration standard dilutions were prepared separately for positive and negative ionization as well as for the two different group of analytes - pharmaceuticals and polar pesticides as well as PFAAs. The calibration range was determined in dependence of the instrument sensitivity and injection volume for each group of analytes and ionization mode separately.

Each calibration solution contained a varying amount of native substance and a constant amount of isotopically labeled equivalent as internal standard. Thus the instrument response was normalized according to the concentration of the internal standard:

$$R_{IScorr.} = A_{native} \cdot \frac{c_{IS}}{A_{IS}} \quad (4.1)$$

where $R_{IScorr.}$ is the internal standard corrected system response, A_{native} and A_{IS} are the peak areas of the native and labeled compound, respectively, c_{IS} is the concentration of the internal standard and c_{native} is the concentration of the native compound. The processing of calibration and quantification data including peak integration, internal standard correction and linear regression was carried out in the QuanLynx module of the MS software MassLynx 4.1 (Waters Corporation, Milford, USA). Response curves plotting the IS corrected response (calculated according to equation 4.1) against the concentration of the native standard substance c_{native} were obtained by weighted linear regression with the inverse native standard concentration $1/c_{native}$ as weighting factor yielding an improved fit for low concentrations. Additionally, the linear regression calculation of the QuanLynx module was verified by processing the integrated peak data with the software OriginPro 9.1 (OriginLab, Northampton, USA).

The instrumental detection limit (IDL) was calculated based on the results from the calibration experiments. Therefore, the standard deviation of the IS corrected response of the lowest con-

centrated standard was used to estimate the peak area of a signal that could still be distinguished from zero with a probability of 99 %:

$$IDL [Area] = t_{\alpha, n-1} \cdot S_{\bar{X}} \quad (4.2)$$

where $t_{\alpha, n-1}$ is the tabular value from the Student's t-distribution for the probability α and the given number $n-1$ of degrees of freedom given by the number of repeated injections. The IDL-area values were converted into concentration values by the corresponding calibration curves issued during instrumental calibration. The applied method for the determination of the IDL was more accurate than calculations based on the signal-to-noise ratio. This is due to the fact that HRMS, especially in combination with tandem-MS methods, achieves a background suppression of nearly 100 % resulting in a noise close to zero or irregular shaped signals which can tremendously affect the IDL-value. Moreover, the calculation of the IDL based on the instrument calibration accounted for the actual spray stability and response of the analytical instrument during calibration acquisition. If the system calibration was generated only by single injections of the calibration standards, the method described above was applied with the values of three subsequent determined instrument calibrations with single injections in order to calculate the standard deviation of at least three injections.

According to the results from method development, separate calibration standard dilutions for one single group of analytes in different solvent compositions of mobile phase A:B were necessary. The standard dilutions were generated using microliter syringes (ILS, Stützerbach, Germany) for dilution from CERTAN vials and calibrated Eppendorf pipettes (Model category Eppendorf Research, Eppendorf AG, Hamburg, Germany) of 10, 100, 200 and 1000 μL volume for all further liquid handling. The dilutions schemes were designed to guarantee maximum pipette precision by working always near the maximum volume of each pipette and avoiding the handling of volumes below 10 μL as far as possible. For full compatibility with the pipettes, all standard dilutions were carried out in 1.5 mL polypropylene tubes (Sarstedt, Nümbrecht, Germany).

4.5.1. Calibration standards for perfluorinated compounds

PFAA calibration standards for 7-point system calibration during operation with nano-scale chromatography and direct injection were prepared from 1 to 100 $\text{pg } \mu\text{L}^{-1}$ with a final volume of 50 μL . The IS was kept at a constant concentration of 80 $\text{pg } \mu\text{L}^{-1}$. The dilution scheme is listed in Table 4.2.

PFAA calibration standards during the operation of micro-scale chromatography were prepared from serial dilution starting at a 200 $\text{pg } \mu\text{L}^{-1}$ native standard solution containing 80 $\text{pg } \mu\text{L}^{-1}$ IS

Table 4.2: Dilution scheme for the preparation of PFAA standards used for calibration of the instrument in nano-scale configuration with direct injection

Standard Conc. [pg μL^{-1}]	Amount of native Standard [μL]	Conc. of native Standard [pg μL^{-1}]	Amount of IS [μL]	Conc. of IS [pg μL^{-1}]	Amount of Solvent [μL]
1	5	10	10	400	35
10	5	100	10	400	35
20	10	100	10	400	30
40	20	100	10	400	20
60	30	100	10	400	10
80	40	100	10	400	0
100	10	500	10	400	30

in a total volume of 40 μL . For serial dilution, five vials with 80 $\text{pg } \mu\text{L}^{-1}$ IS in a volume of 20 μL were prepared. Starting from the 200 $\text{pg } \mu\text{L}^{-1}$ standard, aliquots of 20 μL were transferred from one vial to another resulting in 1:2 diluted standards with native concentrations of 100, 50, 25, 12.5 and 0 $\text{pg } \mu\text{L}^{-1}$ (stopping the serial dilution at 12.5 $\text{pg } \mu\text{L}^{-1}$). This optimized dilution scheme for a six-point calibration helped to reduce the total volume of PFAA standards needed to establish system calibration.

4.5.2. Calibration standards for pharmaceuticals and polar pesticides

With the multi-analyte stock solutions being available in higher amounts and higher concentration for pharmaceuticals and polar pesticides, larger volumes for the preparation of native standard solutions in mobile phase were used that could be kept in the fridge for calibration purposes for up to one month. In order to establish a 10-point calibration, native standard dilutions in mobile phase were prepared at concentrations from 0 to 900 $\text{pg } \mu\text{L}^{-1}$ in equidistant concentration steps of 100 $\text{pg } \mu\text{L}^{-1}$. The dilutions were carried out with an intermediate dilution of the native multi-analyte stock solution with a concentration of 1 $\text{ng } \mu\text{L}^{-1}$. The final volume of each native standard solution was 1 mL.

For the preparation of the final calibration standards, 50 μL from each native standard were diluted with 50 μL IS standard solution with a concentration of 800 $\text{pg } \mu\text{L}^{-1}$ directly in a sample vial. Consequently, the final 10-point calibration consisted of standards with native concentrations from 0 to 450 $\text{pg } \mu\text{L}^{-1}$ in steps of 50 $\text{pg } \mu\text{L}^{-1}$ with a constant IS concentration of 400 $\text{pg } \mu\text{L}^{-1}$. Standard preparation for positive and negative ionization did not require a change within the dilution scheme. However, the calibration standards had to be diluted in

specific mobile phase for positive and negative ionization, respectively.

4.6. Derivatization of catecholamines

The catecholamines dopamine, epinephrine and norepinephrine were analyzed at an early stage of instrumental method development as testing compounds. In order to make catecholamines available for measurement on the employed LC-MS instrument, a derivatization of samples and standards was carried out with a commercially available kit (AccQ-Tag Ultra, Waters, Milford, USA) originally designed for amino acid analysis. Within the derivatization kit, the active ingredient 6-aminoquinolyl-N-hydroxysuccinimidyl carbamate (AQC) reacts with the amine group of the corresponding catecholamine. The reaction is shown in Fig. 20 exemplary for dopamine. The resulting derivatized catecholamine was detected with an m/z -increase of 170.056.

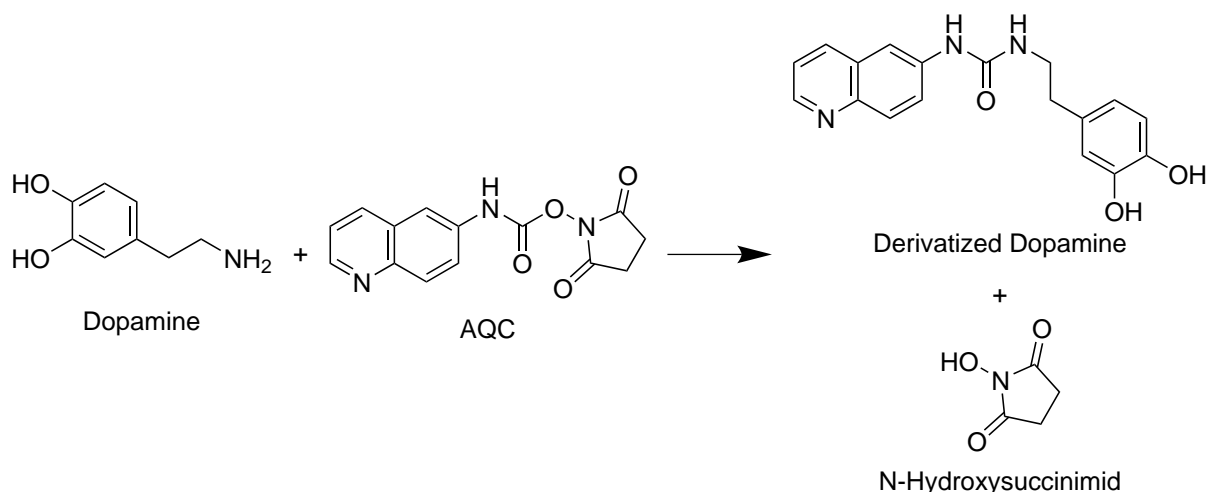


Fig. 20: Derivatization of dopamine with 6-aminoquinolyl-N-hydroxysuccinimidyl carbamate (AQC)

Upon first usage of a new derivatization kit, the reagent powder had to be dissolved in its vial using 1 mL acetonitrile supplied with the kit by mixing with a vortex mixer for 10 seconds. A sample was derivatized by delivering 70 μL borate buffer supplied with the kit and 10 μL aqueous sample into a sample vial. Subsequently, 20 μL of reconstituted AQC was added and the solution was mixed using a vortex mixer for another 5 seconds. Afterwards, the sample was stored at room temperature for 1 minute and subsequently 10 minutes in a pre-conditioned heating block at 55 $^{\circ}\text{C}$. After that the sample was ready for measurement.

4.7. Evaluation of solid-phase extraction cartridges

The applicability of solid-phase extraction cartridges from different manufacturers for the cleanup of pharmaceuticals and polar pesticides was assessed. Therefore, sample aliquots of 1 mL in ul-

Table 4.3: List of evaluated solid-phase extraction cartridges for laboratory cleanup

Cartridge Identifier	Company	Sorbent Type	Sorbent Amount [mg]	Volume [ml]
Chromabond HR-X	Macherey-Nagel	PS-DVB	500	6
Chromabond HR-X	Macherey-Nagel	PS-DVB	200	3
LEOX	BEKOLut	PS-DVB	500	6
Oasis HLB	Waters	PS-DVB	500	6
Bond-Elut PPL	Varian / Agilent	PS-DVB	200	3
Supelclean ENVI-Carb	Sigma-Aldrich	graphitized carbon black	250	3

trapure water with a concentration of $40 \text{ pg } \mu\text{L}^{-1}$ were prepared. The evaluated SPE cartridges and their technical specifications are listed in Table 4.3. The SPE cleanup was carried out using a Visiprep SPE vacuum manifold (Sigma-Aldrich, Steinheim, Germany).

The SPE elution protocol was the same for all cartridges except a volume adjustment factor of 0.5 if using cartridges with 200 or 250 mg sorbent instead of 500 mg:

- **Conditioning** 6 mL acetonitrile:methanol 50:50 (v:v) + 6 mL ultrapure water (3 + 3 mL for 200 mg cartridges)
- **Sample introduction** 1 mL sample solution in ultrapure water + three times rinsing with approximately 300 μL ultrapure water in total
- **Washing** 6 mL ultrapure water:methanol 99:1 (v:v) (3 mL for 200/250 mg cartridges)
- **Drying** 10 min with a vacuum of about -20 mmHg
- **Elution** 10 mL acetonitrile:methanol 50:50 (v:v) (5 mL for 200/250 mg cartridges)

The eluates were evaporated to a volume of about 1 mL using a gentle stream of nitrogen with heating to $40 \text{ }^\circ\text{C}$. Subsequently, the residual volume was transferred to 1.5 mL polypropylene tubes and a volume of 500 μL was adjusted. Until instrumental measurement, the samples were stored at $4 \text{ }^\circ\text{C}$. Instrumental measurement was carried out with nano-scale separation and analyte trapping configuration applying a preliminary instrument calibration without usage of internal standards. Due to the early stage of instrumental method development, SPE evaluation was only carried out for positive ionizing pharmaceuticals and polar pesticides. For measurement, sample aliquots of 50 μL were evaporated within a sample vial to near dryness under a gentle stream of nitrogen and reconstituted in 50 μL of mobile phase A:B 80:20 (v:v). With the initial spiked solution exhibiting a concentration of $40 \text{ pg } \mu\text{L}^{-1}$ in 1 mL volume, total recovery

corresponded to a measured concentration of $80 \text{ pg } \mu\text{L}^{-1}$ within the final sample volume of $500 \text{ } \mu\text{L}$.

4.8. Evaluation of syringe filters

For particle removal from samples ready for injection, syringe filters were evaluated with different filtration material in order to determine analyte recovery or possible introduction of background. Therefore, four sample solutions containing $20 \text{ pg } \mu\text{L}^{-1}$ of native pharmaceuticals and polar pesticides were prepared in mobile phase A:B 80:20 (v:v) ready for measurement. The standards included additionally $20 \text{ pg } \mu\text{L}^{-1}$ of sulfamethoxazole-D4, simazine-D5 and atrazine-D5. One standard solution was transferred into a measurement vial without filtration which served as reference solution. The other three solutions were filtered directly into measurement vials through a $0.45 \text{ } \mu\text{m}$ filter with polytetrafluoroethylene membrane (PTFE, Puradisc 4, Whatman, Little Chalfont, UK), a $0.45 \text{ } \mu\text{m}$ filter with hydrophilic polypropylene membrane (Acrodisc GHP, Pall, Crailsheim, Germany) and a $0.20 \text{ } \mu\text{m}$ filter with regenerated cellulose membrane (RC, SPARTAN, Whatman, Little Chalfont, UK). As the analytical instrument measured the analyte concentration in the test solution, any remaining sample solution on the wetted membrane did not influence the result.

The samples were measured in nano-scale configuration and analyte trapping in positive ionization mode. For the determination of analyte recovery after filtration, peak areas from the filtrated aliquots were compared to the unfiltered solution. Moreover, the spiked internal standard allowed to check whether isotope dilution analysis could correct for any analyte loss.

4.9. Active water sampling system

The established active water sampling system was designed for the on-site enrichment of analytes on self-packed sampling cartridges with a dimension of approximately $220 \times 420 \text{ mm}$ (length x i. d.) and ground joints at both ends. The cartridges can be closed with air-tight glass caps during storage and transportation. Prior to usage, all laboratory glassware was heat-treated up to $450 \text{ } ^\circ\text{C}$ to remove any remaining organic residues. Within the glass cartridges, approximately 50 to 60 g of mixture of XAD-7- and XAD-16-resin 50:50 (m:m) was trapped between a glass frit at one side and heat-treated glass wool at the other side (see Fig. 21). Prior to first usage, the cartridges were placed as a whole in a Soxhlet apparatus and extracted with 800 mL acetone for 24 h which corresponded to 90 full extraction cycles at a time of 16 min. After each extraction, the cartridges were dried within a gentle flow of dry nitrogen for 6 h. The prepared cartridges could now be used for recovery experiments as well as for environmental sampling.



Fig. 21: Self-packed glass cartridge with XAD-resin trapped inside with glass frit and heat-treated glass wool (Picture: Johannes Deyerling)

Additionally, the entrance of large particulates into the sampling cartridges was avoided by using filter cartridges, tightly packed with heat-treated glass wool, that were optionally mounted before the XAD-cartridges within the flow path. The schematic structure of the whole sampling system is shown in Fig. 23.



Fig. 22: OEM peristaltic pump (left) which is operated between 1 and 24 V DC either with battery or dedicated power supply and analog water meter (right)

For sampling, the cartridges were submerged into the water body of interest and water was being sucked through the cartridges with a battery driven peristaltic pump (OEM M3000, Verder, Haan, Germany, Fig. 22). Thereby, the design of the flow path avoided any sampling artifacts that might originate from the employed tubing. The sampling flow rate and volume was monitored with an analog water meter mounted at the water outlet of the pump.

4.10. Laboratory performance evaluation of large volume water sampling

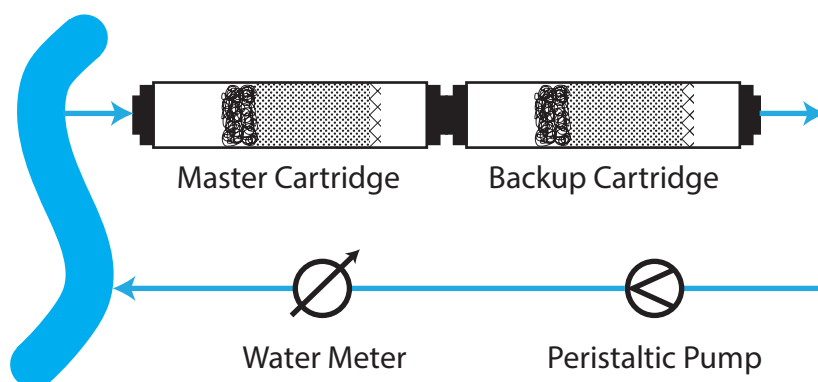


Fig. 23: Schematic illustration of the established water sampling system with self-packed glass cartridges; optionally a filter cartridge could be mounted before the sampling cartridges in the flow path (not shown)

The performance of cartridge extraction and subsequent cleanup of the generated extract by solid-phase extraction was assessed in laboratory recovery experiments. In order to assess sample extraction and cleanup recoveries and to determine matrix effects, pre-cleaned sampling cartridges were spiked with a dilution of the native multi-analyte standard mixture containing pharmaceuticals and polar pesticides in acetonitrile. Typically a total amount of 80 to 90 ng was chosen yielding a concentration of 400 to 450 $\text{pg } \mu\text{L}^{-1}$ in a final sample volume of 200 μL . Besides the evaluation of the extraction technique, artificial water samples were generated in a laboratory environment from spiked distilled water volumes of 25 L. The sample enrichment was carried out with the same setup as for environmental sampling described in section 4.9. A schematic view of the whole sampling system can be seen in Fig. 23. After sampling, excessive water was purged from the cartridges prior extraction by administering a gentle stream of nitrogen for 5 min. The spiked cartridges were extracted for 16 to 24 h over night in a Soxhlet apparatus either with 800 mL acetone, methanol or mixtures of both solvents. Alternatively, the analytes were eluted from the cartridges with 400 or 800 mL acetone. The extracts were evaporated by rotary evaporation to a volume of about 10 mL and finally a volume of about 1 mL was adjusted by a gently stream of nitrogen. After the addition of 2 mL ultrapure water, the extracts were further subjected to a gentle stream of nitrogen for 10 min in order to evaporate any remaining organic solvent. In the following, the samples were cleaned for measurement by solid-phase extraction with HR-X cartridges (500 mg). Thereby, the elution protocol was similar to the one applied during SPE cartridge selection experiments (see section 4.7.):

- **Conditioning** 6 mL acetonitrile:methanol 50:50 (v:v) + 6 mL ultrapure water

- **Sample introduction** 2 mL sample solution in ultrapure water + three times rinsing with approximately 300 μL ultrapure water in total
- **Washing** 5 mL ultrapure water
- **Drying** 40 min with a vacuum of about -20 mmHg
- **Elution** 2 x 5 mL acetonitrile:methanol 50:50 (v:v)

The eluates were collected in pear-shaped flasks and reduced to a volume of approximately 500 μL by rotary evaporation. Finally, the cleaned extracts were transferred to 1.5 mL polypropylene tubes by three times rinsing with a small volume of acetonitrile:methanol (50:50) (v:v) and a volume of 200 μL was adjusted by evaporation in a gentle stream of nitrogen at 40 °C. Until measurement, the samples were stored at 4 °C in the dark.

For measurement, an aliquot of 40 μL of a sample was transferred to a 1.5 mL polypropylene tube and evaporated to near dryness by a gentle stream of nitrogen at 40 °C. Subsequently, the sample was reconstituted in 40 μL of a specific mobile phase mixture (corresponding to the intended measurement) containing 400 $\text{pg } \mu\text{L}^{-1}$ of isotopically labeled pharmaceuticals and polar pesticides. After rigorous mixing using a vortex mixer, the extracts were centrifuged for 30 min at 4 °C and 14,000 x g to remove any remaining particles from the samples. Finally, the supernatant was transferred into measurement vials.

Besides the on-site enrichment of large water volumes, the laboratory enrichment of bottled water samples in the scale of 100 to 500 mL directly on 500 mg Chromabond HR-X SPE cartridges was investigated. Therefore, 100, 250 and 500 mL of ultrapure and tap water were spiked to a concentration of 180 ng L^{-1} with the multi-analyte standard containing native pharmaceuticals and polar pesticides. Consequently, within a final sample size of 200 μL a concentration of 90, 225 and 450 $\text{pg } \mu\text{L}^{-1}$ could be expected for 100 % recovery, respectively. Direct solid-phase extraction was carried out according to the following elution protocol:

- **Conditioning** 6 mL acetonitrile:methanol (50:50) (v:v) + 6 mL ultrapure water
- **Sample introduction** Admission of the spiked sample through a reservoir attached to the SPE cartridge at a flow rate of about 4 mL min^{-1}
- **Drying** 40 min with a vacuum of about -20 mmHg
- **Elution** 2 x 5 mL acetonitrile:methanol (50:50) (v:v)

The preparation of the eluates for measurement could be carried out the same way as described above.

4.11. Environmental sampling and analysis of the Yangtze River

Environmental sampling of the Yangtze River slightly upstream of the Three Gorges Dam in China (see Fig. 24) was conducted in September 2013 with the sampling system described in section 4.9. The sampling location was near the city of Maoping in the middle of the Yangtze River (30.8693° N, 110.9454° E) and was reached by a boat fixed to the middle of the fairway. A water sample size of about 300 L was taken at water depths of 11, 31 and 50 m, respectively. Additionally, one prepared sampling cartridge was carried to the sampling site as field blank for blank correction. For sampling, the sampling cartridges with mounted filter cartridge were placed within a protective stainless steel housing and submerged to the desired water depth. The flow rate was set to about 2.3 L min^{-1} which allowed to collect a sample volume of approximately 280 L within 2 h. After sampling and transport to Germany, the samples were stored at 4°C in the dark until laboratory processing.

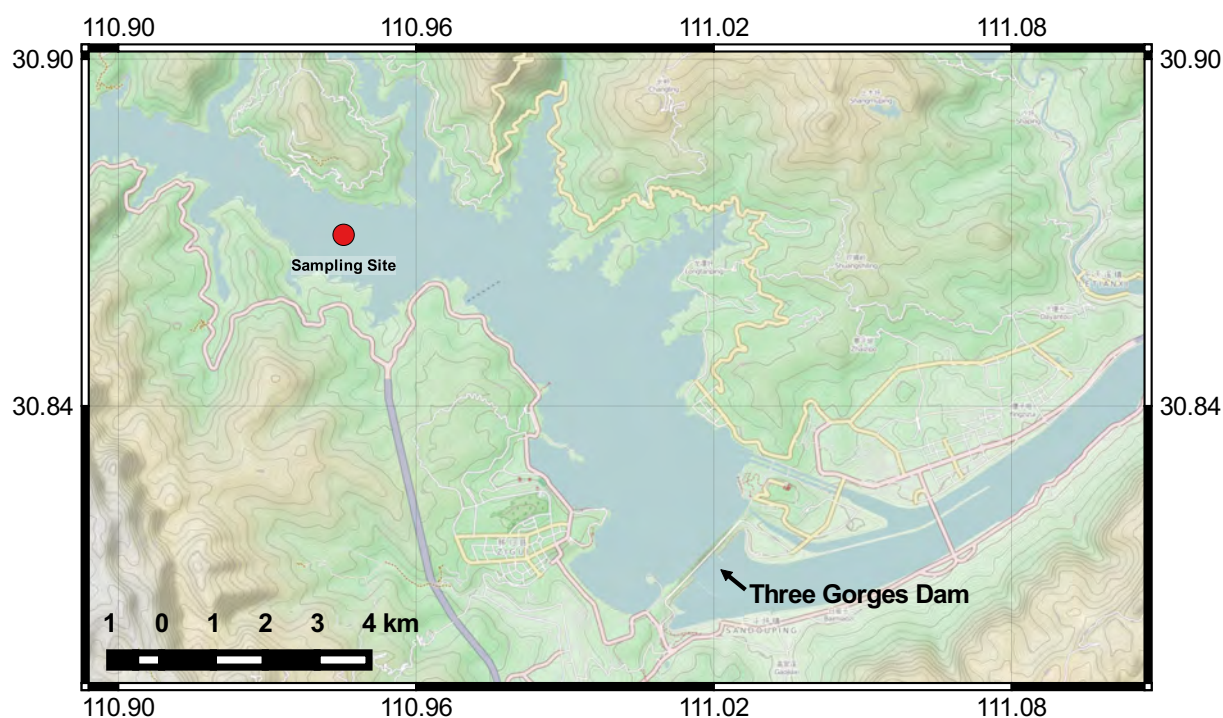


Fig. 24: Map of the Yangtze River near the Three Gorges Dam with highlighted sampling site (© OpenStreetMap contributors [2])

Prior to extraction, the glass cartridges were purged from excessive residual water by a gentle stream of dry nitrogen for 5 minutes. Subsequently, internal standard mixtures containing isotopically labeled pharmaceuticals and polar pesticides as well as PFAAs (according to the purchased standards described in section 4.1.) were administered on the glass wool on top of the sampling and filter cartridges. The sample cartridges were cleaned at the outside using low amounts of acetone in order to remove any remaining residues of sample labels and transferred

to a Soxhlet apparatus. The extraction was carried out with 800 mL of acetone for at least 16 hours corresponding to about 60 extraction cycles over night. After extraction, the samples were evaporated using a rotary evaporator to a residual volume of about 200 mL. Remaining water was removed by directing the extracts through glass filters filled with dry sodium sulfate. The extracts were ready for the following solid-phase extraction cleanup after evaporation to a volume of about 2 mL.

The SPE with Chromabond HR-X cartridges was carried out on a vacuum manifold applying the elution protocol described in section 4.10. The eluate was evaporated by rotary evaporation to a volume of about 200 μL and transferred to a 1.5 mL polypropylene tube (Sarstedt, Nümbrecht, Germany) by three times rinsing with acetonitrile:methanol 50:50 (v:v). Finally, a sample volume of typically 200 μL was adjusted by evaporating excess solvent under a gentle stream of nitrogen and heating to 40 °C.

With the recorded sample volume, environmental water concentrations could be calculated. At first, an enrichment factor F_{EN} was determined according to the following equation:

$$F_{EN} [] = \frac{V_{sampled} [L]}{V_{extract} [\mu L] \cdot 10^{-6}} \quad (4.3)$$

where $V_{sampled}$ and $V_{extract}$ are the volumes of the water sample and the final extract after cleanup, respectively. Consequently, the concentration of a dissolved organic compound i in water $c_{i,w}$ was calculated by multiplication of the determined extract concentration $c_{i,extract}$ and the enrichment factor F_{EN} :

$$c_{i,w} [pg L^{-1}] = c_{i,extract} [pg \mu L^{-1}] \cdot F_{EN} \cdot 10^{-6} \quad (4.4)$$

Analyte values determined in the blank cartridge were referred to the corresponding sample volume with equation 4.4 and the resulting blank concentrations were subtracted from the reported values:

$$c_{i,w,blankcorr} [pg L^{-1}] = c_{i,w} [pg L^{-1}] - c_{i,blank} [pg L^{-1}] \quad (4.5)$$

where $c_{i,w,blankcorr}$ is the blank corrected water concentration of a compound i and $c_{i,blank}$ is the theoretical blank concentration referred to the water sample volume. The limit of quantification (LOQ) could also be calculated based on the blank values:

$$LOQ [pg L^{-1}] = 3 \cdot 0.25 \cdot c_{i,blank} [pg L^{-1}] \quad (4.6)$$

In case of the LOQ-value exceeding the detected concentrations, the compound was regarded as not detected (n. d.).

4.12. Workflow for directed non-target screening

With the recorded HRMS data from environmental samples, the existing targeted analysis and quantification could be enhanced by a non-target screening approach. The screening required only one additional sample injection with low collision energy set enabling the detection of possible targets as positively charged molecular ions. These non-target injections were accompanied by blank mobile phase injections in order to correct the data gathered during non-target runs for irrelevant background noise. Due to the improved sensitivity of the MS and the better ESI stability in positive ion mode, negative ionization mode was neglected for non-target analysis. Sample runs already acquired for targeted analysis with elevated collision energy could be used to gather information about the fractionation behavior of possible analytical targets. Signals from the isotopically labeled internal standards gathered during instrumental calibration were used to calibrate the retention time scale of the chromatographic system with the retention time index (see section 2.1.2.). The RTI-calibration, calculated according to equation 2.6, allowed the estimation of $\log P$ -values of unknown substances which could be included in database research of possible suspects. The developed non-target workflow consisted of the following steps:

1. Subtraction of background collected during blank injection
2. Conversion of blank corrected MS data to NetCDF exchange format for further data processing in MZmime 2.11
3. Cropping of parts of the chromatogram that were not necessary for analysis (early elution, column equilibration)
4. (optional) Mathematical background reduction
5. Peak list generation with a suitable algorithm extracting mass traces forming well-shaped peaks above a certain intensity threshold
6. Deconvolution of extracted ion chromatograms containing more than a single peak into separate chromatograms
7. Removal of duplicates with an isotopic pattern and a mass filter
8. Visible evaluation of suspects and removal of chromatograms that appear to be noise
9. Peak list alignment if multiple samples have been analyzed
10. Estimation of the $\log P$ -values of the possible targets from their individual retention time

11. Suspect identification with the databases STOFF-IDENT, DAIOS and MassBank

The developed workflow was applied first in the analysis of virtual organisms (VOs) which are passive samplers similar to semi-permeable membrane devices (SPMDs). The VOs consist of 25 mm wide and 65 μm thick lay-flat polyethylene tubing (VWR, Ismaning, Germany) cut to a length of 29 cm and filled with 700 μL triolein (Sigma-Aldrich, Steinheim, Germany). Heat seals at both ends of the tubing trapped the triolein inside the sampler. The samplers investigated with the non-target approach in this study were exposed to water in the small river Selke which is a tributary of the river Bode in Saxony-Anhalt (Germany). In total, two exposed samples and one field blank were investigated. The extraction of a VO for analysis was carried out in a Erlenmeyer flask with 100 mL acetonitrile:methanol 50:50 (v:v) by gentle shaking for 16 h overnight. The VO was removed and the extract was evaporated using a rotary evaporator to a residual volume of 2 mL. Subsequently, a cleanup on HR-X SPE cartridges was conducted according to the elution protocol described in section 4.10. The eluate was evaporated to a volume of about 500 μL , transferred to 1.5 mL polypropylene tubes and a final volume of 200 μL was adjusted. The non-target data analysis developed and tested with VO-extracts was also applied to the XAD cartridge samples collected in the Yangtze River in 2013.

5. Results and Discussion

5.1. Chromatographic method development

5.1.1. Nano-scale chromatography with trap column

5.1.1.1. Evaluation of trapping parameters

Chromatograms obtained with nano-scale separation and previous enrichment on a trapping column in general suffered from severe peak tailing when subjected to the analysis of small molecules. The manufacturer of the nano-scale LC instrument specifically designed the trapping setup for the application in proteomics. Consequently the trapping column is capable of the enrichment of large protein fragments. In such application scenarios, the trapping step enables fast analyte enrichment from the sample loop as well as desalting of the sample from the aqueous buffer solution the protein samples are usually solved in. Unfortunately, there was no other column chemistry than Symmetry C-18 available for the trapping column during the time the presented study was conducted, therefore, the method for operation with the given setup was optimized as far as possible.

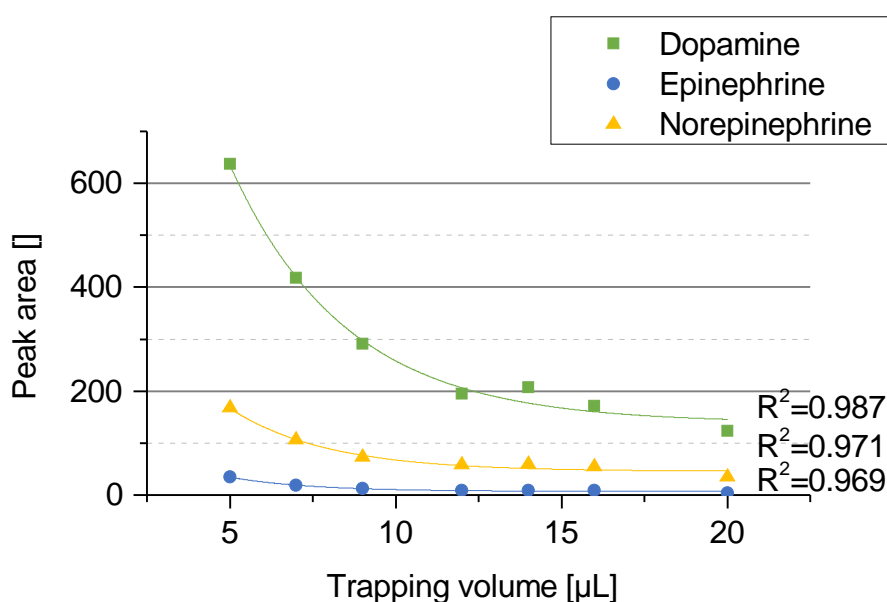


Fig. 25: Dependence of system response (peak area) of derivatized catecholamines on trapping volume: the sensitivity decreased exponentially with trapping volume

The first aspect of method development was the investigation of the trapping parameters and their influence on signal intensity, peak shape and retention time. This investigation was carried out with derivatized catecholamines (dopamine, epinephrine and norepinephrine) which were employed at early stage as test compounds for method development. For this experiment, the

chromatographic gradient was kept constant and only the trapping time and flow rate was altered while carrying out 2 μL full loop injections for analysis. The peak area appeared to be exponentially negative correlated with the solvent volume used for trapping with correlation coefficients between 0.99 and 0.97 (Fig. 25). Besides, there was a slight increase in retention time of about 1 % observable for an increase of trapping volume from 5 to 20 μL .

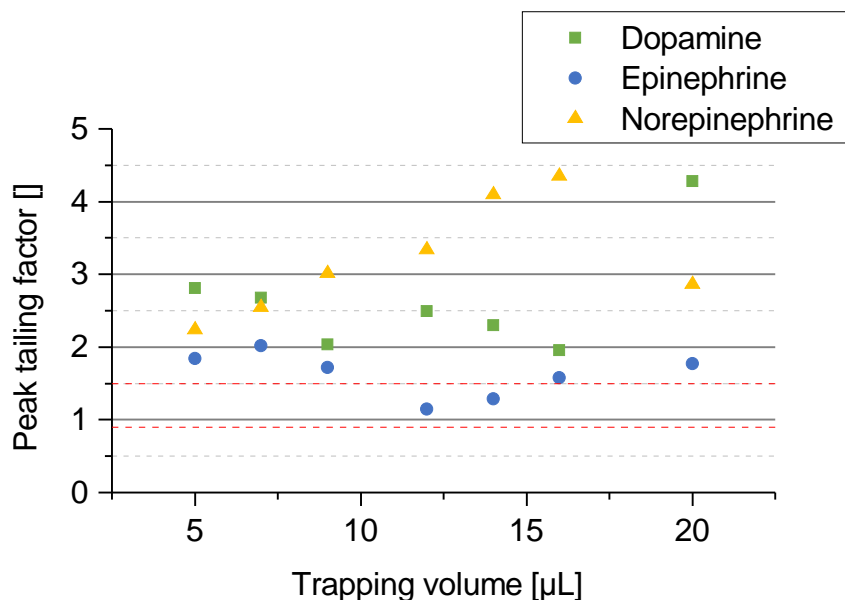


Fig. 26: Relationship of the peak tailing factor and trapping volume: there was no general characteristic dependence observed; acceptable peak tailing factor range is indicated in red (0.9-1.5 according to [102])

Peak tailing, however, seemed not to be characteristically influenced by the trapping volume. In most cases, the USP peak tailing factor was calculated to be higher than 1.5 which is already regarded as insufficient for analytical purposes (Fig. 26) [102]. Nevertheless, the results indicated that peak tailing seemed to increase for norepinephrine with trapping volume in the range of 5 to 16 μL . No characteristic relations could be found between the trapping flow rate, the peak tailing factor and the peak area indicating only a minor influence of this parameter on the chromatographic process.

In summary, the trapping volume was found to be a critical parameter for the sensitivity within the nano-scale chromatographic setup with trapping column. The results did not indicate any possibility to improve the peak shape and reduce peak tailing at this stage of the chromatographic method. The highest response was achieved with the lowest amount of trapping volume tested (5 μL). This finding is well in accordance with the instrument guideline suggesting to use approximately three sample loop volumes as trapping setting [148]. The exponential decrease of system response of the rather polar derivatized catecholamines suggests that the abilities of the trapping column regarding the enrichment of small and polar molecules was limited. More-

over, analytes have likely been lost already with the 5 μL trapping setting. If the retention on the trapping column is not high enough, analyte separation instead of on-column focusing might already be taking place during the trapping step. In this case, peak tailing could be caused by pre-separated compounds that are flushed as broad analyte bands onto the head of the nano-scale separation column. Furthermore, the high flow differences between analyte trapping and elution (e.g. 5 $\mu\text{L min}^{-1}$ trapping flow vs. 0.3 $\mu\text{L min}^{-1}$ analytical flow) might have caused additional band broadening due to diffusion. It has to be considered that the volume of the trapping column was 76 % of the volume of the analytical column. Thus a large additional volume was introduced to the chromatographic system increasing retention time and diffusional band broadening.

5.1.1.2. Trapping and gradient elution with pharmaceuticals and polar pesticides

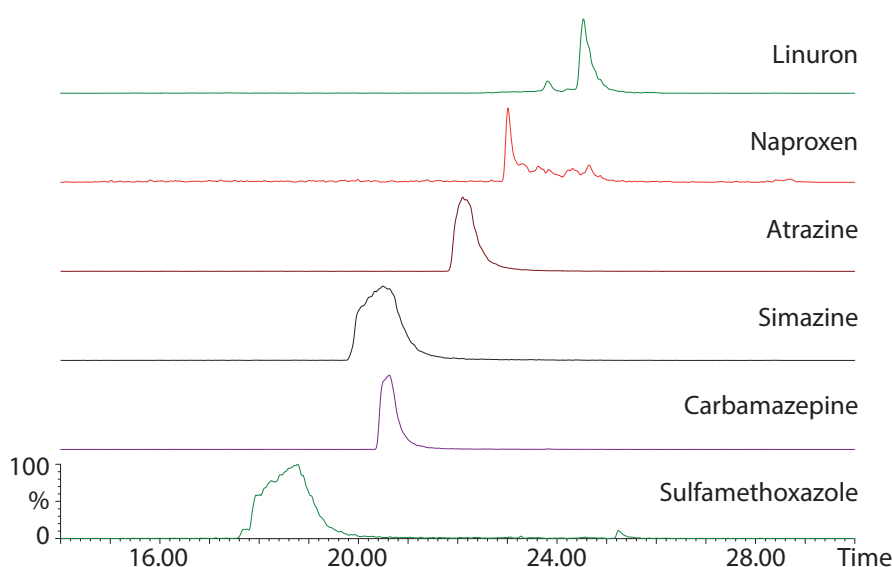


Fig. 27: Extracted ion chromatograms of pharmaceuticals and polar pesticides achieved with the 26.5 min initial linear gradient from 0 % to 100 % solvent B and analyte trapping with subsequent nano-scale separation

Despite the limitations for the analysis of small and polar molecules mentioned above, extended method development was conducted for the analysis of polar pesticides and active pharmaceutical ingredients with the trap and elute setup. Additionally, the influence of the analytical gradient on peak tailing was elucidated. Therefore, the analytical gradient was designed for maximum analyte separation and sensitivity as well as peak shape. Full loop injections with the 2 μL sample loop and a 40 $\text{pg } \mu\text{L}^{-1}$ dilution of the multi-analyte standard mixture in solvent A containing all investigated pharmaceuticals and polar pesticides was used for gradient develop-

Table 5.1: Retention time and resolution of adjacent peaks of pharmaceuticals and polar pesticides during initial gradient elution with trapping and nano-scale separation

Compound	26.5 min gradient		53 min gradient	
	Retention time	Resolution	Retention time	Resolution
Sulfamethoxazole	18.78	1.05	24.03	0.90
Simazine	20.59	0.07	26.99	0.50
Carbamazepine	20.63	2.21	27.89	1.86
Atrazine	22.10	1.24	29.95	2.78
Naproxen	23.01	3.30	32.30	4.32
Linuron	24.53	-	34.75	-

ment. Moreover, method development was carried out with positive ionization enabling the detection of atenolol, paracetamol (acetaminophen), sulfamethoxazole, simazine, carbamazepine, atrazine, naproxen, and linuron. The trapping volume was kept constant at three loop volumes which corresponds to 6 μL as suggested by the manufacturer of the chromatography system. The analytical gradient development was conducted according to the systematic approach of Snyder and Dolan [102]. Therefore, a basic initial gradient chromatogram is recorded based on which the gradient shape is further improved. In the presented study two linear gradients from 0 to 100 % organic solvent (solvent B) with a gradient time of 26.5 and 53 min were employed followed by an isocratic hold at 100 % B for 1 min. After each gradient run a column equilibration time of 15 min was appended at 0 % B corresponding to about 5 column volumes resulting in a total runtime of 42.5 and 69 min, respectively. The obtained chromatograms are shown in Fig. 27 for the 26.5 min gradient. Obviously, band broadening, peak distortion and peak tailing occurred. Atenolol and paracetamol, which are not shown in Fig. 27, were not detectable. The retention times and the separation performance of each two adjacent peaks are listed in Table 5.1.

Besides the limited separation performance overall, the peak pairs simazine/carbamazepine and atrazine/naproxen drew special attention. The initial gradient chromatograms yielded the information at which fraction of solvent B the compounds elute. In case of the 26.5 min gradient, compound elution started at approximately 60 % B whereas the first compound with the 53 min gradient eluted at about 40 % B. Consequently, there was potential for the reduction of lost chromatographic space until the elution of the first compound by increasing the starting fraction of solvent B. The increase of the starting fraction of solvent B to 40 % B obviously decreased the elution window. Additionally, the peaks were compressed and the sensitivity improved. Furthermore, the gradient range was adjusted to the new retention times resulting in a nearly

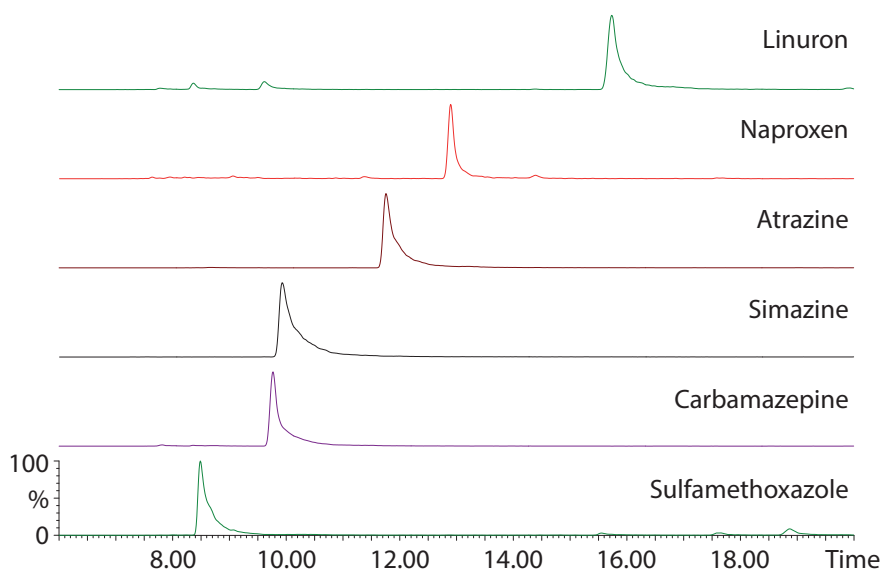


Fig. 28: Extracted ion chromatograms of pharmaceuticals and polar pesticides with the 15 min optimized linear gradient from 40 % to 46 % solvent B and analyte trapping with subsequent nano-scale separation

Table 5.2: Retention time and resolution of critical peak pairs with optimized gradient shape and starting solvent B from 40 to 80 % achieved with trapping and nano-scale separation

Initial %B	Resolution of critical peak pairs	
	simazine/carbamazepine	atrazine/naproxen
40	0.14	1.70
50	0.32	0.77
60	0.51	0.36
70	0.68	0.17
80	0.64	0.41

isocratic gradient starting at 40 % B, slowly increasing to 46 % B during 15 min, followed by 15 min of equilibration at 40 % B again. The total run time of 31 min corresponds to a reduction of 27.1 and 41.5 %. The resulting chromatogram is shown in Fig. 28. Obviously, the issues causing peak distortion and band broadening could be resolved, however, peak tailing persisted also with the optimized gradient. Further gradient optimization was conducted by raising the initial % B in steps of 10 % up to 80 % B while preserving the gradient shape. Table 5.2 shows the resolution between the critical peak pairs.

The optimization of the separation between simazine and carbamazepine was found to be orthogonal to the separation of atrazine and naproxen. Therefore, the gradient starting with 40 % B yielded baseline separation of the atrazine/naproxen peak pair whereas the 60 % B gradient represented a compromise yielding the best achievable resolution for the two critical

peak pairs at the same time.

5.1.1.3. Trapping and gradient elution with perfluorinated compounds

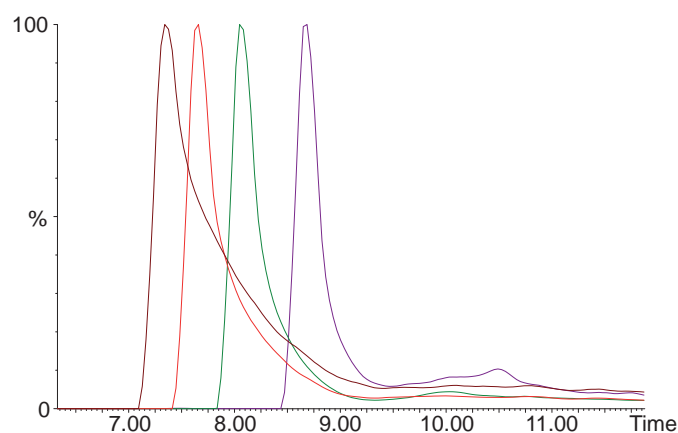


Fig. 29: Overlapping extracted ion chromatograms of PFBS, PFHxS, PFOS and PFDS (peaks from left to right) achieved by linear gradient elution starting at 80 % solvent B with trapping and nano-scale separation

Peak tailing and limited separation with the trapping setup was also observed during method development with perfluorinated alkyl acids (PFAAs) under operation with negative ionization. In comparison to the mixture of pharmaceuticals and polar pesticides, the investigated PFAAs are a group of structural homologs with a systematic polarity distribution according to their chain length. Therefore, an increasing retention time with increasing chain length could be expected.

By analogy with the method development for pharmaceuticals and polar pesticides, it was discovered that initial broad and tailing peaks could be compressed by increasing the starting concentration of organic solvent B in the analytical gradient. For the investigated linear PFAAs, however, only above 70 % B reasonable peaks without excessive band broadening were formed. Therefore, the starting % B was increased in steps of 10 % from 60 % to 90 %. The gradient consisted of a 24 min linear ramp to 100 % solvent B from the corresponding starting concentration followed by a re-equilibration time at the starting concentration of 15 min. Fig. 29 exemplary shows the separation of investigated perfluoroalkylsulfonates in overlay. It can be clearly recognized that the peak tops have already been well separated. Due to the pronounced peak tailing, however, signal overlapping could not be avoided. The peak tailing factor achieved with the different starting gradients is shown in Fig. 30. In general, peak tailing seemed to decrease with increasing carbon chain length. The gradient starting at 60 % B caused severe peak distortion and peak tailing resulting in difficulties with peak tailing factor determination and thus extraordinary high values. The boxplot in Fig. 30 illustrates that the gradients with 70 to

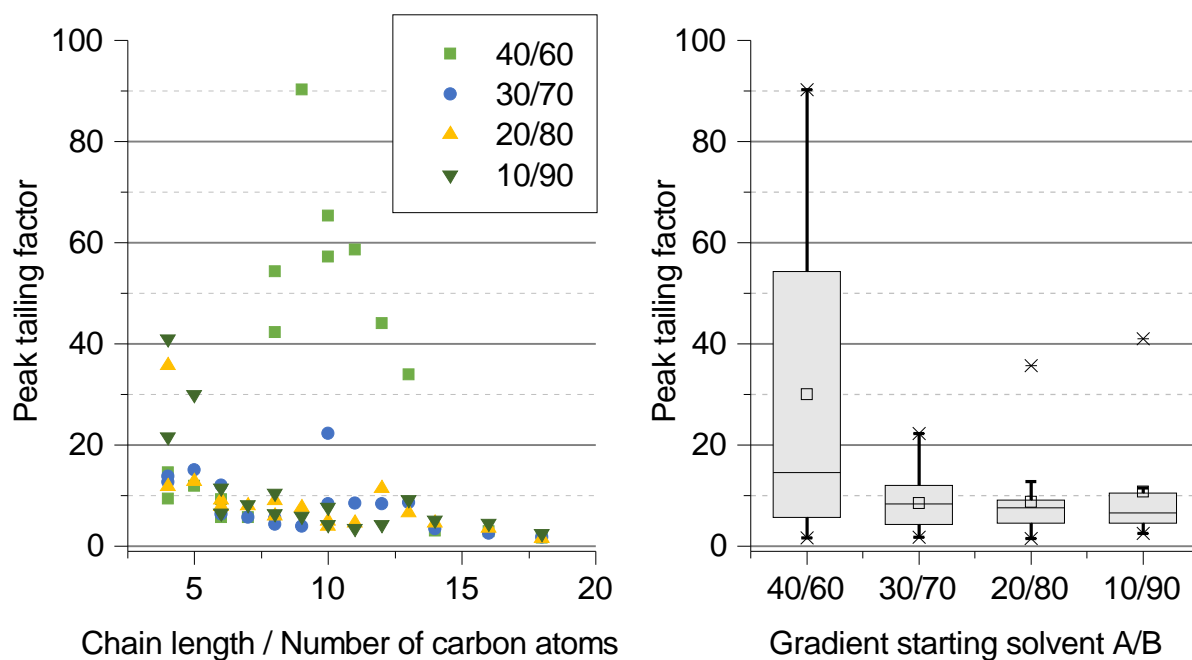


Fig. 30: Left: USP peak tailing factors of PFAAs against their chain length determined with gradients starting at different solvent A/B ratios; right: boxplot for the illustration of the USP peak tailing factor spreading achieved with the different starting solvent A/B ratios

90 % solvent B as starting solvent composition yielded comparable results in terms of peak tailing. All developed elution methods for PFAAs with analyte trapping, however, could not reduce the peak tailing factor to values below 1.5, consequently, the peak shape could not be regarded as acceptable. Besides, the pronounced peak tailing rendered the determination of chromatographic resolution impossible.

5.1.2. Nano-scale chromatography with direct injection

5.1.2.1. Gradient elution with pharmaceuticals and polar pesticides

The removal of the trapping column and change of the fluidic configuration to direct injection (DI, see also Fig. 17) required the addition of gradient time needed for the flushing of the sample loop at the low analytical flow rates between 0.25 and 0.3 $\mu\text{L min}^{-1}$. This was achieved by introducing an isocratic hold with 0 % B at the beginning of the analytical gradient adjusted to the loop volume installed (the 2 μL sample loop was predominantly used for nano-scale separations with DI). The inserted isocratic hold at the beginning of the gradient leads to a concentration of the sample at the top of the column, at least for the compounds showing reasonable retention on the employed C-18 column chemistry. This process is also referred to as on-column focusing. Compounds with insufficient retention on the stationary phase, however, arrive as severely broad and tailing signals with low intensity at the detector rendering their

analysis impossible.

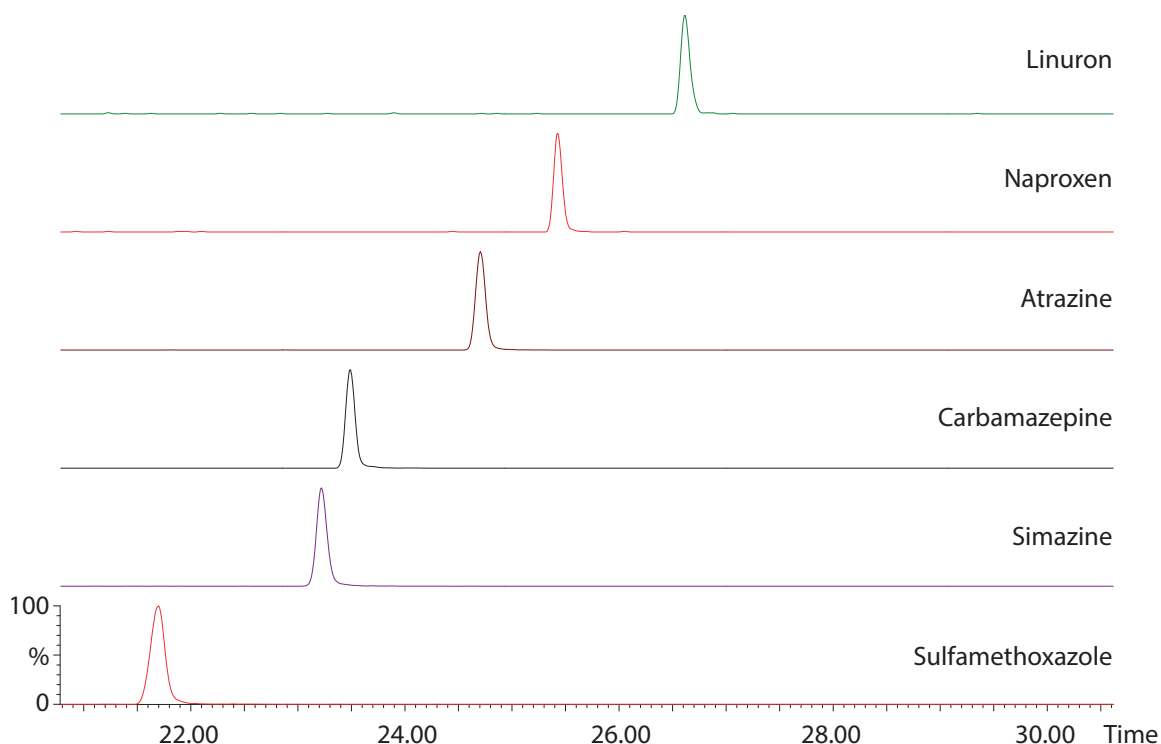


Fig. 31: Extracted ion chromatograms of pharmaceuticals and polar pesticides achieved with 20 min linear gradient from 0 to 100 % solvent B and nano-scale separation with direct injection of 0.5 μL 200 $\text{pg } \mu\text{L}^{-1}$ multi-analyte standard

Reasonable compound separation and high signal intensity could be achieved with a basic linear gradient from 0 to 100 % solvent B at 0.25 $\mu\text{L min}^{-1}$: initial isocratic hold at 0 % B for 8.20 min, increase to 100 % B until 28.00 min, isocratic hold at 100 % B until 40.00 min followed by column equilibration at 0 % B until 59 min. Fig. 31 shows a representative chromatogram achieved with direct injection of 0.5 μL multi-analyte standard with a concentration of 200 $\text{pg } \mu\text{L}^{-1}$. Obviously, peak tailing and peak distortion were absent in DI configuration. Moreover, the separation performance could be clearly improved. Atenolol and paracetamol, however formed irregular peaks with low intensity (chromatograms not shown). The characteristic retention times and resolution between two adjacent eluting compounds are listed in Table 5.3. The retention times altogether were within the linear gradient time. Baseline separation (resolution > 1.5) was achieved for all monitored compounds including the critical peak pair simazine/carbamazepine. Besides, the separation between atrazine and naproxen did not get critical as for some of the gradient approaches with analyte trapping (see section 5.1.1.2.). Consequently, the chromatographic method employing nano-scale separation with DI was in general suitable for sample analysis.

The presented gradient elution with DI, however, was found to be particular sensitive for the

Table 5.3: Retention time and resolution of adjacent peaks during gradient elution of pharmaceuticals and polar pesticides achieved with nano-scale separation and direct injection

Compound	Retention time	Peak tailing factor	Resolution
Sulfamethoxazole	21.70	0.94	6.67
Simazine	23.22	1.20	1.53
Carbamazepine	23.49	1.03	6.98
Atrazine	24.70	1.07	4.32
Naproxen	25.43	1.04	7.21
Linuron	26.61	1.24	-

solvent in which the standards were solved. Routinely, standard dilutions were carried out in the aqueous mobile phase A for full compatibility with the starting gradient at 0 % solvent B. Under this condition, basically all compounds were detectable but the response for naproxen and linuron was very weak. Nevertheless, the response for substances with comparably higher hydrophobicity (in this case $\log P$ -values > 3.00) could be improved by solving the standard in a mixture of mobile phase A and B. Increasing concentration of solvent B, however, decreased the system response for highly polar compounds like sulfamethoxazole. Therefore, either a compromise was determined for further calibration experiments or two separate calibration curves were recorded, covering polar and less polar compounds with reasonable system response. For the evaluation of system response for the single substances, dilutions of the multi-analyte standard stock solution were prepared with solvent compositions from 100:0 to 0:100 A:B (v:v) in steps of 10 %. Fig. 32 illustrates the peak area change normalized to injections with the standard dissolved in pure solvent A. Peak areas of distorted peaks were not determined and are not shown in the illustration. The most polar compound, sulfamethoxazole, yielded maximum response when dissolved in 90:10 A:B. Higher fractions of solvent B in the standard solution decreased the system response for this particular compound and in the 60:40 A:B sample, peak distortion occurred. For simazine, carbamazepine and atrazine, the results indicated a 50 to 140 % increased response while increasing solvent B in the sample up to 50:50 A:B. The greatest gains in sensitivity of 1670 and 2020 %, however, could be achieved for naproxen and linuron comparing the sample in 100:0 A:B to the 50:50 A:B sample.

These results had to be taken into account for further measurements and calibration purposes. As a compromise, the solvent composition 90:10 A:B could be used for polar compounds, increasing the system response for sulfamethoxazole and simazine by more than 50 %. Less polar compounds, could be detected with 50:50 A:B yielding optimized response for atrazine, carbamazepine, naproxen and linuron at the same time. The need for the preparation of two

separate calibration curves with different solvent A:B ratio lead to an increase in routine laboratory work. Moreover, samples for analysis had to be reconstituted two times which again increased laboratory processing time, measurement time and sample consumption.

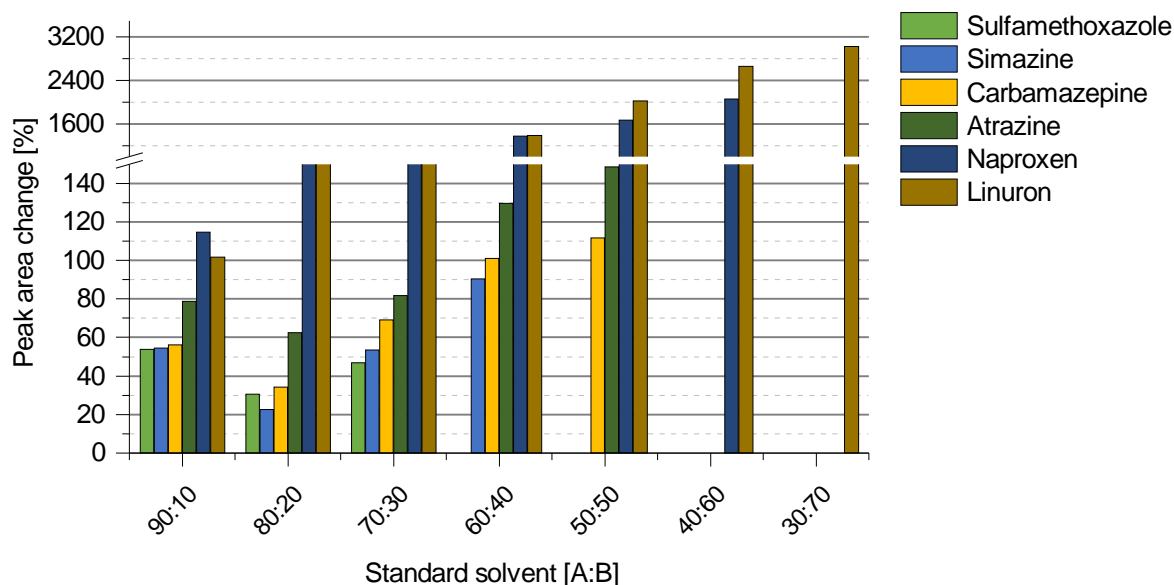


Fig. 32: Peak area of the multi-analyte standard with pharmaceuticals and polar pesticides dissolved in mobile phase A:B mixtures from 100:0 to 30:70; the peak area is normalized to the standard solution solved in 100:0 A:B; peak areas were only determined for non-distorted peaks

All in all, the direct injection configuration rendered it possible to analyze the selected pharmaceutical residues and polar pesticides with the nano-scale chromatographic setup without the need of additional analyte trapping. The total effort including runtime per injection, measurement of samples in two different solvents and nano-ESI-operation for instrumental analysis with the nano-scale setup had to be regarded as time-consuming. Nevertheless, the system yielded high sensitivity allowing the reduction of sample consumption to 0.5 μL or less.

5.1.2.2. Gradient elution with perfluorinated compounds

PFAAs could be separated in direct injection configuration with similar gradient settings as for pharmaceuticals and polar pesticides: initial isocratic hold at 0 %B for 8.20 min, linear increase to 100 % B until 28.00 min, isocratic hold at 100 % B until 36.00 min followed by equilibration at 0 % B until 55.00 min. By analogy with the results for pharmaceuticals and polar pesticides, peak tailing was also absent during the analysis of PFAAs with nano-scale chromatography and direct injection configuration. Baseline separation was achieved for all compounds within the group of PFCAs and PFAS. Due to the structural similarity between the two investigated groups of homologs, coelution occurred for PFHpA and PFHxS, PFNA and PFOS as well as for

PFUdA and PFDS. The differences in polarity between sulfonates and carboxylic acids became obvious as coelution only occurred between likewise functionalized PFAAs of different carbon chain length.

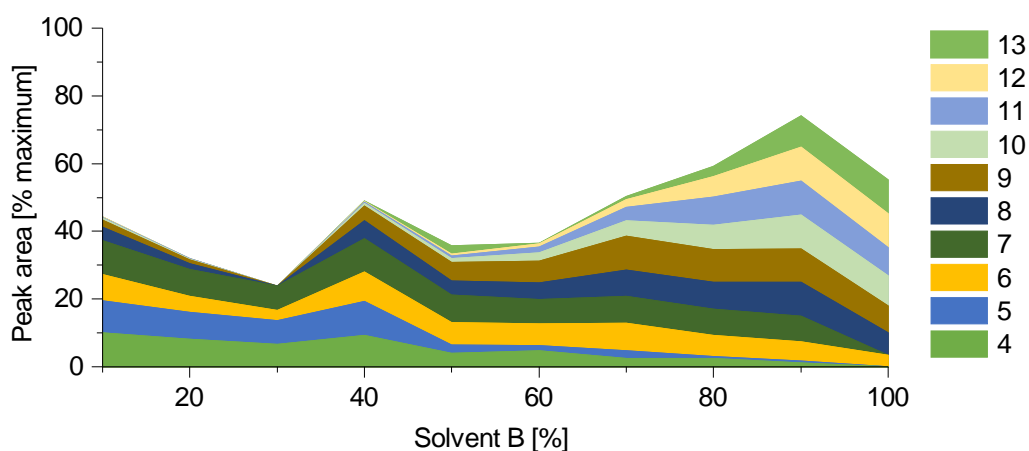


Fig. 33: Normalized system response for PFAAs with direct injection and nano-scale separation in dependence on the standard solvent categorized by carbon chain length

Similar to the analysis of pharmaceuticals and polar pesticides, the system response was found to be sensitive regarding the sample solvent composition. Consequently, the system response for PFAAs was determined by solving the multi-analyte PFAA standard in different solvent A:B ratios from 90:10 to 0:100 in steps of 10 % at a final standard concentration of $20 \text{ pg } \mu\text{L}^{-1}$. The peak area dependency of the compounds on the fraction of solvent B in the sample solvent categorized by their carbon chain length is illustrated in Fig. 33. According to the results, the response of PFAAs with a chain length of 4 and 5 improved with decreasing amount of solvent B. These short-chain PFAAs have the highest polarity at the same time of the group of homologs. Unfortunately, only the retention for PFBS was high enough for on-column focusing whereas PFBA did not form a regular peak even with the standard being diluted in pure aqueous solvent A. The response of the short-chain PFAAs decreased with increasing solvent B as standard solvent. The response of PFAAs with a carbon chain length of 6 and 7 proved to be independent from the standard solvent composition and no peak distortion was recognized. Finally, PFAAs with a chain length of 8 or more, showed better intensity with increasing amount of organic solvent B in the sample solvent. PFCAs with a chain length higher than 13, namely PFTeDA, PFHxDA and PFODA, showed reasonable response only with the standard being diluted in pure solvent B. Their absolute signal intensity, however, was about 70 % lower than for other PFAAs. Therefore, based on the results, a compromise was found by generating two calibration curves, one for samples diluted in 100:0 A:B (v:v) and a second one accounting for a dilution ratio of 30:70 A:B. Using this methodology, PFAAs with carbon chain lengths between 4 and 13 could

be investigated with nano-scale separation and direct injection configuration.

5.1.3. Micro-scale chromatography with direct injection

Chromatographic separations in micro-scale dimension were conducted by employing a column with an inner diameter of 300 μm . Apart from the diameter, the properties of the column did coincide with the ones of the employed nano-column. Hence, the established nano-scale gradient elution method could be transferred to the microscale setup running at 4.00 instead of 0.25 $\mu\text{L min}^{-1}$. Additionally, the increased analytical flow rate allowed the routine application of a 5 μL sample loop for sensitivity enhancement without the need for on-column focusing. In fact, the equilibration time at the end of each injection could be shortened. Finally, the gradient for micro-scale separation was found to be suitable for operation with water-acetonitrile and water-methanol mixtures covering experiments with positive and negative ionization. The gradient started with an isocratic hold at 0 % B for 1.5 min followed by a linear increase to 100 % B until 25 min, an isocratic hold at 100 % B until 30 min and ended with column equilibration at 0 % B until 35 min. Overall, the micro-scale setup appeared to be less sensitive to the solvent in which standards and samples were solved in.

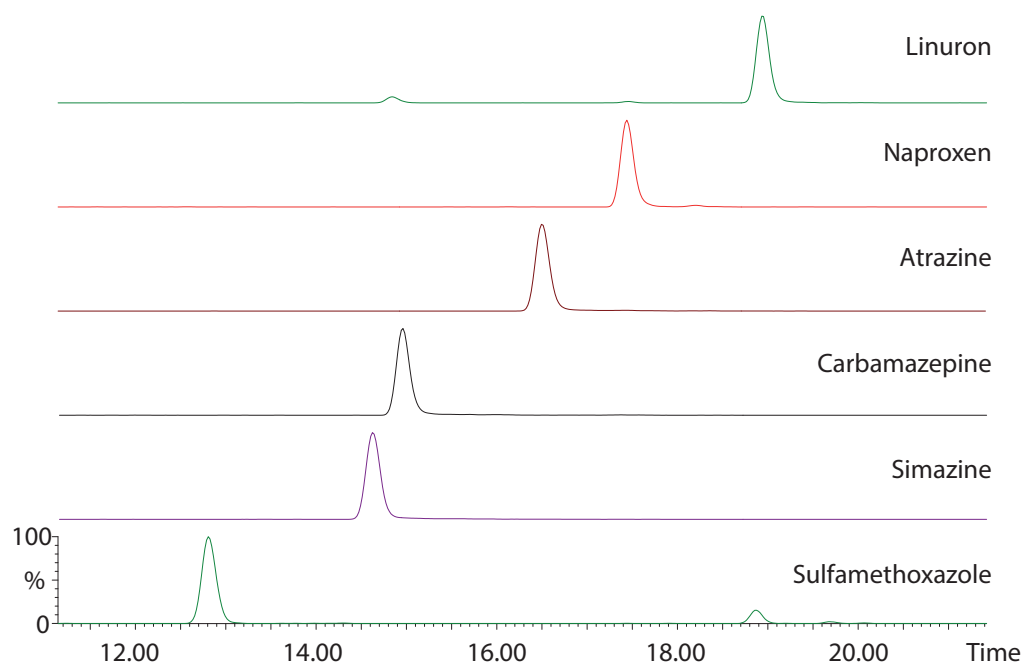


Fig. 34: Extracted ion chromatograms of a standard with 200 $\text{pg } \mu\text{L}^{-1}$ pharmaceuticals and polar pesticides in 90:10 A:B (v:v) achieved with 23.5 min linear gradient from 0 to 100 % solvent B and micro-scale separation with direct injection

Fig. 34 exemplarily shows the extracted ion chromatograms of a 5 μL injection of multi-analyte standard containing pharmaceuticals and polar pesticides with a concentration of 200 $\text{pg } \mu\text{L}^{-1}$

diluted in 90:10 A:B (v:v). Baseline separation was achieved for all compounds shown in Fig. 34 including the critical peak pair simazine/carbamazepine (resolution 1.62). Again, the analysis of atenolol and paracetamol was not possible due to them forming split peaks and generating weak signals. In contrast, the system response for naproxen and linuron was acceptable. Consequently, it was not necessary to set up a separate calibration and measurement with standards and samples at different solvent composition for positive ionizing pharmaceuticals and polar pesticides. The lower overall sensitivity of the system due to the usage of the standardized ESI source could be compensated by performing full loop injection with the 5 μL sample loop installed analog to the setup with the trapping column. Consequently, the instrument could be operated in the same calibration range with both the micro-scale and nano-scale configuration.

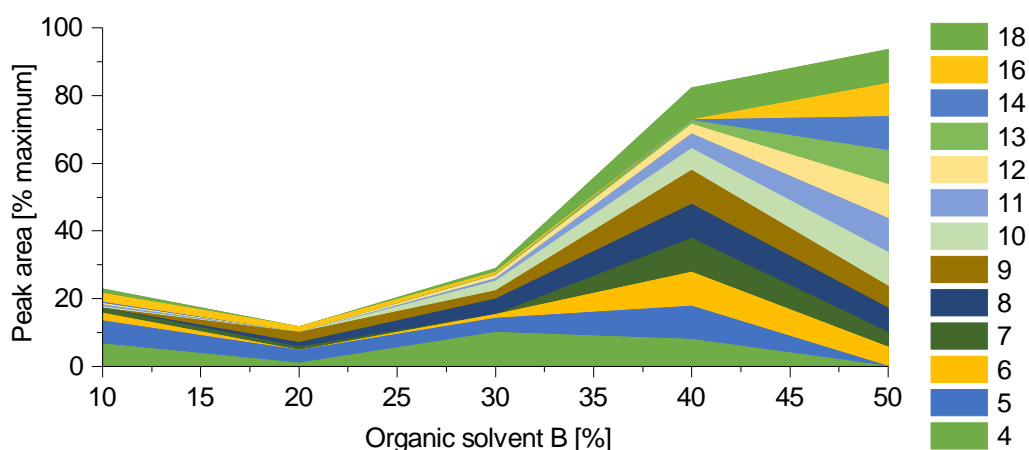


Fig. 35: Normalized system response for PFAAs with direct injection and micro-scale separation in dependence on the standard solvent categorized by carbon chain length

The performance for the response and separation of PFAAs in negative ionization mode with micro-scale separation was comparable to nano-scale separation. For the wide group of homologs, the system response was found to be dependent on the standard solvent again. Therefore, 5 μL injections of 100 $\text{pg } \mu\text{L}^{-1}$ multi-analyte PFAA standards from 90:10 to 40:60 A:B (v:v) in steps of 10 % were carried out to determine the response behavior in the micro-scale setup. The results are shown in Fig. 35 as peak area normalized to the corresponding maximum response of a certain PFAA chain length. The general dependence of the system response on the fraction of solvent B is comparable to the one with the nano-scale setup and direct injection. Short-chain PFAAs exhibited the highest response for low amounts of solvent B in the sample. Increasing amounts of solvent B helped to improve the response for mid to long chain PFAAs. The response using the micro-scale setup for the PFAAs with the shortest (4-5) and the longest carbon chain lengths (14-18) was better than in the nano-scale setup. Nevertheless, the absolute

intensity and signal stability for PFBA, PFTeDA, PFHxDA and PFODA was still insufficient for reliable calibration and quantification. In comparison to the nano-scale setup, lower amounts of solvent B were enough to cover the maximum response for PFAAs with more than 8 carbon atoms. Based on the results, further PFAA measurements with micro-scale separation were carried out either in pure solvent A for optimized response of short-chain PFAAs or in 40:60 A:B (v:v) for good response of mid- and long-chain PFAAs.

5.1.4. Applicability of the fluidic configurations for calibration and quantification

Three different fluidic setups were evaluated regarding their applicability for the analysis of a selection of pharmaceutical active ingredients, polar pesticides and PFAAs. Taking the results achieved with nano-scale chromatography and analyte trapping into account, it has to be concluded that this fluidic configuration is not suitable for the analysis of small (<1000 Da) and polar molecules. The trapping column could be identified as the main reason for low sensitivity and peak tailing in this setup. The analyte loss during the trapping step was found to be exponential negatively correlated with the trapping volume. The observed peak tailing was absent in two other tested setups without analyte trapping. Consequently, the analyte trapping step could be identified as cause for the peak tailing issues which could not be resolved by the adjustment of the analytical gradient. It was suggested that polar analytes might already get partly separated during the trapping step which causes broad analyte bands which are flushed onto the analytical column for separation. Unfortunately, due to the limited commercial availability and compatibility of pre-columns with the employed chromatography system, it was not possible to evaluate the performance of the system with other trapping columns.

With both possible DI configurations in nano- and micro-scale, peak tailing was absent and the separation performance clearly improved. Baseline separation could be achieved for most substances by employing a simplified linear gradient that needed only minor optimizations. In general, both configurations were suitable for calibration and quantification experiments. The DI configuration harnessed the extended capabilities of the analytical column regarding the retention of highly polar substances. Thereby, the sample is concentrated at the top of the column (on-column focusing) instead of preconcentration on a separate trapping column. Consequently, analytes which showed only limited retention on the employed column chemistry eluted as broad bands or were not detectable at all. Both setups lead to a systematic overload of the analytical columns as the injected sample volume is large compared to the column volume. In that sense, DI with nano-scale separation demonstrated the highest degree of column overloading. The column dimensions of 75 μm i. d. and 150 mm length correspond to a capillary column volume of 0.66 μL . The injection volume in the autosampler, however, could only be

reduced to a minimum of 0.2 μL independently from the sample loop volume. This injection volume already corresponds to 30 % of the total column volume. Moreover, the complete flushing of the 2 and 5 μL sample loop in each analytical run required 3.02 and 7.55 column volumes, respectively. The micro-scale setup demonstrated the effect of a larger column volume on the separation while leaving the injection loop volumes constant. With 10.60 μL , the 300 μm i. d. column had a 16 times higher column volume than the nano-column. The 2 and 5 μL sample loop volumes now corresponded to only 0.19 and 0.47 column volumes. Judging from the results, the micro-scale column enabled the decrease of the run-time of a single injection while maintaining separation performance. The operation at higher flow rate with larger column volume, however, automatically leads to higher sample dilution and lower total system sensitivity. This drawback could be compensated by increasing the sample injection volume. This relationship between sample consumption and system response was important for defining the goals of the method development: comparing the system sensitivity with nano- and micro-scale setup, the response was higher with the nano-configuration due to less sample dilution and higher efficiency factor of the nano-ESI. While the sensitivity was increased, the injection volume had to be decreased at the same time to avoid the exceeding of the column capacity. Consequently, sample analysis could only benefit from the increased sensitivity of the nano-scale setup when decreasing the sample volume. If sample volume is not a limiting factor, the micro-scale setup can yield a comparable system response just by increasing the sample volume by a factor of 10 from 0.5 to 5 μL . It has to be remarked that the total sample consumption per injection was 10 μL (with a loop overfill factor of 2).

Although the preparation of standard solutions for calibration purposes was established with pipettes that allowed precise liquid handling in the range between 100 and 1000 μL , it was challenging to guarantee high precision and accuracy of calibration standards below a volume of 100 μL which were necessary to profit from the nano-system sensitivity. Furthermore, the technical needle placement precision of the autosampler was found to reach its limits for the reliable and reproducible injection of sample volumes below 20 μL . Although sample vial inserts were employed to increase the sample needle immersion distance for small volumes, the response deviation between standard injections was found to be higher for standards injected from small volumes than from standards in higher volumes (50 to 100 μL). For one main goal of the work presented, the development of a reliable method for quantification, reproducibility between injections for system calibration and sample measurement was critical. Qualitative measurements, like application in proteomics, for which reproducibility and precision is of minor interest but sample amount is limited, the full advantages of nano-scale chromatography could be capitalized.

Nevertheless, the most important benefit achieved by scaling from nano- to micro-dimension is not due to chromatographic reasons in the first place but to the necessity and possibility to operate the standard ESI source at the MS inlet due to the higher flow rate. The operation of this MS interface for routine analysis proved to be much more convenient and reproducible than the operation of the nano-ESI. Details regarding ESI operation will be discussed in section 5.2.

5.2. Mass spectrometric method development

5.2.1. Operation of the nano-electrospray interface

For nano-scale chromatographic separations, a stable operation of the nano-ESI interface at flow rates between 0.25 and 0.30 $\mu\text{L min}^{-1}$ was found to be critical to achieve useful and reliable results. Especially for the aim of this study to establish a quantification method based on isotope dilution, a stable operation of the ESI interface was necessary in order to conduct the acquisition of response factors with the same sensitivity and response as sample analysis. Therefore, a stable ESI operation in a time frame of two to three weeks without the necessity of any major configuration changes had to be regarded as minimum requirement. Unstable ESI operation during single injections may lead to distorted chromatographic peaks, decreased peak intensity or even no ion signal (see Fig. 36). Variations in spray stability between injections may also negatively affect the linearity of the response curve as well as the precision of the produced analytical results. Partially blocked nano-ESI emitters lead to higher back pressure at the capillary column outlet. The junction between the nano-scale column and its capillary outlet, however, is only designed to withstand pressures of up to 200 psi. Higher back pressures produced by partially blocked emitters lead to a leak forming at the column outlet whereas the junction is (according to the manufacturer) designed to be self-healing. Consequently, the replacement of a blocked emitter yields also a regeneration of the fragile junction at the outlet of the nano-scale column. Gradually emerging emitter blockages, however, resulted in slightly shifting retention times due to leak formation during long-time experiments such as instrument calibration.

Several aspects in nano-ESI operation could be identified as critical for its stable operation. At first, the installation and connection of the nano-ESI emitter tip was found to be challenging. Improper handling of the emitter at this stage may lead to the blockage of the emitter necessitating its replacement. New fused silica emitters had to be cut at the end distal to their tip due to the emitters being delivered with a sealed distal end (see also Fig. 39). The connection of the capillary column outlet and the emitter with the transparent zero dead volume connector was controlled using a magnifying glass in order to identify possible leakages at an early stage.

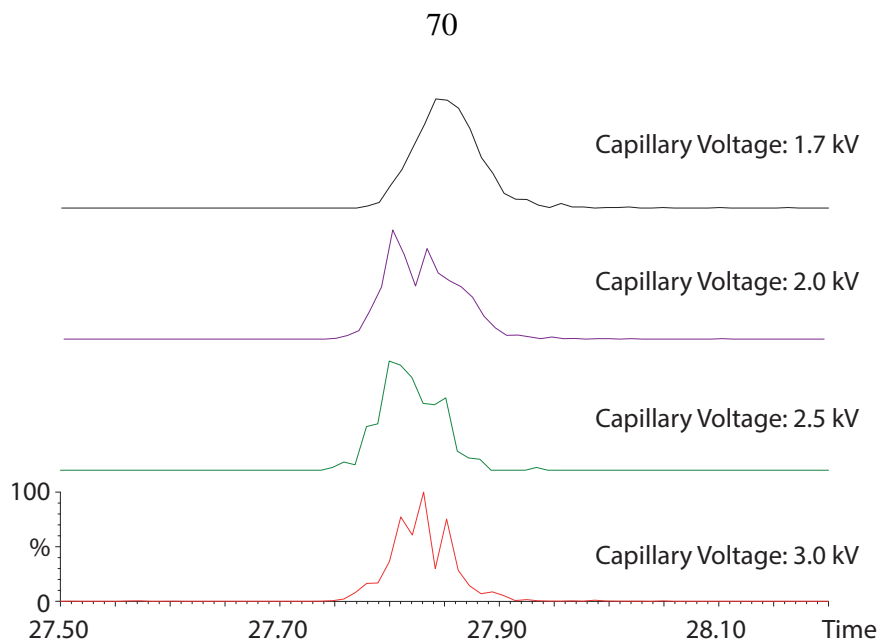


Fig. 36: Peak shape of PFHpA measured with nano-scale chromatography in direct injection configuration and negative ionization at different capillary voltages

Nevertheless, the formation of visible droplets at the outlet of transfer capillaries took approximately between 10 and 30 seconds at the employed nano flow rates and was barely visible in case of pure organic solvent due to evaporation. The connection of the column outlet with the emitter was carried out with running as well as with stopped chromatographic flow. As no clear differences regarding connection reliability could be observed, the flow was stopped during the capillary connection as this was suggested by the manufacturer of the capillary connector.

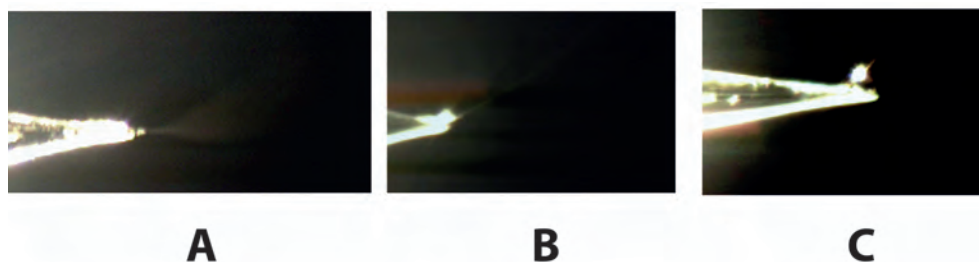


Fig. 37: Different states of nano-ESI operation observed with the microscope surveillance of the nano-ESI source: stable taylor cone (A), spindle mode (B), droplet formation (C)

Once the capillary connection was established, the capillary voltage was gradually increased until a stable spray formation could be observed (see Fig. 37 A). Usually, spray formation started at capillary voltages from 1.5 kV and stabilized at 1.8-2.0 kV. The spray stability, however, obviously varied with the following parameters:

- **Tip position:** Due to variations within the electrical field force at the MS inlet, the position of the nano-emitter influenced the formation of a stable Taylor cone. During

source tuning, a compromise had to be found to guarantee the stable formation of an electrospray and the guidance of the ion beam with good yield into the MS inlet.

- **Capillary voltage:** The electrical field force could be directly varied by the setting of the potential administered to the capillary. Especially the operation with methanol-water mixtures and highly aqueous gradients required the partial rising of the capillary voltage to 2.0 or 2.5 kV. Otherwise droplet formation did occur (see Fig. 37 C).
- **Solvent surface tension:** Due to its higher surface tension, water was obviously more difficult to spray than organic solvents. A compromise had to be found to yield a stable spray at the part of the analytical gradient during which the investigated compounds eluted.
- **Emitter aging:** Even during correct nano-ESI operation, the fused-silica emitter tip suffered aging effects such as sintering at the tip due to the high voltage. Additionally, the distal conductive coating of the emitter was suspected to wear out due to the high voltage and due to an improper capillary connection which exposes the coating to aggressive organic solvents that may decrease the lifetime of the coating.
- **Flow rate stability:** The establishment of a stable spray for calibration and tuning solutions using a syringe pump connected to the nano-ESI interface was found to be unreliable. In cases of a successful infusion with the syringe pump, the resulting ion currents were observed to be pulsating, indicating instable liquid delivery (see Fig. 38). In contrast, this behavior could not be reproduced with the binary pump (BSM) or the trapping pump (ASM) of the chromatographic system which are both optimized for the delivery of precise nano flow rates.

The emitter lifetime during this work could be considerably increased by several means. At first, a particularly clean working environment during the installation of a new emitter was mandatory to avoid the necessity of removing dust or other contamination from the conductive coating or even from the tip. Additionally, the blades of the capillary cutter had to be replaced to improve the smoothness of the cut surface and to reduce the formation of glass particles that might be pushed into the fluidic channel during capillary connection (see Fig. 39 C). Finally, the employed water purification system for the production of ultrapure water was suspected of particulate emission. During periods in which ultrapure water was used without further treatment, emitter blockages occurred frequently (see Fig. 39 D). This finding is well in accordance with experiences made by many customers of the emitter manufacturer, advising further treatment of

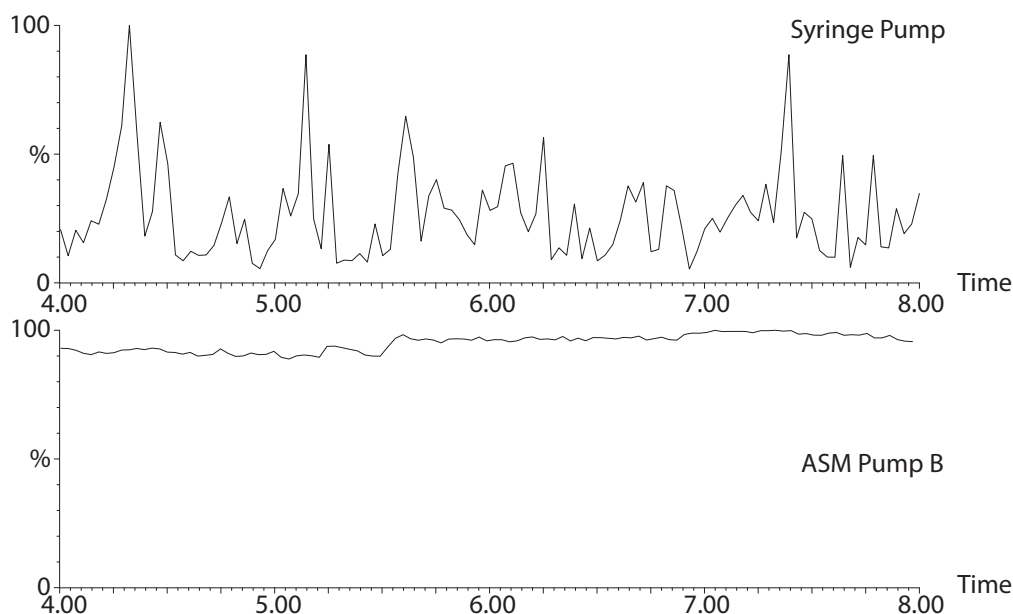


Fig. 38: Total ion current (TIC) of direct infusion of 0.1 % phosphoric acid in 50:50 acetonitrile:water (v:v) at a flow rate of $0.30 \mu\text{L min}^{-1}$ with the nano-ESI interface: the ion signal obtained with the syringe pump is pulsating compared to the signal obtained with pump B of the ASM

ultrapure water produced with water purification systems. Thus, an additional water purification step for the aqueous mobile phase employing subboiling distillation was introduced which noticeably reduced emitter blocking.

All measures discussed above allowed the continuous operation of a single emitter tip up to two months enabling extended calibration and quantification experiments with comparable sensitivity. The setup of the nano-ESI interface for negative ionization and water-methanol mixtures, however, remained unreproducible.

5.2.2. Operation of the standard electrospray interface

The operation of the standard-sized electrospray interface was only necessary and possible with micro-scale chromatography and flow rates of at least $4 \mu\text{L min}^{-1}$. In contrast to the nano-ESI, the spray formation is routinely pneumatically supported by the introduction of heated desolvation gas and nebulizer gas which both help to stabilize the obtained spray and the resulting ion beam. The stainless steel capillary appeared to act as robust emitter which was virtually immune to blockages and nonsensitive to aging. Routine replacement of the stainless steel capillary on a yearly basis was sufficient for reliable and reproducible measurements.

With the manufacturer only supplying basic values for the pneumatic parameters and the tip position, the ESI source was tuned while infusing a tuning solution of leucine-enkephalin obtained from the manufacturer at a flow rate of $4 \mu\text{L min}^{-1}$ solved in acetonitrile:water 50:50

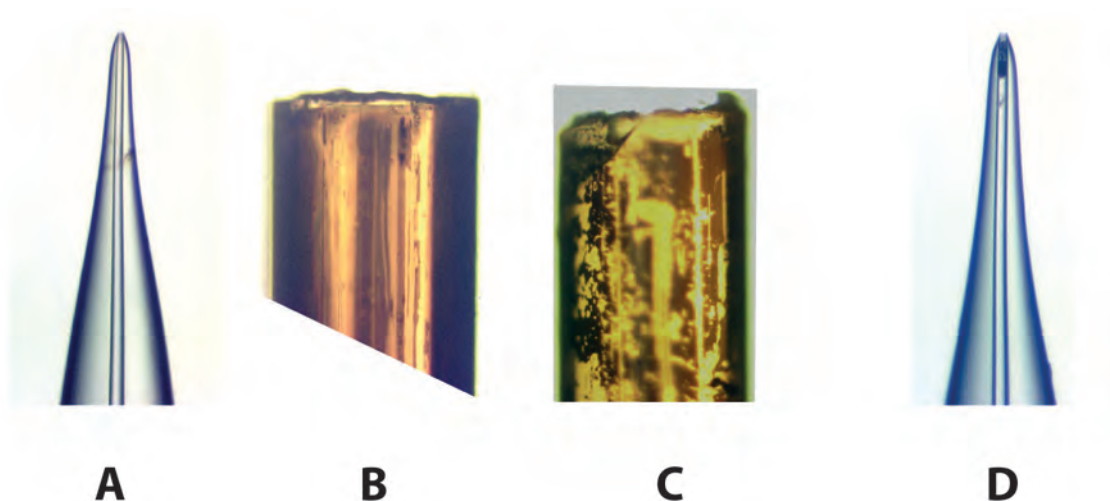


Fig. 39: Pictures of the fused silica nano-emitter obtained in the light microscope: new emitter (A), properly cut distal emitter end with conductive coating (B), irregular cut of distal end with damaged conductive coating (C), clogged emitter with visible black residue (D)

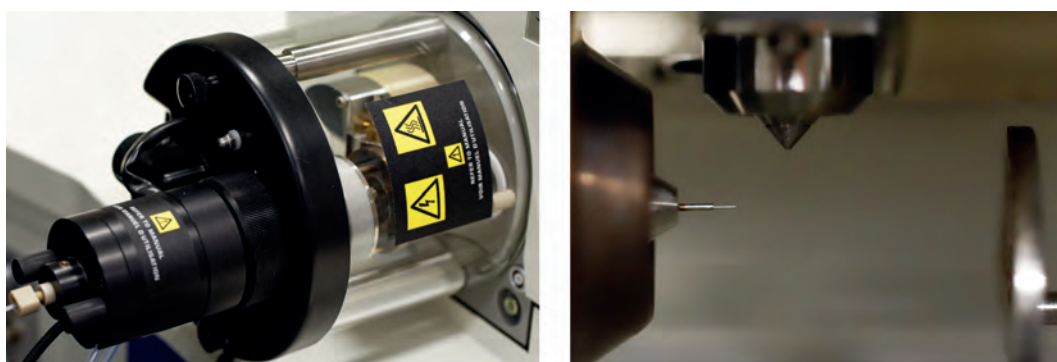


Fig. 40: Mounted standard electro spray interface with screw connection (left) and stainless steel capillary tip and sample cone tuned for operation at $4 \mu\text{L min}^{-1}$ (right) (Picture: Johannes Deyerling)

(v:v) with 0.1 % formic acid at a concentration of $1 \text{ ng } \mu\text{L}^{-1}$ with a syringe pump. Other ionizable compounds were also found suitable for source tuning, however, it was important for them being solved in a mixture that contained at least 50 % water. Otherwise the tuning resulted in pneumatic parameters that were not compatible for the spraying of highly aqueous solvents. Pneumatic parameters and the emitter tip were adjusted within the boundaries given by the manufacturer for maximizing the ion signal with the tuning solution. Compared to the nano-ESI source, the standard-sized interface performed excellently with the syringe pump yielding stable ion beams that eased the tuning process.

The stable operation with the syringe pump could be utilized for the determination of cone voltages and collision energies for the single analytes. These parameters could be used for measurements either in nano- or micro-scale due to these values being compound-specific and

thus independent from the interface.

After initial tuning, the standard-sized ion source did not require any further attention (tuned source see Fig. 40). Especially the micro-scale column outlet connected with a screw fitting to the ESI source was easier to operate than the ZDV connection in nano-scale. With the simplified operation of the ion source, method development could be focused on the laboratory sample preparation. Additionally, the time needed for the development of a micro-scale chromatographic method was obviously shorter than in nano-scale due to the reduction of time in which issues with the ion source had to be addressed.

5.2.3. Operation of the Q-TOF mass spectrometer

During method development, the MS was mainly operated in TOF-MS mode harnessing the detection capabilities of time-of-flight detection for simultaneous analysis of a wide mass range without scanning. With basic MS tuning, only singly charged positive or negative molecular ions could be expected for the analysis of small molecules. For quantification experiments, however, the product ion scan mode was also used in order to select specific target ions for fragmentation. The usage of fragmentation products for quantification was beneficial for a significant reduction of background signals in environmental samples. Even the high mass resolution in TOF-MS mode in some cases was not high enough to discriminate the target signals from the background sufficiently for peak integration.

MS instrument sensitivity was considerably influenced by the scan time which tells the instrument how many mass spectra to combine for one data point in the chromatogram. MS instrument response was found to be directly proportional to the scan time. However, the scan time had to be set with respect to peak width within the chromatogram: only results with more than 10 data points per peak were found to be sufficient for acceptable reliable peak integration and signal precision. In general, the peak width in nano-scale and micro-scale chromatography allowed a scan time of 1 s in TOF-MS mode for recording more than 10 data points per peak. Both MS modes used exhibited some drawbacks due to instrument limitations. The optimized compound-specific values for cone voltage and collision energy, determined during tuning of the MS by direct infusion of individual standard solutions, could not be directly used in TOF-MS mode: in this type of experiment, the MS software did not allow to set varying collision energies. Consequently, multi-residue analysis had to be carried out with a compromise collision energy set for the corresponding investigated group of analytes which did decrease the possible maximum sensitivity. In contrast, the cone voltage could be adjusted according to the retention time of the eluting compounds for maximizing system response. However, overlapping peaks, either caused by coelution or peak tailing, and peaks with marginal separation

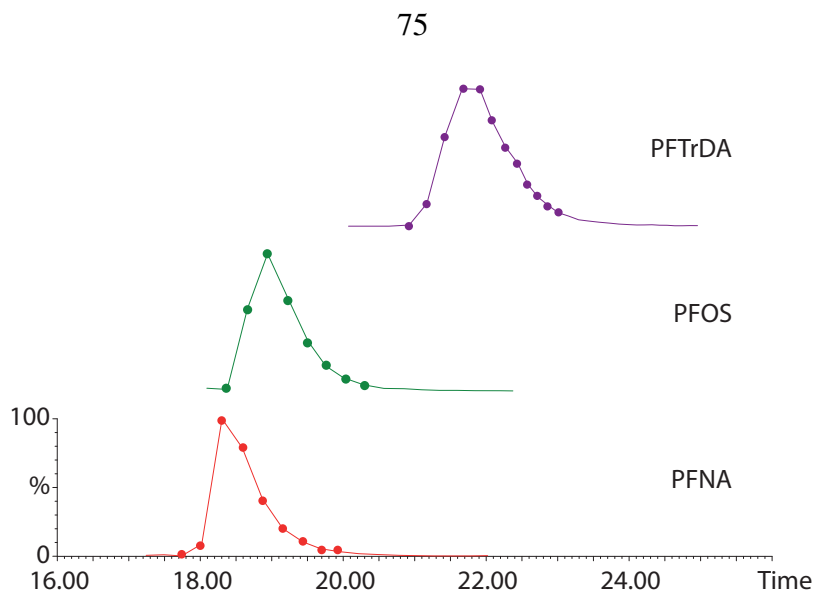


Fig. 41: Extracted ion chromatograms with indicated data points of PFNA, PFOS and PFTrDA acquired in parallel MS functions due to coelution with 2 s scan time (limited separation due to nano-scale configuration and analyte trapping)

resulted also in overlapping MS experiments called functions. Although the MS allows to process multiple functions simultaneously, it had to be recognized that depending on the scan time set, the MS processed parallel functions in alternating fashion only one at a time. Consequently, the number of recorded data points per peak was reduced by the number of parallel MS functions which can negatively affect signal reproducibility. In order to keep the recorded number of data points per peak constant, the scan time had to be reduced by half resulting in a reduction of instrument sensitivity by the same factor due to the direct proportionality. If the scan time was not adjusted, the MS method partly yielded chromatograms with a too low amount of data points per peak. Fig. 41 illustrates single mass traces of PFNA, PFOS and PFTrDA recorded in individual MS functions that had to be processed in parallel due to coelution. Using a scan time of 2 s, parallel function acquisition lead to a reduction of data points which finally yielded triangular shaped peaks. Although peak smoothing algorithms allow the interpolation of additional data points and finally produce Gaussian shaped peaks, the error regarding precision in the determination of peak area still increases. Thus, the results were not regarded as suitable for quantitative measurements.

The product ion scan mode or MS/MS mode allowed to set both compound-specific parameters, cone voltage and collision energy, individually for each MS function. Therefore, each compound could be analyzed with optimized MS tuning. Once again, the processing of multiple MS functions at the same time, however, negatively affected instrument sensitivity and the amount of data points. Especially for quantitative measurements with stable isotope dilution, the coelution of native compounds and isotopically labeled equivalents was obviously inevitable.

Table 5.4: Peak area of internal standards (IS) determined in TOF-MS and MS/MS mode achieved by injecting 0.5 μ L of a calibration standard for pharmaceuticals and polar pesticides

Compound	IS Area TOF-MS	IS Area MS/MS
Sulfamethoxazole-D4	133.2	45.7
Simazine-D5	261.3	60.1
Carbamazepine-D10	120.7	175.1
Atrazine-D5	209.8	144.0
Naproxen-D3	4.3	7.9
Linuron-D6	7.0	2.8

With the quadrupole MS selecting specifically one ion for fragmentation, two parallel MS functions were necessary to acquire the signal for the native and mass-labeled compounds at the same time. Consequently, coelution or nearby elution of two individual substances with corresponding isotopically labeled standards resulted in an overlap of four MS functions, decreasing sensitivity down to one fourth. Nevertheless, the background reduction in MS/MS mode in some cases compensated decreased MS sensitivity. Table 5.4 exemplarily lists the peak areas of internal standards (pharmaceuticals and pesticides) in subsequent injections acquired in TOF-MS and MS/MS mode. For sulfamethoxazole, simazine, atrazine and linuron the system response clearly decreased applying MS/MS measurements. This observation is not only due to simultaneous MS functions but also due to different fragmentation behaviour and efficiency of the single molecules. Peak area comparison for carbamazepine and naproxen demonstrated that benefits from compound-specific tuning parameters and compound fractionation could also overcompensate the drawbacks in instrument sensitivity in MS/MS mode.

MS/MS and TOF-MS methods employing multiple functions were dependent on stable retention times as the compound-specific parameters were saved in fixed time frames. Retention time shifts, like observed during operation with nano-scale separation, were compensated by using longer MS functions that exhibited a certain safety margin around analyte signals (see Fig. 42). However, the MS function overlap had to be increased for covering these safety margins. Additionally, MS methods including multiple functions had to be adjusted frequently while working with nano-scale separation. Especially the day-to-day variation resulted many times in large retention time shifts that lead to only partially recorded signals rendering further processing impossible.

Another important aspect regarding partial MS function overlap is the possible negative influence on response linearity. Although this relationship could not be doubtlessly confirmed with results obtained during instrument calibration, instrument sensitivity may change during acqui-

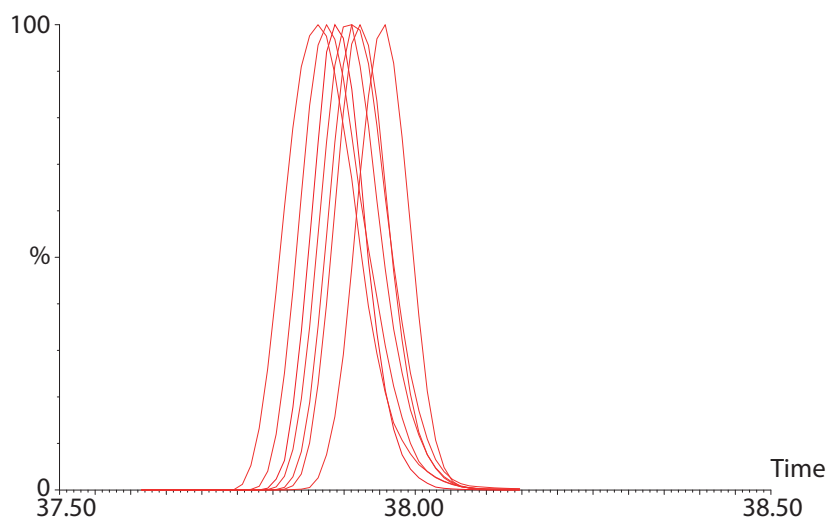


Fig. 42: Overlapping extracted ion chromatograms of mass labeled PFNA during injection of different calibration standards with nano-scale chromatography and direct injection

sition if MS functions from other compounds start or end during the elution window of another compound. Overlapping functions were particularly necessary for acquiring the signals for all PFAAs including PFCAs and PFAS with their corresponding isotopically labeled IS in one single analytical run. Fig. 43 A illustrates the resulting MS function layout as indicated by the instrument software. Each row and bar represents an individual MS/MS function. Simultaneous pairs of bars represent the acquisition of native and labeled compounds in parallel. The PFAA method appears particularly crowded in the middle due to the coelution of PFCAs and PFAS. Ending MS functions in the middle of an elution window of another compound lead to a MS sensitivity increase by 50 % within peak acquisition. This issue was addressed by separating the analysis of PFCAs and PFAS into two individual analytical runs which avoided overlapping MS functions between single compounds to a large extent (see Fig. 43 B). The total time necessary to establish a complete instrument calibration for PFAA quantification, however, was doubled by this approach.

The dynamic range of the MS with a TDC as the ion counting device (see section 2.2.) was limited from 0 to approximately 400 counts per second for each individual mass channel. Signals with higher intensity saturated the detector and significantly deviated from linear response. In this case, the intensity was underestimated and the resulting data point was situated below the linear response curve. Fig. 44 B and C show the centered mass spectra recorded for atrazine with 10 and 80 $\text{pg } \mu\text{L}^{-1}$ concentration, respectively. For the molecular ion with highest intensity at m/z 216, a shift of the centroid of m/z 0.0065 was observed due to detector saturation. Thereby, the maximum ion current at m/z 216 was 429 and 1580 counts per second for the 10 and 80 $\text{pg } \mu\text{L}^{-1}$ standard, respectively. Nevertheless, the detector saturation occurred individu-

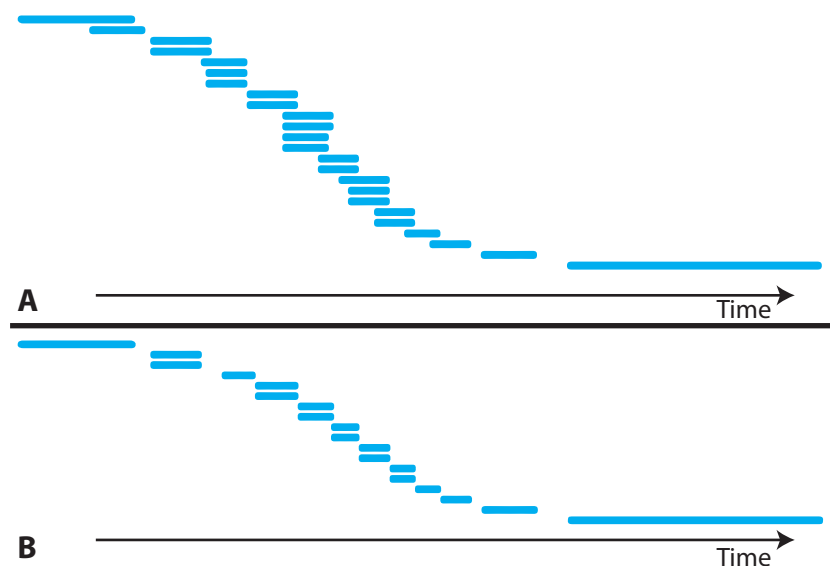


Fig. 43: Individual MS functions indicated as bars in single rows against the method time: (A) combined MS/MS method for the detection of PFCAs and PFAS, (B) PFCA-only MS/MS method for avoiding MS function overlap between PFAAs

ally in dependence on the mass channels. This is due to the fact that ions of identical m/z -values saturate the detector only at specific point of time. Consequently, ions of other m/z -values arriving at a different point of time, are not affected by the saturation of a specific mass channel. Therefore, compounds achieving high system response could still be quantified by choosing less intensive ions from their isotopic pattern for quantification. This technique could also be applied to already acquired datasets as postprocessing due to the ability of TOF-MS always to record all ions in parallel.

The benefits regarding background reduction achieved in MS/MS mode in combination with the preservation of the sensitivity and parallel detection ability known from TOF-MS mode could be established with a new approach. Unlike in MS/MS mode, the new approach included quadrupole scanning for the transmission of molecules of a wide mass range into the collision cell. An elevated collision energy resulted in the fragmentation of all ions while the TOF-MS allowed the sensitive and precise detection of all formed fragmentation products in parallel. The resulting all ion fragmentation (AIF) method was introduced while operating the micro-scale chromatography setup. For AIF experiments, the instrument was basically set to TOF-MS mode with elevated collision energy. As already discussed previously, the MS software only allowed to set a fixed collision energy for TOF-MS runs. Consequently, the presented AIF method suffered the application of a fixed collision energy for the fragmentation of all investigated compounds. This lead to a higher degree of fragmentation for some compounds and for others to incomplete fragmentation. The fractionation of mass labeled and native compounds side-by-

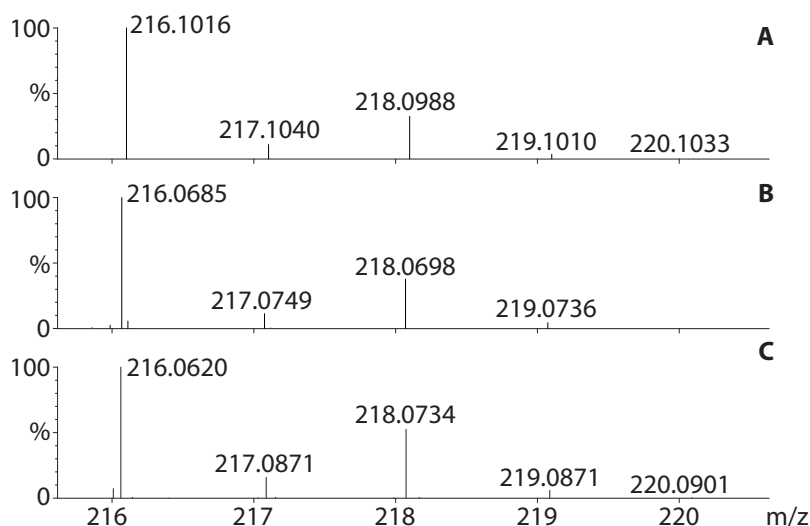


Fig. 44: Centered MS spectra of atrazine: (A) predicted spectrum of MH^+ -ion, (B) spectrum during maximum intensity of $10 \text{ pg } \mu\text{L}^{-1}$ standard, (C) spectrum during maximum intensity of $80 \text{ pg } \mu\text{L}^{-1}$ standard

side lead in rare cases to the formation of product ions with the same mass. Consequently, this particular transition was unavailable for quantification. Nevertheless, other transition pathways could replace unintended overlap in those cases. In total the AIF method exhibited several benefits:

- **Retention time independency:** The AIF method was set up as a single MS function for the whole chromatographic run eliminating the necessity of adjustment of the MS method for compound retention times. Even in the case of a retention time shift (e. g. due to differing fraction of organic solvent in a sample), the analytic results still remained processable. In total, the MS operation was simplified as one general AIF method could be used for all analytes.
- **Parallel detection:** Due to the detection of coeluting substances side-by-side, the AIF mode was particularly suitable for isotope dilution analysis. While only one MS function had to be processed at a time, the MS acquired enough data points per peak even if multiple analytes had to be detected simultaneously.
- **Background reduction:** By analogy with the MS/MS mode, the detection of fractionation products (daughters) from the corresponding parent molecules lead to the reduction of chemical background noise during the analysis of laboratory and environmental samples. The specifically monitored ion transitions decreased the probability of analytic background of similar parent mass but different molecular structure to yield a fractionation product of the same mass at a given collision energy.

- **Improved sensitivity:** The operation of the quadrupole mass analyzer in scanning mode resulted in higher ion transmission yields than using the quadrupole as mass analyzer in MS/MS mode for the selection of a precursor ion for fragmentation. Additionally, all fragmentation products could be detected in parallel with only a single TOF-MS function avoiding the sensitivity-decreasing simultaneous function processing.
- **Fractionation of unknowns:** The AIF method allowed the fractionation of unknown compounds in cases of non-target analysis. Therefore, TOF-MS data acquired at low collision energy in a separate run accompanied with AIF data could be used for the identification of unknown compounds with fractionation databases in non-target analysis.

In summary, two MS modes were found to be particularly suitable for application in a method for quantification. The TOF-MS mode with low collision energy was applicable for instrument calibration, tuning and chromatographic method development. Furthermore, this MS method was used for gathering data of non-fractionated, singly charged molecules for non-target analysis. Besides, the mode could also be used for quantification purposes in cases where analytical background did not negatively affect the peak shape in extracted ion chromatograms. The TOF-MS mode with higher collision energy (in this work called AIF mode) was developed as a compromise for the application in environmental sample analysis achieving background reduction while preserving comparably high sensitivity. Moreover, fractionation data of unknown compounds was gathered within the same analytical run used for the quantification of known targets.

5.3. Instrumental calibration and linearity

5.3.1. Nano-scale chromatography with direct injection

The establishment of a system calibration while operating the instrument with nano-scale chromatography was found to be a challenging task due to the instability of the ion beam. Nevertheless, progress in nano-ESI operation (see section 5.2.1.) allowed the stable operation for prolonged time periods enabling the determination of response factors. Reasonable results were only obtained in nano-scale chromatography with direct injection. The limited separation and severe peak tailing apparent with analyte trapping configuration rendered calibration purposes with this fluidic configuration difficult.

For pharmaceuticals and polar pesticides, a 10-point calibration from 0 to 450 pg μL^{-1} resulted in an acceptable system response with an injection volume of 0.5 μL . Within the standards in

solvent A:B 90:10, the absolute response for naproxen and linuron was weak, therefore, an additional calibration run for these two substances was necessary with standards solved in A:B 50:50. The correlation coefficient listed in Table 5.5 indicated a good linear fit ($R^2 \geq 0.99$) for all substances of this group and the relative standard deviation of the IS signal represented stable ESI conditions with values below 10 %. Additionally, the slope of the calibration curve was near 1 for most of the compounds indicating a balanced response between the native and mass-labeled standard substance.

Table 5.5: List of parameters and results from system calibration obtained with nano-scale chromatography and direct injection; pharmaceuticals and polar pesticides were calibrated with single injections, PFAAs with triplicate measurements

Compound	Ion-ization [+/-]	Solvent Composition [A:B]	Correlation Coefficient R^2 []	Slope []	RSD IS Response [%]	IDL [pg μL^{-1}]
Sulfamethoxazole	+	90:10	0.997	1.02	8.5	15.7
Simazine	+	90:10	0.996	1.06	6.5	40.2
Carbamazepine	+	90:10	0.990	0.83	4.0	29.7
Atrazine	+	90:10	0.990	0.97	4.7	22.5
Naproxen	+	50:50	0.995	0.67	4.0	55.0
Linuron	+	50:50	0.996	0.95	6.1	45.2
PFPeA (n=5)	-	100:0	0.987	0.65	27.5	4.4
PFHxA (n=6)	-	100:0	0.999	0.80	27.5	3.4
PFHpA (n=7)	-	30:70	0.993	1.14	15.6	2.2
PFOA (n=8)	-	0:100	0.994	0.98	58.4	0.58
PFNA (n=9)	-	0:100	0.996	0.95	56.3	1.06
PFDA (n=10)	-	0:100	0.993	0.92	53.5	1.8
PFUdA (n=11)	-	0:100	0.992	0.98	45.2	1.4
PFDoA (n=12)	-	0:100	0.996	0.88	12.7	1.7
PFTTrDA (n=13)	-	0:100	0.978	0.73	12.7	-
PFTeDA (n=14)	-	0:100	0.957	0.62	12.7	-
PFHxDA (n=16)	-	0:100	0.779	0.42	12.7	-
PFODA (n=18)	-	0:100	0.789	0.03	12.7	-
PFBS (n=4)	-	100:0	0.990	5.74	20.7	8.1
PFHxS (n=6)	-	30:70	0.994	1.10	15.6	11.6
PFOS (n=8)	-	0:100	0.990	0.92	33.5	6.5
PFDS (n=10)	-	0:100	0.985	0.56	33.5	13.9

In this case, naproxen displayed an exception with a slope of 0.67, indicating a lower response for the native substance within the standard than for the mass-labeled one. The presented values

were determined with a single injection of each standard solution. With a total run time of one hour per injection, the total system calibration for positive ionizing pharmaceuticals and polar pesticides took 24 hours of measurement time including 4 blank injections. Therefore, the IDL was determined combining three individual calibration attempts. Although variations of the instrument response should have been compensated by IS correction, the standard deviation between the single calibration experiments resulted in high IDLs between 15.7 and 55.0 pg μL^{-1} . The standard deviation between the independent calibration attempts might have also been increased by the absolute error of standard amounts during liquid handling. The detection of the negative ionizing pharmaceuticals, ibuprofen and diclofenac, was not possible with the nano-chromatography setup. The lower system response in negative ion mode in combination with a low sensitivity for these compounds rendered their calibration not suitable for further measurements.

The absolute response of PFAAs in the nano-ESI with negative ionization was high. Therefore, 0 to 100 pg μL^{-1} was chosen as the calibration range for this group of compounds and an injection volume of 0.5 μL was set. The large group of homologs helped to identify the limitations of the detection system. The detailed calibration results are also listed in Table 5.5. In order to increase the analytical span of the instrumental setup, three complete calibration standard series were prepared in solvent A:B 100:0, 30:70 and 0:100. The calibration standards solved in A:B 100:0 and 0:100 were injected in triplicate which improved the estimation of the IDL.

The PFCA with the shortest chain, PFBA, was not detectable. Additionally, the results indicated a lower linear fit and low response for PFCAs with a higher chain length than 12. Reasonable response was achieved only for PFAAs with a chain length between 5 and 10. The correlation coefficient of the linear regression indicated a good linear response for these PFAAs. The high relative standard deviation of the IS of up to 56.3 % indicated unstable nano-ESI operation in negative ion mode caused mainly by water-methanol mixtures as mobile phase which proved to be more challenging for stable spray formation. Thus, the more unreliable response for PFPeA, PFTrDA, PFHxDA, PFODA and PFDS could be also explained due to them not existing as isotopically labeled counterpart in the IS mixture. For these compounds, the mass-labeled homolog with the lowest difference in carbon chain length was chosen for internal standard correction (see Table 4.1 for IS mapping). In case of spray instabilities, however, the system response varies in dependence of the gradient time. For compounds not contained in the mass-labeled IS mixture, the IS response correction was unable to compensate for spray fluctuations as an IS with different carbon chain length elutes at a different point of time and thus under different nanospray conditions. For compounds with corresponding mass-labeled substance, however, the high absolute signal fluctuations could be successfully compensated. Isotope dilution anal-

ysis in this case helped to correct for analyte loss and matrix effects in environmental samples as well as for signal instabilities originating from nanospray formation. Structural differences between mass-labeled and native standards were reflected in the slope of the calibration curve. Long-chain PFCAs ($n > 12$) with low response resulted in slope values smaller than 1 due to the corresponding mass-labeled standard yielding higher response. The signal for PFBS was particularly higher than the signal from the corresponding IS (PFHxS) resulting in a steeper calibration curve.

The estimated IDL values for PFAAs were clearly lower than the values determined for positive ionizing pharmaceuticals and polar pesticides. This observation might be explained by the concentration of only $1 \text{ pg } \mu\text{L}^{-1}$ of the PFAA standard which was used for IDL estimation. Additionally, all three measurements were carried out with the same calibration standards and did not originate from separately prepared calibration dilutions as it was the case for pharmaceuticals and polar pesticides.

5.3.2. Micro-scale chromatography with direct injection

The basic parameters regarding instrument calibration could be transferred from nano-scale to micro-scale chromatography. The lower system response during operation with micro-scale chromatography could be compensated by increasing the injection volume by the factor 10 from 0.5 to 5 μL . Consequently, the calibration range for the single compounds could be kept similar to the range used in nano-scale. The results of the micro-scale system calibration are listed in Table 5.6.

The calibration for positive ionizing pharmaceuticals and polar pesticides was carried out at 10 concentration levels from 0 to 450 $\text{pg } \mu\text{L}^{-1}$ as for the nano-scale setup. The signal intensity for positive ionizing pharmaceuticals and polar pesticides was high enough to calibrate all compounds solved within solvent A:B 90:10. Moreover, the application of the pneumatically stabilized standard ESI source allowed the quantification of negative ionizing pharmaceuticals with water-methanol mixtures as mobile phase. The correlation coefficient indicated a good linear fit and the relative standard deviation of the IS below 10 % represented stable ESI operation. The deviation of the slope from 1 was higher compared to the results obtained with nano-ESI indicating a more unbalanced response between native and mass-labeled compounds which rather was a result from standard preparation than from the instrumental setup. With micro-scale separation, the runtime of a single injection could be reduced to 35 min, thus a system calibration for positive ionizing pharmaceuticals and polar pesticides with single injections took 7 hours of measurement time. The establishment of a corresponding calibration with triplicate measurements took 20 hours which was still 4 hours less than for nano-scale separation and

single injections. The more stable and reproducible operation is also reflected by particularly decreased IDL-values in comparison to the nano-scale setup which were now all below the concentration of the lowest standard concentration ($50 \text{ pg } \mu\text{L}^{-1}$). The compound naproxen which could be detected in positive and negative ionization mode demonstrated the general drawback experienced with negative ionization. Although the absolute response of this compound was higher with negative ionization, a lower IDL could be achieved with positive ionization. This result could be explained by a more stable ion beam during positive operation which reduced the standard deviation between injections, also reflected by the RSD of the internal standard.

Table 5.6: List of parameters and results from system calibration obtained with micro-scale chromatography and direct injection with triplicate measurements for pharmaceuticals and polar pesticides and single measurements for PFAAs

Compound	Ion-ization [+/-]	Solvent Composition [A:B]	Correlation Coefficient R^2 []	Slope []	RSD IS Response [%]	IDL [pg μL^{-1}]
Sulfamethoxazole	+	90:10	0.996	1.02	4.1	9.8
Simazine	+	90:10	0.994	1.31	8.3	5.9
Carbamazepine	+	90:10	0.991	0.95	5.0	15.1
Atrazine	+	90:10	0.996	1.47	7.3	4.9
Linuron	+	90:10	0.990	0.97	8.5	7.4
Naproxen	+	90:10	0.996	0.73	6.5	9.26
Naproxen	-	70:30	0.993	1.47	9.4	16.3
Diclofenac	-	70:30	0.995	0.76	7.6	4.4
Ibuprofen	-	70:30	0.991	1.47	7.0	16.8
PFPeA (n=5)	-	100:0	0.980	0.40	15.8	6.1
PFHxA (n=6)	-	100:0	0.993	1.09	15.8	3.0
PFHpA (n=7)	-	100:0	0.997	1.47	15.8	0.3
PFOA (n=8)	-	40:60	1.000	1.11	10.3	2.2
PFNA (n=9)	-	40:60	1.000	1.08	12.8	1.2
PFDA (n=10)	-	40:60	0.996	0.84	21.7	1.5
PFUdA (n=11)	-	40:60	0.995	1.03	40.0	12.4
PFDoA (n=12)	-	40:60	0.992	1.50	65.8	5.8
PFTTrDA (n=14)	-	40:60	0.984	1.02	65.8	15.4
PFTeDA (n=15)	-	40:60	0.855	0.51	65.8	13.2
PFHxDA (n=16)	-	40:60	0.553	0.06	65.8	-
PFBS (n=4)	-	100:0	0.995	0.60	8.6	3.9
PFHxS (n=6)	-	40:60	1.000	1.43	10.5	3.4
PFOS (n=8)	-	40:60	0.996	1.47	11.1	9.6
PFDS (n=10)	-	40:60	0.992	1.37	11.1	2.9

The PFAA response with micro-scale chromatography was recorded with serial-diluted standards of the concentration 200, 100, 50, 25, 12.5 and 0 $\text{pg } \mu\text{L}^{-1}$ and an injection volume of 5 μL . With the micro-scale setup being less dependent on solvent composition, the standards only had to be dissolved in mobile phase A:B 100:0 and 40:60 in order to achieve a sufficient response coverage for PFAAs reducing calibration effort and runtime. The detailed calibration parameters recorded for PFAAs with the micro-scale setup are also listed in Table 5.6.

PFBA was again not detectable even in the standard solved in pure solvent A. The linear fit was good for PFCAs with a carbon chain length from 6 to 12. Moreover, correlation coefficients larger than 0.99 were achieved for all PFAS. IS signal intensities, however, varied with up to 65.8 % indicating less stable spray formation when operating in negative mode with water-methanol mixtures. This fact also influenced the IDL for PFAAs. Especially PFCAs with a longer carbon chain than 10 suffered higher IDLs due to the lower total system response. Moreover, the standard concentration for IDL determination was higher at 12.5 $\text{pg } \mu\text{L}^{-1}$ than for nano-scale experiments due to the different dilution scheme.

5.3.3. Applicability of the instrumental calibrations for quantification

Judging the results, both instrumental setups and calibrations could be used for quantification purposes. Considering the calibration parameters only, however, is not sufficient to account for the applicability of the nano- and micro-scale calibration. The increased effort necessary during nano-scale operation, especially for negative ionization, resulted in several drawbacks in comparison to the micro-scale fluidic configuration.

The necessity for the preparation of three independent standard dilutions particularly increased the amount of standards needed for system calibration. With running the calibration prior each sample batch run, especially the amount of isotopically labeled PFAAs grew considerably high although calibration standards were prepared in small aliquots of 50 μL . Besides, the sample consumption and preparation time increased due to the reconstitution in three different mobile phase compositions. In fact, the benefit of low sample consumption (0.5 μL instead of 5 μL) of the nano-scale chromatography system was vanished because of the preparation of each sample being only possible with sample amounts above 10 μL that could still be precisely handled with pipettes in the laboratory. The total analysis time for one sample regarding all analytes with positive and negative ionization took several days. In addition, the necessary change of mobile phase for the switching between positive and negative ionization required frequent re-tuning or replacement of the nanospray emitter. Furthermore, with calibration experiments prior sample injection taking more than 24 hours, nanospray stability during quantification experiments evolved to be a critical factor. The most important drawback of the nano-scale setup, however,

proved to be the reproducibility of the system response. The determination of detection limits already indicated high standard deviations between injections. Finally, the calibration results for negative ionizing PFAAs presented in section 5.3.1. could not be reproduced at a later point of time due to severe difficulties in tuning and stabilizing the nanospray for operation with water-methanol mixtures. An increase of injection volume lead to band broadening and could not be utilized to compensate lower system response.

In contrast, the micro-scale setup allowed reproducible calibration and analysis in a decreased amount of time. Especially analysis with negative ionization and water-methanol mixtures could be carried out more reliably. Due to the lower time per analytical run, system response factors determined with three injections of each standard concentration could be utilized as reference. Calibration experiments determined with single injections were used for system calibration prior sample analysis. Standard and sample consumption were reduced because of a lower dependency of the chromatography on the sample solvent. Moreover, sample preparation was simplified with only less solvent reconstitution steps being necessary. The sample volumes between 20 and 50 μL already utilized with nano-scale analysis were also applicable for 5 μL full-loop injections during micro-scale analysis. Consequently, no further adjustments from the procedures developed during nano-scale analysis were necessary. More stable operation also lowered the IDL for the single analytes. Especially positive ionizing compounds could be detected more reproducibly and sensitively. All in all, the calibration results and the operational aspects observed during system calibration clearly indicated the micro-scale setup being more suitable for the application in routine analysis and quantification. It was possible to demonstrate that a reasonable calibration with the nano-scale setup is possible, too, albeit with an uneven higher operational effort.

5.4. Laboratory recovery experiments

5.4.1. Selection of a solid-phase extraction chemistry

Different SPE cartridges were evaluated for their applicability in cleanup of positive ionizing pharmaceuticals and polar pesticides. This experiment was carried out at an early stage of instrumental method development during tests with nano-scale chromatography and analyte trapping which was not the final recommended configuration for quantification experiments (see section 5.1. and 5.3.). Thus, the recovery evaluation also included the analytes atenolol and paracetamol that were not quantified within the final method.

The determined cleanup recoveries are illustrated in Fig. 45. The two groups of compounds were separated for improved visibility and the analytes were sorted within each group according

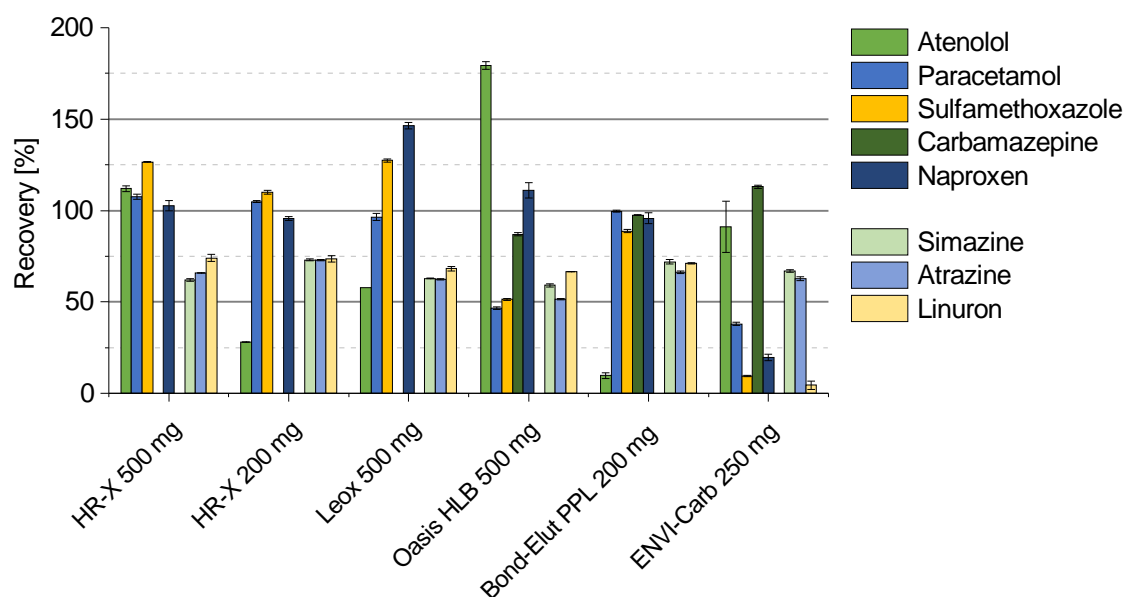


Fig. 45: Recoveries of positive ionizing pharmaceuticals and polar pesticides from spiked 1 mL water solutions; mean value of two measurements ($n=2$); carbamazepine was not included in the experiments

to an ascending log P -value. The recovery of pharmaceuticals varied to a large extent between 10 and 180 % which demonstrated the importance of SPE phase selection. The in total lowest recovery for pharmaceuticals was experienced with the cartridge containing graphitized carbon black (ENVI Carb). All PS-DVB based sorbents achieved recoveries higher than 50 % for most pharmaceuticals. However, especially the highly polar compound atenolol ($\log P=0.16$) challenged the tested SPE cartridges. Regarding the HR-X cartridges, atenolol breakthrough could be avoided with a higher amount of sorbent. With the Bond-Elut PPL cartridge, similar breakthrough behavior could be observed which might have been compensated by an increased amount of sorbent, too. The Oasis HLB cartridge disturbed the quantification of atenolol which lead to intensive signal enhancement. For the Leox cartridge, a trend between ascending log P -value and recovery could be observed, indicating a retention mechanism predominantly based on reversed-phase. However, a more balanced recovery distribution was necessary for the given application. Therefore, the results achieved with Bond-Elut PPL and the 500 mg HR-X cartridge proved to be promising. The results represent the challenging task of retention for a structural highly irregular shaped group of analytes. Nevertheless, all investigated pharmaceutical residues consist of at least one aromatic ring. Different substitution patterns, however, result in steric differences and a high log P range of 3.04 between atenolol and naproxen that has to be retained by the SPE sorbent. The hydrophobicity of the co-polymeric sorbent PS-DVB is reduced by the introduction of polar modifications by the usage of monomers with heterocycles or polar residues in mixture with styrene and divinylbenzene during sorbent production.

According to the degree of polar modification, the retention behaviour for the polar pharmaceutical residues varied. Consequently, the results suggested a higher degree of polar modification of the HR-X chemistry than for the other tested SPE phases.

Regarding the pesticides simazine, atrazine and linuron, recovery was more balanced between the single PS-DVB cartridges. Although the ENVI-Carb cartridge failed to retain the most lipophilic compound linuron, all other cartridges achieved recoveries larger than 50 %. Again the Bond-Elut PPL as well as the HR-X cartridges were able to gain the highest recoveries of up to 74 %. The more comparable retention of these analytes could be explained by structural similarities. In atrazine and simazine a 1,3,5-triazine represents the core structure whereas linuron consists of a substituted benzene ring. Nevertheless, both core structures are aromatic. All three herbicides contain chloro-atoms attached to their aromatic core which invokes a reduction of electron density within the aromatic ring. Besides, the compounds exhibit nitrogen bridged alkyl substitutions attached to their core. In case of linuron, urea can be identified as structural motive within this substitution. Atrazine and simazine have the highest similarity and are only discriminated by one methyl-group at a nitrogen bridged sidechain. The structural similarity of these compounds is also reflected by their smaller $\log P$ -value difference of 1.02 compared to the investigated pharmaceuticals. With their aromatic ring structure, the retention mechanism of the pesticides on PS-DVB and carbon phases can be expected to be based on π - π -interactions besides hydrophobic interaction. Therefore, PS-DVB cartridges were particularly suitable for the retention of small organic molecules with aromatic ring structure. The observed differences between the single PS-DVB sorbents might also be explained by certain structural modifications that the manufacturers introduce into the polymers in order to influence polarity and hydrophobicity of the sorbents as mentioned above. With these modifications being not available to the public and with retention predictions being challenging anyway, a suitable SPE sorbent bed could only be judged by empirical testing.

All in all, the HR-X cartridge with 500 mg sorbent appeared to show a balanced performance for the retention of highly polar pharmaceutical residues as well as a reasonable recovery of the three investigated polar pesticides. Comparable performance was achieved with the Bond-Elut PPL cartridge with only a sorbent bed of 200 mg which remarkably avoided signal enhancement and only lacked the retention of the highly polar atenolol. Based on the results, HR-X cartridges with 500 mg sorbent were used as laboratory cleanup step for environmental samples.

5.4.2. Syringe filter evaluation

With both the nano- and micro-scale chromatography system not being protected by in-line filters or specific guard columns, an additional sample cleaning step was evaluated just before injection as a precautionary method to avoid the build up of excessive back pressure or even total column blockages, increasing the total lifetime of an analytical column. Therefore, centrifugation or filtration prior to injection were considered as possible precautionary methods. To judge the applicability of syringe filters for final sample cleanup, clean standard test solutions were filtered prior to injection through a polytetrafluoroethylene membrane (PTFE), a hydrophilic polypropylene membrane (GHP) and a regenerated cellulose membrane (RC) and the signal was compared against the one of an unfiltered standard solution of the same concentration. In general, analyte loss was expected due to interaction of target compounds with the membrane material.

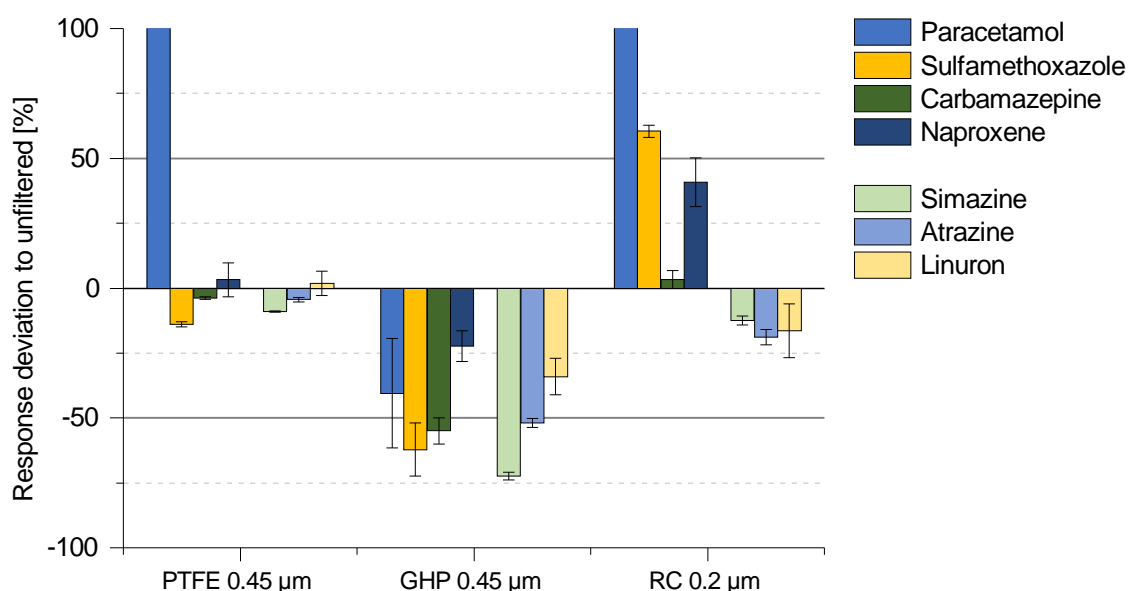


Fig. 46: Response deviation of syringe filtered standard solutions to unfiltered standard of native positive ionizing pharmaceuticals and polar pesticides (non-IS corrected, n=3)

The determined relative response deviation to the signal in the unfiltered standard solution is represented in Fig. 46. Obviously, the analyte content within the filtered standard solutions differed from the unfiltered solution. Predominantly, analyte loss of up to 75 % could be observed. The smallest deviations from the reference solution were achieved with the PTFE filter. Nevertheless, this membrane type introduced analytical interferences for paracetamol leading to a signal enhancement of more than 100 %. The GHP membrane negatively affected the response of all monitored target compounds resulting in a signal suppression of up to 75 %. With the RC membrane, acceptable performance for polar pesticides could be achieved but an-

alytical background for the determination of pharmaceutical residues was introduced leading to overdetections of more than 50 %.

The GHP membrane is known to offer low protein binding affinities making it especially suitable for the filtration of proteinaceous samples. Moreover, the membrane is resistant against organic acids and aggressive organic solvents. However, the results suggested that this membrane type is not suitable for application in organic trace analysis of small molecules. Syringe filters with RC membrane are commonly suggested for standard HPLC sample preparation with compatibility for water, acetonitrile and methanol solutions. The presented results however indicated the introduction of background resulting in a strong influence on the analytical results. Thus, this membrane could not be recommended for the intended use in trace analysis. Finally, PTFE membranes appeared promising for the filtration of solutions containing aggressive organic solvents. The polymer, consisting of thoroughly fluorinated carbon chains, does not exhibit any active centers for analyte adsorption which resulted in the highest analyte recoveries for all tested compounds. Furthermore, the membrane did not introduce analytical background except for the analyte paracetamol. However, the filter membrane generated high back pressures during filtration due to the membrane being hydrophobic and not wettable by the aqueous sample.

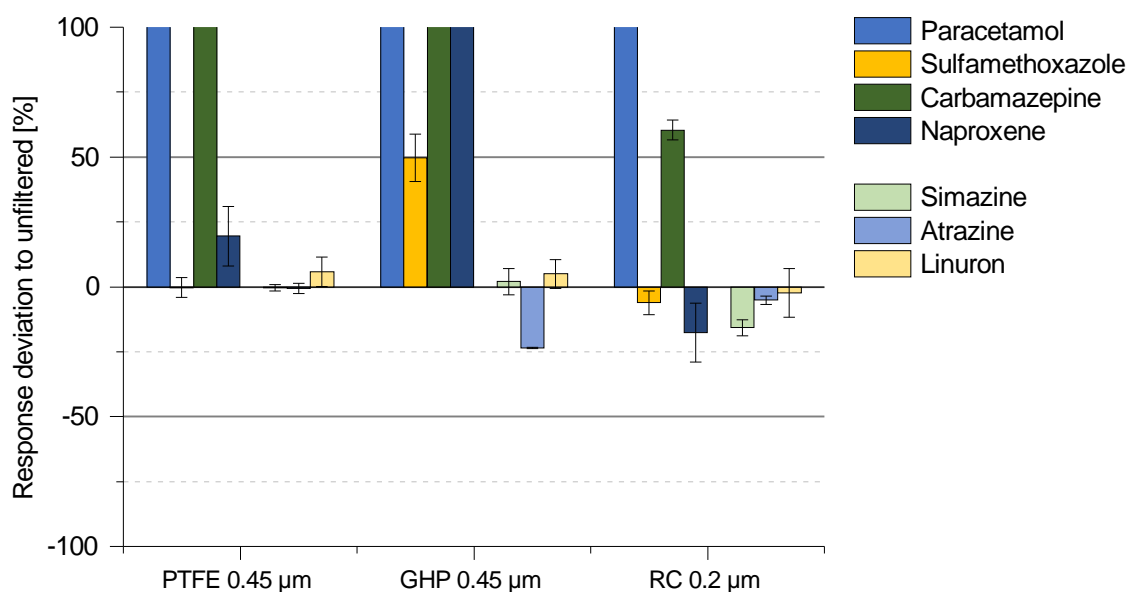


Fig. 47: Response deviation of syringe filtered standard solutions to unfiltered standard of native positive ionizing pharmaceuticals and polar pesticides (non-IS corrected, n=3)

With the standards containing isotopically labeled sulfamethoxazole, simazine and atrazine, results could be corrected with the corresponding internal standard signals. The IS-corrected results are presented in Fig. 47. In comparison to the uncorrected results in Fig. 46, the signal deviation due to matrix effects and analyte loss could be reduced down to 0.02 % in mean for sub-

stances with corresponding IS. The remaining pharmaceuticals were corrected with the signal of mass-labeled sulfamethoxazole whereas linuron was corrected with mass-labeled atrazine. In most cases, however, this IS assignment lead to severe overcorrection of the analyte signals. Consequently, probable mechanisms explaining response deviations like adsorption onto the filtration membrane or background interferences appeared to be highly compound specific and could only be corrected with structurally identical isotopically labeled substances as IS.

The evaluation of syringe filters demonstrated that even rather simple steps within a laboratory cleanup may have a tremendous influence on the analytical result. Due to the discovered drawbacks of syringe filtration, ultracentrifugation was applied as a further precautionary cleanup element to remove particles from samples prior to injection. This step avoided the introduction of unknown background interferences and the unnecessary reduction of signal intensity due to membrane filtration which finally helped to decrease the method detection limit. Furthermore, the minimum sample volume for filtration of approximately 500 μL , needed to yield a sufficient sample amount of about 100 μL (due to the dead volume caused by membrane wetting and filter compartment), could be further reduced to below 100 μL using centrifugation.

5.4.3. Performance evaluation of large volume water sampling

The active water sampling system involving on-site enrichment of analytes on XAD-cartridges was evaluated in laboratory tests for possible extraction and cleanup techniques. Reliable results were only achieved during experiments where quantification with the micro-scale chromatography setup was possible. Sensitivity deviations between single injections during operation with the nano-scale setup rendered the judgement of deviations between experiments doubtful. Therefore, the laboratory recovery studies presented here were determined with the micro-scale setup unless otherwise noted.

The extraction experiment of pre-cleaned spiked sampling cartridges allowed the assessment of extraction and cleanup recoveries as well as matrix effects. By adding isotopically labeled internal standards only prior to injection, two methodological performance parameters could be monitored at the same time. The response of native compounds on the one hand corresponded to the extraction and cleanup recoveries while IS correction allowed to separate any occurring matrix effects from this observation. On the other hand, the absolute signal intensity of the mass-labeled IS compared to the absolute signal intensity during instrumental calibration allowed the quantification of matrix effects. Therefore, that instrumental calibration was carried out just before or right after the quantification of samples to be able to compare the absolute response for the IS. Otherwise, changes in response due to instabilities in the ESI would have directly affected the judgment of the matrix effect. Adding up both, analyte recovery and matrix

effect allowed the judgement of the total observed recovery that could be expected in environmental samples.

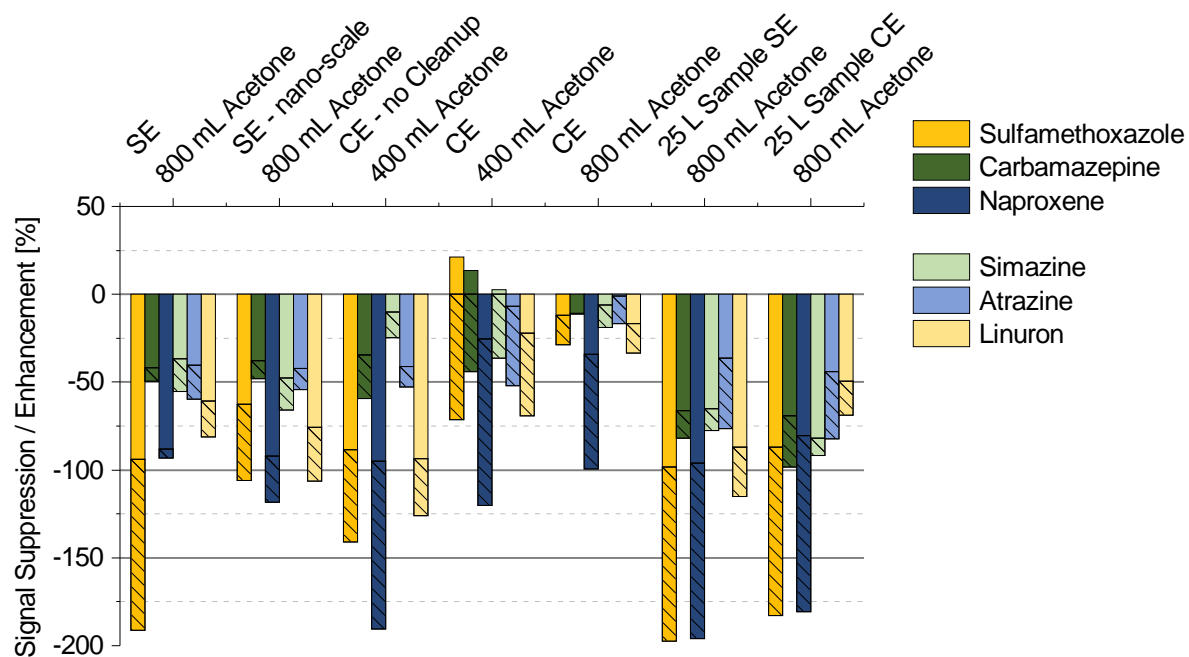


Fig. 48: Signal suppression and enhancement during extraction and cleanup of artificially spiked sampling cartridges; losses due to extraction and cleanup indicated as hatched column parts, matrix effects as plain column parts; SE:= Soxhlet extraction, CE:= cartridge elution

The results from the laboratory extraction and cleanup experiments are summarized in Fig. 48. Obviously, the addition of analyte loss and matrix effect reduced the total recovery by more than 50 % in most cases. A signal reduction of more than 100 % is the result of the individual determination of matrix effect and recovery. These cases indicate that the quantification of these compounds within an environmental sample would be challenging due to barely visible IS signals. Overall, the results demonstrate that the extraction of the self-packed and pre-cleaned sampling cartridges and the concentration of large solvent amounts lead to a formation of a pronounced matrix effect which suppresses the IS signals by up to 98 %. This effect was even increased in case of cartridges being exposed to water for sampling.

The experimental recovery determination for Soxhlet extraction with 800 mL acetone could be carried out with nano- and micro-scale chromatography. Therefore, the results allowed the comparison between the matrix effect compensation capability of nano-ESI and the standard ESI source. Nano-ESI at very low flow rates is known to exhibit special abilities in matrix effect reduction. However, these beneficial effects were only observed for flow rates below $0.02 \mu\text{L min}^{-1}$ whereas at $0.05 \mu\text{L min}^{-1}$ already pronounced matrix interference was apparent [147]. The presented results support this finding as the matrix effect (operating at

0.25 $\mu\text{L min}^{-1}$) was comparable between the micro-scale and the nano-scale measurement (plain part of the column in Fig. 48). Consequently, nano-scale chromatography in combination with nano-ESI was not capable of the reduction of matrix effects within the measurements.

The comparison of the results achieved with elution of a spiked sampling cartridge with 400 mL acetone without and with subsequent cleanup demonstrates the abilities of the applied SPE cleanup for the removal of interfering background substances. Without SPE, severe matrix effects were apparent, especially for sulfamethoxazole and naproxen, reducing their signal intensity by 89 and 95 %, respectively. After SPE, a slight signal enhancement for sulfamethoxazole was recognized (21 %), whereas for naproxen the suppression could be reduced to 26 %. At the same time, however, the gain in matrix effect reduction was at the expense of analyte loss during cleanup. Nevertheless, the total recovery with applied SPE cleanup was improved for all investigated compounds except simazine which showed more independence from matrix effects overall. Besides the direct influence of analytical matrix on the signal intensity during measurement, matrix compounds might invoke influence on the retention behavior on SPE cartridges, too. Thereby, sample matrix could block binding sites and lead to a cartridge saturation which finally may result in analyte loss. Moreover, sample properties like pH and salinity could influence the affinity of analytes onto the SPE sorbent. Both mechanisms could explain a decreased recovery in addition to the occurring matrix effect.

Some analytes appeared to be especially sensitive to interfering matrix. Suppression due to matrix was higher than 80 % for sulfamethoxazole, naproxen and linuron in several cases. Although the applied HR-X SPE was capable of the enrichment of these compounds (see section 5.4.1.), severe interferences in the XAD-extracts prevented their reliable detection which could not be totally compensated with the applied cleanup.

The best total recovery from spiked sampling cartridges was achieved by cartridge elution with a volume of 800 mL. The matrix effects appeared to be minimized while the extraction and cleanup recovery was convincing except for naproxen. Cartridge elution with 400 mL acetone reduced the matrix effects slightly, but resulted in a decreased analyte recovery indicating that the solvent volume passing through the cartridge was not sufficient for full analyte recovery. Soxhlet extraction yielded slightly better analyte recoveries compared to 400 mL cartridge elution but introduced matrix effects at the same time. Comparing Soxhlet extraction and cartridge elution with 800 mL acetone clearly demonstrates the benefits of cartridge elution. Comparable extraction recoveries and a clear reduction of matrix effects increased the total analyte recovery when applying the elution technique.

The extraction of analytes from 25 L artificial water sample showed acceptable enrichment and extraction yields for carbamazepine, simazine, atrazine and linuron. Matrix effects, however,

clearly increased compared to the extraction experiments conducted with cartridges which have not been exposed to water before. Although cartridge elution reduced the matrix effects for the analysis of spiked sampling cartridges, this advantage was lost to a large extent when processing cartridges used for sampling of the artificial water sample. Still, the matrix effects observed for most of the compounds was lower with the cartridge elution technique than with Soxhlet extraction.

The enrichment of positive ionizing pharmaceuticals and polar pesticides on sampling cartridges in laboratory-scale with the final sampling layout allowed the determination of the partition of analytes between the master and backup cartridge. Thus the enrichment dynamics and the retention of analytes on the deployed XAD resin could be examined.

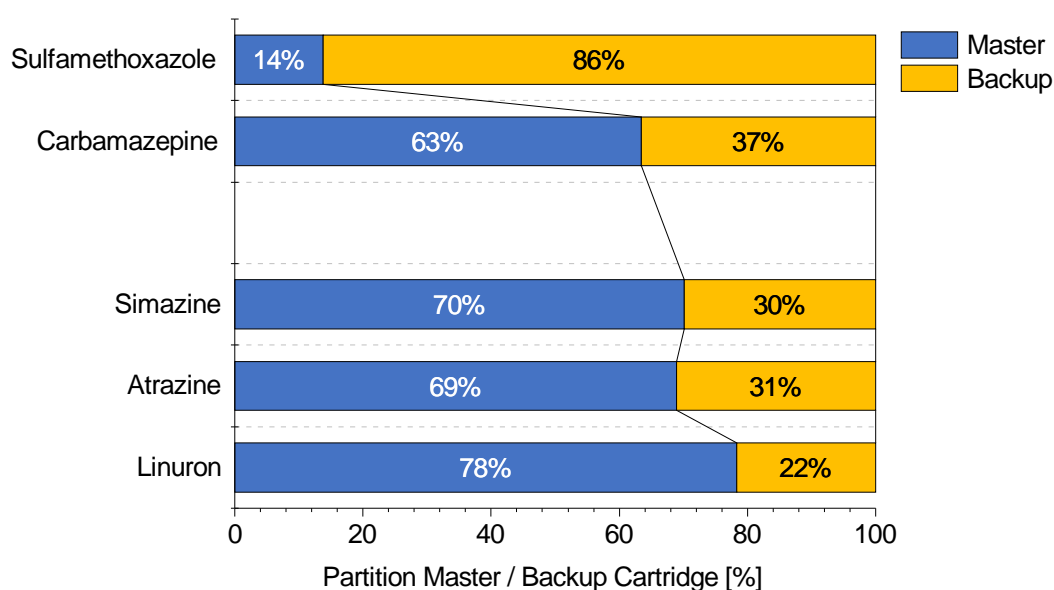


Fig. 49: Analyte partition between master and backup sampling cartridge for positive ionizing pharmaceuticals and polar pesticides observed while sampling 25 L artificially spiked distilled water; mean of three independent extraction tests; the signal intensity of naproxen in the extracts did not allow this calculation

Fig. 49 illustrates the relative partition of pharmaceuticals and polar pesticides measured with positive ionization. Unfortunately, the signal intensity of naproxen did not allow its reliable determination which further supports the previous findings regarding a pronounced matrix effect for this compound. The breakthrough into the backup cartridge was particularly high for the most hydrophilic compound sulfamethoxazole ($\log P$ -value: 0.89). Obviously, there was a trend between analyte partition and hydrophobicity. Compounds with a $\log P$ -value above 2.00 were found in fractions above 63 % within the master cartridge. The results indicate, however, that there is a considerable analyte breakthrough with the deployed sampling layout. Consequently, measurements carried out with this sampling method have to be regarded as semi-quantitative

as some compounds escape from the sampling cartridges leading to an error in the calculation of water concentration based on the measured analyte amounts within the sampling cartridges. Different reasons might explain the observed partition of analytes. One aspect is the employed polymeric XAD resin which seemed to be not capable of the quantitative retention of the highly polar target compounds. Although XAD-7 is stated by the manufacturer to enrich antibiotics and ionic species [149], the retention in the laboratory experiment seemed to be insufficient. Inorganic salts and other organic substances like fulvic and humic acids can be excluded as factors of influence on retention as the artificial water sample consisted of a spiked distilled water volume. Finally, the adjusted sampling rate of 2 L min^{-1} might have been too high to yield complete equilibration between liquid and solid phase.

Due to the pronounced matrix effects experienced with high volume water enrichment on self-packed XAD-cartridges, the enrichment of volumes between 100 and 500 mL on 500 mg HR-X SPE cartridges was evaluated as an alternative for positive ionizing pharmaceuticals and polar pesticides. In contrast to on-site analyte enrichment, smaller volumes could be collected in the environment and processed in the laboratory. The performance of direct SPE was determined with spiked 100, 250 and 500 mL ultrapure and tap water samples with a constant concentration of 180 pg mL^{-1} . Additionally, a 250 mL water sample collected at the Partnach creek (Bavaria, Germany) near its source was spiked with the same concentration, enriched and measured. The resulting signal suppression or enhancement is illustrated in Fig. 50.

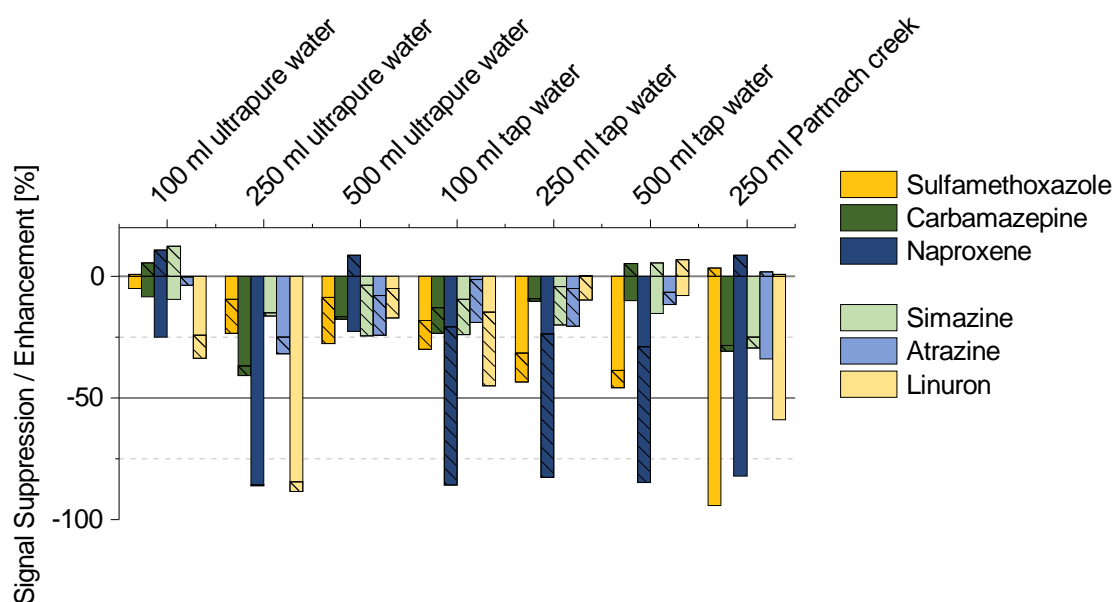


Fig. 50: Signal suppression and enhancement determined with direct solid-phase extraction of artificially spiked water samples; losses due to extraction indicated as hatched column parts, matrix effects as plain column parts

Otherwise as expected, matrix effects were comparable between water volumes and indepen-

dent from background in tap water. In general, matrix effects were clearly less apparent with direct SPE compared to the enrichment on XAD-cartridges. The results for 250 mL ultrapure water exhibited exceptional values for the suppression of carbamazepine, naproxen, atrazine and linuron. As the values of this measurement did not fit within the global trend of the presented results, they were excluded from the following discussion. In most cases, the observed matrix effect invoked a signal suppression below 25 %. The SPE recoveries determined by IS corrected signals of the native compounds, stayed in the range above 80 % for most of the compounds. Issues, however, could be observed again in the enrichment of naproxen. Whereas the matrix effect for naproxen stayed comparable in nearly all samples, a slight over-determination within ultrapure water and a grave analyte loss in tap water was observed. With naproxen and its carboxylic acid function exhibiting a predicted pKa-value of 4.19 (ChemAxon), it should prevail as ionic species within a neutral solution. With the recovery in ultrapure water being 75 % and higher, the enrichment of the ionic species seems not to have negative influence on enrichment on HR-X SPE cartridges. Additionally, the loss of naproxen had to be attributed to the enrichment step as the signal for the IS which was added after extraction stayed comparable between ultrapure and tap water samples. Consequently, some kind of other matrix seemed to be introduced with tap water which lead to a decreased recovery of naproxen. The results regarding the 250 mL environmental sample were less promising. Although the SPE performed good with up to 100 % IS corrected recovery, pronounced matrix effects were apparent especially for sulfamethoxazole (-94 %), naproxen (-82 %) and linuron (-59 %). Overall, the results for the environmental sample faced comparable issues as observed within the XAD extracts. Nevertheless, due to the good analyte recovery, quantification should result in more accurate concentration values. Besides, the suppression for the signal of carbamazepine, simazine and atrazine around 25 % is less than half of the suppression observed in the extracts of XAD sampling cartridges. Direct solid-phase extraction on HR-X cartridges could be a good alternative for the sampling of high water volumes due to the high analyte recovery. Modifications of the active water sampling system might also enable the on-site enrichment on HR-X cartridges at the sampling location avoiding the necessity of liquid transport, storage and optional preservation. This sampling technique can be suggested in applications where the lower total enrichment factor and thus higher method detection limit is acceptable. With IDLs for positive ionizing pharmaceuticals and polar pesticides between 4.9 and 15.1 pg μL^{-1} , the presented direct-SPE method with 250 mL volume yields method detection limits (MDLs) between 3.9 and 12.1 ng L^{-1} . In order to reduce the MDL further for the quantification in the pg L^{-1} dimension, either the IDL has to be reduced or the sample size has to be increased. Consequently, sampling on XAD-cartridges can be seen as large volume alternative if quantification of very

low amounts of analytes is necessary.

5.5. Evaluation of large volume sampling with samples from the Yangtze River

In contrast to the laboratory experiments, environmental sampling of the Yangtze River slightly upstream of the Three Gorges Dam in China was carried out with the optional glass wool filter cartridge which hindered large particles from entering the sampling cartridges. These filter cartridges were also extracted in order to determine compounds which tend to adsorb on glass wool or on trapped suspended particles. Fig. 51 summarizes the partition observed between filter, master and backup cartridge for investigated pharmaceuticals and polar pesticides.

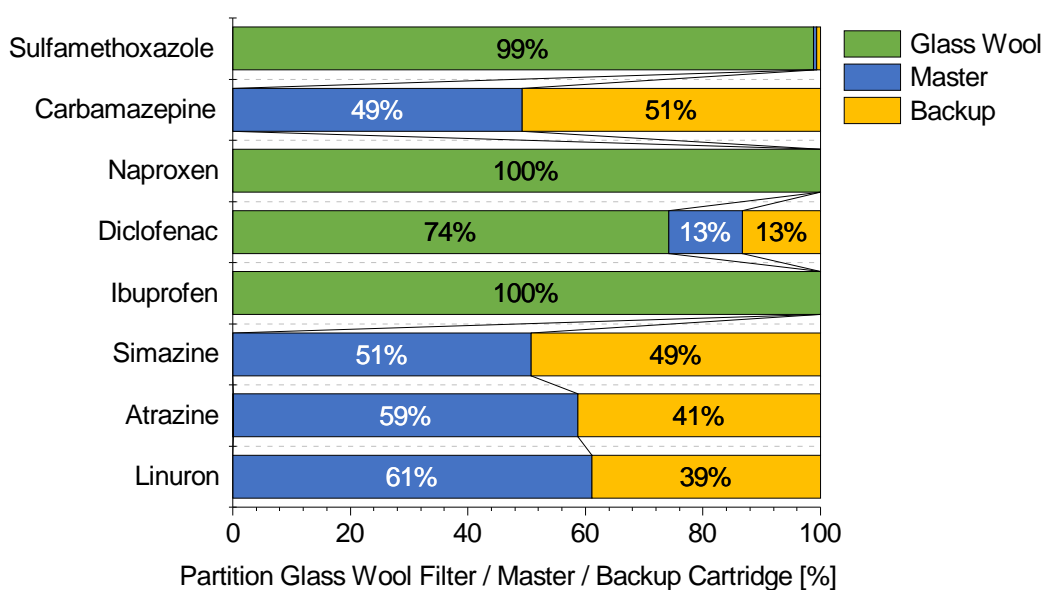


Fig. 51: Partition of pharmaceuticals and polar pesticides between filter, master and backup sampling cartridge observed during sampling at the Three Gorges Dam (China); mean value of the measurements in 11, 31 and 50 m water depth

The results indicated that sulfamethoxazole, naproxen, diclofenac and ibuprofen mainly resided within the glass wool filter cartridge. Nevertheless, this observation was rather a consequence of matrix effect than the reflection of actual analyte partition. Higher absolute IS recovery in the glass wool filter than in the XAD cartridge extract indicated that the potential matrix effect from the filters was lower and thus the analyte signal was higher than the IDL. Analyte partition for carbamazepine, simazine, atrazine and linuron meanwhile met expectations that particle association for these polar compounds is less common. In well accordance with the findings from the laboratory investigation, there was a trend observable indicating an increasing analyte fraction in the master cartridge for increased hydrophobicity of the compounds. However, compared to the laboratory recovery experiment, the fraction of analytes in the master cartridge was lower,

ranging from 49 to 61 %. The higher total mean sampling volume of 340 L and a more complex environmental matrix might explain the decreased analyte retention. Moreover, the flow rate during environmental sampling was adjusted to 3 L min⁻¹ which was 1 L min⁻¹ higher than during the laboratory experiment which might have led to a decreased retention in the master cartridge if no complete equilibrium between the XAD resin and the aqueous phase was reached.

Fig. 52 illustrates the partition of PFAAs within the single parts of the sampling system. The polarity within the group of PFCAs and PFAS decreases with the carbon chain length. Consequently, higher retention for hydrophobic PFAAs could be expected and thus a higher recovery within the master cartridge. The results, however, did not reveal a global trend between carbon chain length and proportion in the master cartridge. The more polar PFHxS and PFHxA were mainly found in the master and filter cartridge which is in opposite to reasonable expectations. In contrast, PFPeA and PFHpA were nearly exclusively detected within the backup cartridge indicating a decreased retention and high breakthrough for these compounds. PFAAs with a chainlength between 8 and 11 showed meanwhile comparable partition whereas beginning from PFDA a slightly increasing proportion was found within the filter cartridge which could be explained with increasing hydrophobicity.

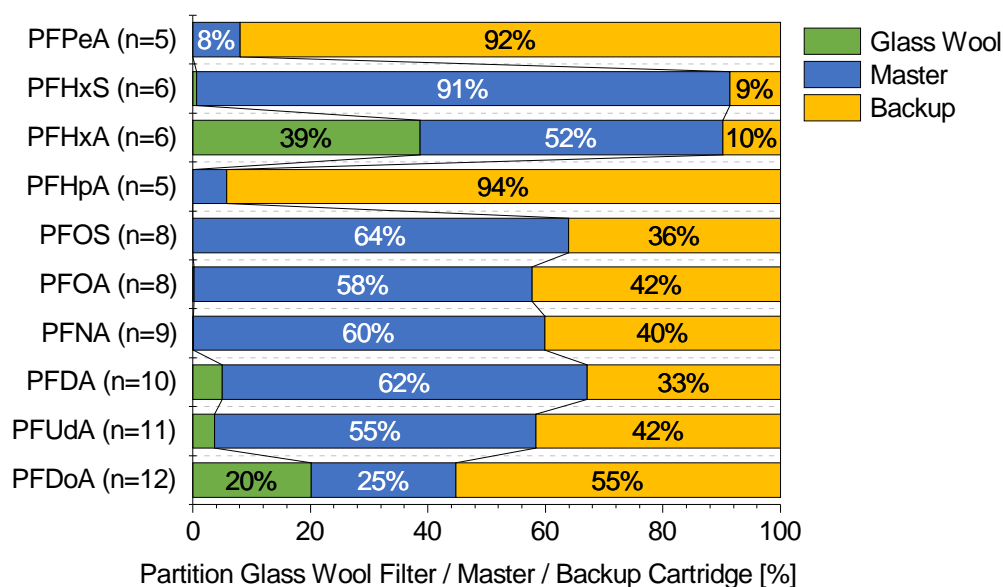


Fig. 52: Partition of perfluorinated alkyl acids (PFAAs) between filter, master and backup sampling cartridge observed during sampling at the Three Gorges Dam (China); mean value of the measurements in 11, 31 and 50 m water depth

The partition of PFAAs within the sampling system could be expected to a large extent and was similar to the results achieved for polar pesticides. The results did not indicate a strong evidence for particle association of these compounds or adsorption onto the glass wool itself. With an

overall mean fraction of 54 % of PFAAs residing in the master cartridge, the sampling results for PFAAs did not allow the calculation of accurate absolute water concentrations. However, the determined data was available for qualitative evaluation.

Within Fig. 53 and Fig. 54 the determined depth profiles for pharmaceuticals, polar pesticides and PFAAs are presented. The profiles illustrate the abundance of the single analytes highlighting the most abundant species. Each profile summarizes all analyte amounts found within the filter, master and backup cartridges. Due to the observed breakthrough and resulting error, absolute water concentrations contained only limited information and will only be discussed for judging the dependency of concentration and water depth.

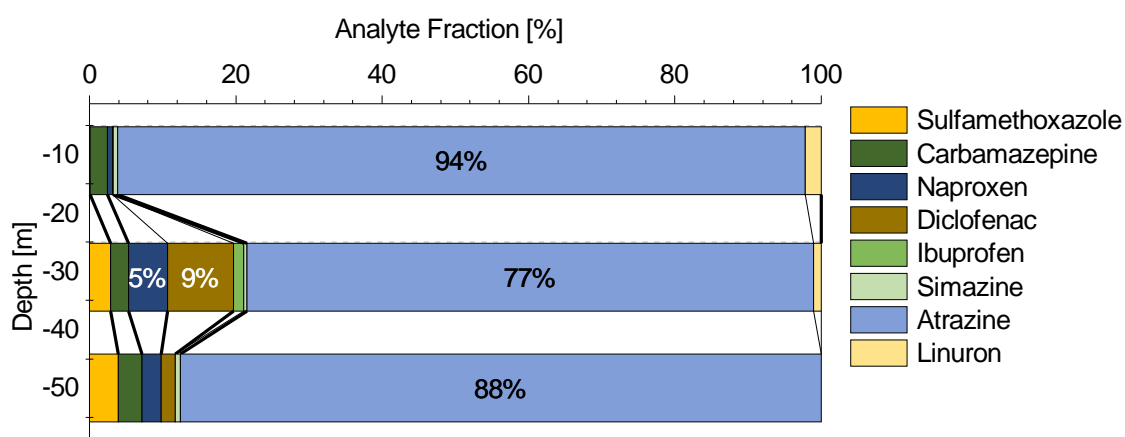


Fig. 53: Depth profile of pharmaceuticals and polar pesticides determined in the Yangtze River upstream from the Three Gorges Dam in September 2013

The depth profile presented in Fig. 53 was dominated by the abundance of the herbicide atrazine. In comparison, the amounts of the other investigated herbicides simazine and linuron was low. In case of linuron, pronounced matrix effects negatively influenced the accurate determination of this compound. Regarding pharmaceuticals, sulfamethoxazole, naproxen and diclofenac contributed to a higher fraction of the total analyte amount. With increasing water depth, a slight increase of the pharmaceutical fraction was observed with a maximum in the measurement in 31 m depth. In total, the determined analyte profile did not reveal a characteristic trend with water depth.

Judging the determined absolute amounts in water, a decreasing trend was observed for the three herbicides. In case of atrazine, this meant a reduction of 73 % from 11 m to 50 m water depth. In contrast, the results indicated a less homogeneous picture for the investigated pharmaceuticals. Naproxen and diclofenac showed highest abundance in 31 m water depth and a lower comparable absolute value in 11 and 50 m depth. In case of sulfamethoxazole and carbamazepine, no characteristic trend could be determined.

The inhomogeneous fractions and absolute amounts within this group of analytes between the different water depths could have been caused by several reasons. As already mentioned, the investigated group of pharmaceuticals and polar pesticides consists of organic molecules with a high degree of structural differences which results in differences in their behavior in the environment. Besides the discussed matrix effects that tend to have different intensity on the single analytes, environmental stability can be an important influence factor on their quantification. The inhomogeneous depth profile might also be an indicator for a not well-mixed water body. With the flow velocity of the Yangtze River being decreased in front of the Three Gorges Dam, flow turbulence might not have been sufficient for the homogeneous dispersion of the analytes within the water body.

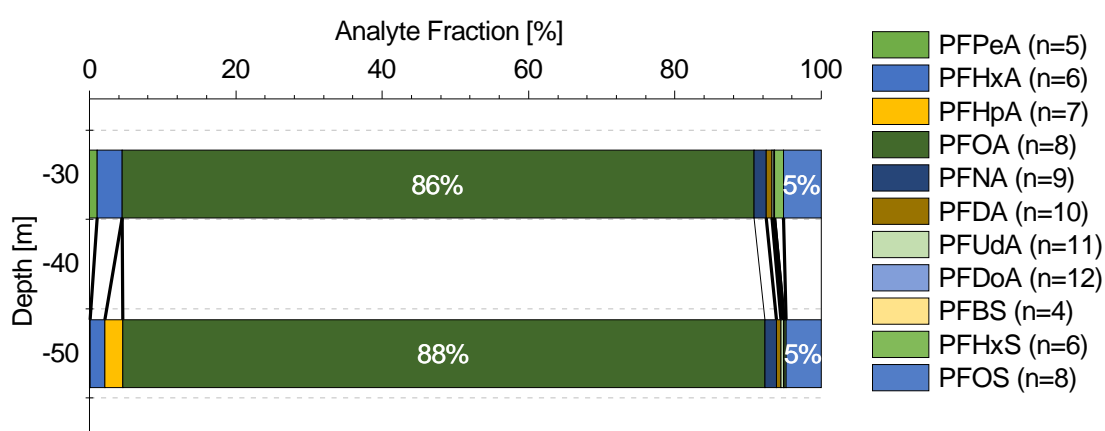


Fig. 54: Depth profile of PFAAs determined in the Yangtze River upstream from the Three Gorges Dam in September 2013

PFOA and PFOS, both with a chain length of 8 carbon atoms, represented more than 90 % of the PFAAs found within the samples. In general, the results for this group of analytes proposed a more homogeneous distribution with water depth. Besides the most abundant homologs, PFPeA and PFHxA were found in slightly higher quantities whereas all other PFAAs were only detected in very low quantities. Comparing the profiles determined in 31 and 50 m depth, only minor differences mostly within a range of 10 % could be observed. Whereas the fraction of PFOA and PFOS remained nearly constant, the fraction of PFHxA decreased from 31 to 50 m depth slightly from 3 to 2 %. In contrast, PFHpA could exclusively be detected in 50 water depth but only with a total fraction of 2 %.

Absolute PFAA amounts in water indicated a slightly increasing abundance of 9.9 % with water depth in respect to the total mean amount. This increase was mainly attributed to PFOA with all other investigated PFAAs playing a minor role. The more homogeneous dispersion of PFAAs depicts a contrast to the investigated pharmaceuticals and polar pesticides. The group of ho-

mologs exhibits comparable chemical properties in terms of structure and chemical behavior as mainly the hydrophobicity of the compounds is influenced by the chain length. The results indicated a homogeneous dispersion in the environment based on the similar chemical properties. The hypothesis of a not well-mixed water body as possible explanation for an inhomogeneous dispersion of pharmaceuticals and polar pesticides could not be supported judging the PFAA results.

With environmental sampling at the Three Gorges Dam, it could be shown that the presented sampling system allows the convenient on-site enrichment of large water volumes on easily portable sampling cartridges. The analytic results were capable to reveal qualitative information about the abundance and apportionment of analytes at the investigated sampling site. With sampling in three different water depths, hints for the distribution of analytes with water depth could be drawn. The sampling system applied in the environment, however, coped with comparable issues that could already be identified within the laboratory extraction experiments: the large cartridge design by itself and the exposure to large water volumes lead to pronounced matrix effects which hindered proper quantification. Moreover, the retention within the sampling cartridges was not sufficient for a quantitative recovery of analytical target substances from surface water. The large sample size, higher sampling flow rate and more complex environmental matrix could explain the even more decreased analyte recovery on the sampling cartridges compared to the laboratory experiments. Nevertheless, alternative functional resins within the cartridges, a slightly decreased sample size and lower sampling flow rates would be promising parameters to increase analyte retention to a level that can be considered as quantitative.

5.6. Inclusion of non-target analysis into the presented method

The HRMS data gathered during targeted analytical runs was used to enhance the existing targeted analysis of compounds with a non-target screening approach. Possible suspects were identified by database research using not only the exact mass but also the $\log P$ -value as identifier. The partition coefficient could be estimated from in-situ calibration of the retention times with standards from the targeted analysis approach. This procedure was especially beneficial due to the fact that the employed MS instrument was lacking a permanent mass calibration surveillance like a lockspray ion source. Consequently, a mass accuracy of about 500 ppm was still sufficient for compound identification in combination with the $\log P$ -value as additional identifier. Once possible structure suggestions had been identified, the possible suspects were checked for plausibility. This was established by taking the chemical knowledge about the sampling, extraction, cleanup and analysis into account. The knowledge about possible shortcomings regarding enrichment capability of the applied sampling technique clearly reduced the

amount of possibly enriched substances. Laboratory extraction and cleanup impose a step of choosing a certain polarity range in which possible target compounds may reside. Finally, chromatographic and mass spectrometric results from targeted analysis could be taken into account as a last suspect filter to identify promising targets. Once compounds passed the plausibility check, further verification could be achieved with entries in mass spectrometric fractionation databases which were compared with fractionation products formed during targeted analysis sample runs as these have been carried out at elevated collision energy in AIF-mode.

For the development of a suitable data processing workflow, samples acquired from an exposed VO passive sampler were analyzed. Targeted analysis could not detect any investigated compounds within the prepared blank and exposed sampler extracts. The concurrent non-target analysis generated suspect lists of the two exposed VOs with 15 and 20 possible hits, respectively. The most important criterion for the exclusion of background signals was the response threshold. With both VOs being exposed at the same sampling site, the results have been aligned which revealed only two independent signals which could be found in both exposed passive samplers. These suspects were regarded as the most promising ones. One of these compounds could be identified as *N,N*-diethyl-*m*-toluamide (DEET) with the database STOFF-IDENT with a high likelihood. The substance is commonly used as insect repellent. The calculated exact mass-to-charge ratio of the positively charged molecular ion is m/z 192.1388 whereas the ions acquired had a m/z of 192.1343 and 192.1464, respectively, in the individually measured samples. Consequently, the acquired mass deviated between 23 and 40 ppm from the calculated exact mass which is an acceptable value for the employed MS instrument. Nevertheless, the mass accuracy did not allow doubtless identification of the suspect. Besides the exact mass, the logP-value was estimated with the help of the RTI-calibration to 2.70 and 2.74 which corresponds to a maximum deviation of 0.24 to the predicted value of the ChemAxon algorithm for the suspect. Moreover, the polarity of the suspect is in well accordance with the retention capabilities of the HR-X SPE as well as the detection capabilities of the analytical instrument. Furthermore, a certain structural similarity of the suspect with the small organic molecules investigated in targeted analysis assured the availability of the compound for electrospray ionization. Further verification of the suspect was possible with MS fragmentation data about the compound available in the databases DAIOS and MassBank. In total, three characteristic mass fragments of DEET (119.05, 91.06 and 72.05) were detected in measurements with higher collision energy at the same retention time. Without injection of DEET as standard substance, the analytical results gave already strong evidence that the detected substance within the exposed VOs was indeed DEET. Finally, the injection of DEET as a dilution from a purchased analytical standard solution further supported the results from non-target analysis. The substance gener-

ated a signal with a retention time difference to the suspect of only 0.06 min and an acquired exact mass of 192.1389. At the same time, fragmentation products at 119.06 and 91.06 could be detected. As summary, the substance detected with a mean m/z of 192.1404 within the VO-extracts could be identified as the organic substance DEET. Further possible suspects found in the passive samplers with a lower level of verification are listed in Table 5.7.

Table 5.7: List of possible suspects detected in extracted VO samplers from the river Selke in Saxony-Anhalt (Germany) and their corresponding verification level

Suspect	Possible Compound	$\Delta m/z$	$\Delta \log P$	Amount of matched MS/MS fragments	detected in Blank	Detected in both exposed VOs
[m/z]		[ppm]	[]	[]	[yes/no]	[yes/no]
192.1404	<i>N,N</i> -diethyl- <i>m</i> -toluamide	32	+0.20	3	no	yes
214.0827	salicylanilide	19	-0.42	2	yes	no
185.1498	γ/δ -undecalactone	24	+0.74	3	no	no
283.2529	artemisinin	347	-0.08	0	no	no

After the development and application of the non-target workflow with the VO-samples, data gathered during the analysis of the XAD sampling cartridges from the Yangtze River were screened for possible analytical targets. The non-target analysis was carried out for the XAD sampling cartridges used in 31 and 50 m water depth. The extract amount from the water sample taken in 11 m depth was not enough to append a sample injection for non-target analysis. The extract of the XAD cartridge field blank was used to correct the data for analytical background. Nevertheless, the XAD cartridge extract exhibited clearly a higher noise level than observed in the VO-extracts. Consequently, the non-target analysis was focused on the most intense ion signals which allowed to simplify the dataset to a large extent. One of the most effective tools for judging the produced peak lists was the alignment of the results between the 31 and 50 m as well as master and backup cartridges. Therefore, only signals with a certain abundance pattern were regarded as valid suspects:

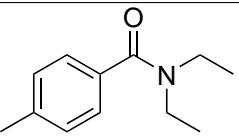
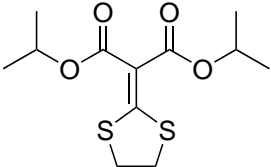
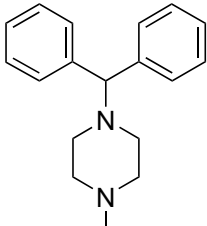
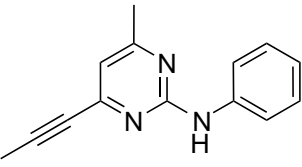
- found in all 4 sampling cartridges
- found in the master and backup cartridge of one sampling depth
- found in either both master or both backup cartridges from 31 and 50 m depth

These criteria helped to reduce the suspect list from 96 to 23 entries. Obviously, there might have been unknown substances in one cartridge and one water depth only but the probability of this case could still be regarded as low. Substances within the polarity range of the compounds investigated in the targeted approach should also tend to cause breakthrough from the master to the backup cartridge and hence should have been detectable in both cartridges. Certainly, the presented approach covers substances with high retention within the sampling cartridges with the only prerequisite that these compounds were found in both sampling depths. The largest error imposed by the established criteria might be the discarding of highly polar substances only detectable in the backup cartridges. In this case, prevailing analyte loss might have led to a total loss of polar unknowns in one sampling depth whereas the compound would still be detectable in the other water depth. The error caused by excluding compounds from the latter case, however, was regarded as acceptable due to its low probability and the focus on substances with medium polarity.

7 suspects yielded either no possible substance in database research or structures which were unlikely to be detected due to the parameters of the analytical method or unavailability to LC-MS. For further 8 suspects, a possible organic molecule could be proposed but no further verification was possible as no MS fractionation data was available in the employed databases DAIOS and MassBank. 4 structure suggestions from database research matched regarding log P -values and acquired exact mass but could be rejected as the formed fractionation ions did not match the datasets gathered from the fractionation databases. Finally, 4 compounds included in the final suspect list could be verified with at least one mass fragment each abundant in the MS/MS run, forming a well-shaped peak at the retention time of the suspect. The suspects exhibiting a higher probability overall are presented in Table 5.8.

The substance with the highest verification level was again DEET which could be verified with 2 mass fragments, analytical availability and matching retention time and fragmentation behavior with the purchased analytical standard substance. Besides, the fungicide isoprothiolane was detected with a high probability. Although the suspect was detected with a mass deviation of 348 ppm, database research benefited from filtering results with a log P -value larger than the one from linuron as the suspect eluted after the last eluting substance of the targeted approach. The suspect could be verified with two matching mass fragments in the MS/MS run. Furthermore, the structure of isoprothiolane contains two sulfur atoms which were reflected in the isotopic pattern of the mass peak of the suspect. The fungicide is commonly used in rice cultivation and has already been reported in the Yangtze River [150]. The suspects cyclizine and mepanipyrim could both be verified with one MS/MS fragment only. Their acquired exact mass deviated by 316 and 238 ppm from the predicted exact mass of the suggested structures. Nevertheless, judg-

Table 5.8: List of possible suspects detected in extracted XAD sampling cartridge extracts from the Yangtze River (China), their verification level and abundance in the sampling cartridges

Name of Suspect	Chemical Structure	$\Delta m/z$ [ppm]	Verified MS/MS fragments []	Detected in 31 m Master+Backup / 51 m Master+Backup / Field Blank [+/-]
<i>N,N</i> -diethyl- <i>m</i> -toluamide (DEET)		360	2	+ + + + +
Isoprothiolane		348	2 (+ isotope pattern)	+ + + + +
Cyclizine		316	1	+ - + + +
Mepaniprym		238	1	+ + + + +

ing their retention time and corresponding logP-value were found to be plausible. Mepaniprym is like isoprothiolane used as a fungicide in agriculture for the protection of wine, strawberries, tomatoes and cucumber [1]. In contrast, cyclizine is a first-generation antihistamine used in the treatment of nausea, vomiting and dizziness [1].

The developed and presented non-target analysis approach offered the possibility to evaluate additional information based on already acquired data. It was applied on samples of two different origins and can be transferred from its nature also towards other workflows. If standard targeted analysis on the LC-MS instrument is carried out, only one additional sample injection and one blank injection are enough to enable this kind of analysis in post-processing. In enhancement to targeted analysis, the directed non-target approach might indicate shortcomings in the selection of target compounds which have not been in focus. Some of these substances might even be

of interest for the given analytical application. Therefore, ensuring the requirements for non-target analysis during the acquisition of data for targeted analysis can be seen as an integrated approach combining the possibility for quantification with screening the environment for new possible targets. The limited mass accuracy and mass resolution of the employed LC-MS instrument, however, did not allow the prediction of sum formulae from the exact mass which excludes the acquired exact mass to act as main descriptor for non-target suspects. Nevertheless, the employed approach including the retention time or partition coefficient as additional parameter for identification could partly compensate the limits of the LC-MS instrument.

6. Conclusion and Outlook

Active pharmaceutical ingredients, polar pesticides and PFAAs can survive the ordinary municipal wastewater treatment and are released into the environment in large quantities. Once released, depending on their chemical properties, they can exhibit endocrine activity or tend to bioaccumulate. Active pharmaceutical ingredients like antibiotics used for humans or livestock can impose selection pressure on bacteria and are known to invoke the formation of multi-resistant bacteria strains. Therefore, analytical methods are needed for the surveillance of the abundance of these anthropogenic substances in the environment. Within surface water, however, analytical targets tend to be diluted in large water bodies like rivers and lakes, making their detection and quantification a challenging task. Consequently, most analytical techniques for the analysis of organic trace substances in water include a sample pre-concentration step right before instrumental quantification.

The presented work covered the complete development of a new analytical method for the determination of emerging organic pollutants in surface water. The method included a sampling system designed for the enrichment of water volumes up to 300 L, a suitable laboratory extraction and cleanup as well as an advanced instrumental method and detection with LC-MS.

At the beginning of this study, the capabilities of the chromatographic and mass spectrometric detection system had to be evaluated in order to conduct further testing of extraction and cleanup performances in the laboratory with a stable operating analytical instrument. Chromatographic method development was focused on the establishment of a suitable fluidic configuration that allowed a reproducible, precise and sensitive detection of the targeted analytes. The available analytical instrument allowed separations to be conducted in nano- and micro-scale. Moreover, an optional trapping column could be installed for pre-concentration and washing samples from salts during operation in nano-scale. The investigation of the capabilities of the chromatographic instrument with nano-scale configuration revealed that the trapping setup was not suitable for the analysis of small polar molecules. It could be demonstrated that a large proportion of analytes was lost during trapping and pronounced peak tailing was observed as a consequence. Moreover, this issue could not be resolved with adjusting the analytical gradient. With the removal of the trapping column from the flow path, peak tailing was absent and the separation performance as well as sensitivity could be improved. Most of the analyzed compounds could be baseline separated which improved the sensitivity and response linearity during the mass spectrometric detection.

The micro-fluidic setup was more simple in operation and was found to be more versatile and fast for the routine analysis of small organic molecules. Although the larger system scale exhib-

ited a system intrinsic handicap regarding detection sensitivity, the benefits in operation were found to be convincing to apply mainly this configuration for further recovery testing and environmental sample analysis.

The sensitivity and peak shape during gradient elution of pharmaceuticals, polar pesticides and PFAAs was found to be strongly dependent on the solvent composition of the sample solvent but independent of the fluidic configuration. This dependency was elucidated and optimized parameters for environmental sample analysis could be determined.

In parallel to chromatographic method development, the abilities of the employed mass spectrometer were investigated. Thereby, the stable operation of standard-scale and nano-scale ESI proved to be crucial for reproducible analysis runs. The stabilization of the nano-scale electrospray required several prerequisites which had to be validated in an extended empirical process. Therefore, it was necessary to identify and optimize several operational parameters like solvent purity, capillary voltage, tip position and flow rate. As a result, an uninterrupted operation in nano-scale for more than 4 weeks could be achieved. The most challenging issues during nano-scale operation were caused by the limited lifetime of nanospray emitters. The knowledge gained about the mentioned operational parameters was important for reproducible analytical results which were needed for subsequent conducted laboratory experiments.

The operation of the MS required the evaluation of different operation modes in terms of suitability for quantification. Analytical background could be successfully reduced with operation modes using collision induced dissociation. However, instrumental limitations were discovered in the parallel processing of MS functions to allow isotope dilution analysis. The issue was investigated and negative effects on response linearity, acquisition frequency and sensitivity were discovered. Taking these results into account it was possible to develop MS methods with respect to the instrument limitations. A dedicated MS/MS method for the detection of analytes side-by-side as well as a combined approach for fragmenting all ions at once have been developed and were both suitable for application in further quantitative measurements.

With the combined progress in the chromatographic and mass spectrometric development, the instrument could be calibrated for quantification and recovery experiments. Achieving a reasonable and linear response with the nano-scale setup required several adjustments in the preparation of calibration standards. In contrast, calibration standard preparation could be simplified during micro-scale operation.

With the known instrumental parameters, an applicable cleanup for environmental samples based on solid-phase extraction was developed. The comparison of different PS-DVB-based SPE cartridges revealed huge differences in the retention performance of the single sorbents. Based on the test results a promising SPE chemistry was chosen which allowed the reasonable

enrichment of highly polar target compounds. Besides SPE cartridges, different syringe filters for sample preparation were compared. It could be demonstrated that even simple laboratory steps like filtration can invoke a huge loss of analyte and the introduction of analytical matrix. The introduction of background substances was minimized by replacing extract filtration with a centrifuge step.

Different extraction techniques for sampling cartridges used for large volume water sampling were compared and the matrix effect, cleanup and extraction performance were analyzed. It could be concluded that the work with high solvent amounts and large sampling cartridges generated a pronounced matrix effect which could only be partially compensated by the conducted SPE cleanup. Additionally, the sampling of spiked 25 L water volumes allowed a laboratory controlled study of the enrichment performance of the self-packed sampling cartridges. The results indicated that the retention of highly polar compounds was weak and that a certain analyte breakthrough could be expected with the tested sampling layout. For comparison an alternative sample pre-concentration step involving direct SPE was tested. Thereby, improved compound recovery and less pronounced matrix effects were observed. However, the analysis of a spiked environmental water sample indicated issues with matrix effects also with the direct SPE and a decreased sample amount.

The processing of environmental samples from the Yangtze River was used to further characterize the abilities of the developed active water sampling system. Again the issue of analyte breakthrough was encountered rendering the analytical results semi-quantitative. Nevertheless, depth profiling at the sampling site could be conducted with the comparison of analyte fractions with sampling depth.

Finally, the targeted analysis method was enhanced by a comprehensive non-target approach for the identification of interesting analytical targets which might be included in future measurements. The workflow was successfully applied on samples from a passive sampler as well as the samples collected in the Yangtze River. Both analyses yielded promising suspect lists which were identified with high probability within the environmental samples.

The sampling of large water volumes could still be optimized in the future. The evaluation of new sorption resins within the sampling cartridges exhibits huge potential for the improvement of analyte retention. The experiments conducted with direct-SPE already demonstrated that a highly specific sorption medium allows a quantitative recovery of medium polar analytes. Besides, further attention regarding sample cartridge extraction techniques seems reasonable for further reduction of matrix effects.

7. Appendix

List of Figures

Fig. 1	Map of the Yangtze River drainage basin with highlighted major tributaries as well as related provinces with their capitals (© OpenStreetMap contributors [2])	2
Fig. 2	Climate diagram of the city Yichang located in proximity to the Three Gorges Dam in Hubei Province, China (data obtained from [11])	3
Fig. 3	Molecular structures of typically produced and investigated perfluorinated compounds (pKa-values obtained from [34]; logP-values of FTOHs from [35])	6
Fig. 4	Main paths of emission of pharmaceuticals intended for human use and livestock into the environment (according to [64])	9
Fig. 5	Illustration of possible fortunate and unfortunate pathways through the packed column (Eddy diffusion) according to [95]; a narrow size distribution of the column bed helps to reduce this effect	14
Fig. 6	Band broadening due to diffusion in and against the direction of the linear flow in the chromatographic column (longitudinal diffusion); faster elution yields a reduction of this effect	14
Fig. 7	Mass transfer between mobile and stationary phase according to [95]; higher linear flow velocity leads to higher spatial differences between adsorbed and free analyte molecules and consequently to band broadening	15
Fig. 8	Exemplary plot of the van Deemter curve with its components plotted as dotted lines; LC separation performance optimizes at the linear flow rate u_{opt} with H_{min}	15
Fig. 9	Model structure of a silica particle surface modified with octadecylsilane (ODS) and end-capped with trimethylchlorosilane (C-18 column chemistry); the alkyl chains form a dynamic lattice fence-like structure	17
Fig. 10	Illustration of a typical internal layout of a Q-TOF mass spectrometer; ions are transferred by multipoles in r.f.-only mode; the pusher transforms the continuous ion beam into pulsed ion packets that can be measured in the field-free drift-space of the TOF tube (according to [112])	22

Fig. 11	Illustration of a electrospray ion source with Z-spray layout; the spray is pneumatically stabilized allowing regular liquid flows between 4-200 $\mu\text{L min}^{-1}$ and up to 1 mL min^{-1} in megafLOW operation; differential pumping achieved with rotary and turbomolecular pumps (according to [112])	24
Fig. 12	Schematic representation of electrospray formation within an ESI interface; the high voltage leads to a deformation of the ionic liquid into a Taylor cone; the resulting droplets shrink due to solvent evaporation and finally release free ions	25
Fig. 13	Different types of disposable cartridges for solid-phase extraction (SPE) (Picture: Johannes Deyerling)	27
Fig. 14	Molecular structures of catechol and the catecholamines dopamine, epinephrine and norepinephrine ($\log P$ -values from PHYSPROP database [118])	28
Fig. 15	Molecular structures of the investigated pharmaceutical residues and pesticides, their application and their $\log P$ -value (experimental values from PHYSPROP database [118]); NSAID = Nonsteroidal anti-inflammatory drug	34
Fig. 16	Ultra high-performance liquid chromatography system Waters nanoAcquity UPLC (Picture: Johannes Deyerling)	36
Fig. 17	Fluidic configuration for direct injection; the illustrated injection valve state fits compound elution or loading of the sample loop	37
Fig. 18	Fluidic configuration for dual-pump trapping with reverse flushing of the trap column: the indicated valve state fits for elution of preconcentrated compounds from the trap column to the analytical column	38
Fig. 19	Picture of the nano-electrospray interface (dismounted) with three axis manipulator in operating position (left) and service position (right) (Picture: Johannes Deyerling)	39
Fig. 20	Derivatization of dopamine with 6-aminoquinolyl-N-hydroxysuccinimidyl carbamate (AQC)	44
Fig. 21	Self-packed glass cartridge with XAD-resin trapped inside with glass frit and heat-treated glass wool (Picture: Johannes Deyerling)	47
Fig. 22	OEM peristaltic pump (left) which is operated between 1 and 24 V DC either with battery or dedicated power supply and analog water meter (right)	47
Fig. 23	Schematic illustration of the established water sampling system with self-packed glass cartridges; optionally a filter cartridge could be mounted before the sampling cartridges in the flow path (not shown)	48

Fig. 24	Map of the Yangtze River near the Three Gorges Dam with highlighted sampling site (© OpenStreetMap contributors [2])	50
Fig. 25	Dependence of system response (peak area) of derivatized catecholamines on trapping volume: the sensitivity decreased exponentially with trapping volume	54
Fig. 26	Relationship of the peak tailing factor and trapping volume: there was no general characteristic dependence observed; acceptable peak tailing factor range is indicated in red (0.9-1.5 according to [102])	55
Fig. 27	Extracted ion chromatograms of pharmaceuticals and polar pesticides achieved with the 26.5 min initial linear gradient from 0 % to 100 % solvent B and analyte trapping with subsequent nano-scale separation	56
Fig. 28	Extracted ion chromatograms of pharmaceuticals and polar pesticides with the 15 min optimized linear gradient from 40 % to 46 % solvent B and analyte trapping with subsequent nano-scale separation	58
Fig. 29	Overlapping extracted ion chromatograms of PFBS, PFHxS, PFOS and PFDS (peaks from left to right) achieved by linear gradient elution starting at 80 % solvent B with trapping and nano-scale separation	59
Fig. 30	Left: USP peak tailing factors of PFAAs against their chain length determined with gradients starting at different solvent A/B ratios; right: boxplot for the illustration of the USP peak tailing factor spreading achieved with the different starting solvent A/B ratios	60
Fig. 31	Extracted ion chromatograms of pharmaceuticals and polar pesticides achieved with 20 min linear gradient from 0 to 100 % solvent B and nano-scale separation with direct injection of 0.5 μL 200 $\text{pg } \mu\text{L}^{-1}$ multi-analyte standard	61
Fig. 32	Peak area of the multi-analyte standard with pharmaceuticals and polar pesticides dissolved in mobile phase A:B mixtures from 100:0 to 30:70; the peak area is normalized to the standard solution solved in 100:0 A:B; peak areas were only determined for non-distorted peaks	63
Fig. 33	Normalized system response for PFAAs with direct injection and nano-scale separation in dependence on the standard solvent categorized by carbon chain length	64
Fig. 34	Extracted ion chromatograms of a standard with 200 $\text{pg } \mu\text{L}^{-1}$ pharmaceuticals and polar pesticides in 90:10 A:B (v:v) achieved with 23.5 min linear gradient from 0 to 100 % solvent B and micro-scale separation with direct injection	65

Fig. 35	Normalized system response for PFAAs with direct injection and micro-scale separation in dependence on the standard solvent categorized by carbon chain length	66
Fig. 36	Peak shape of PFHpA measured with nano-scale chromatography in direct injection configuration and negative ionization at different capillary voltages .	70
Fig. 37	Different states of nano-ESI operation observed with the microscope surveillance of the nano-ESI source: stable taylor cone (A), spindle mode (B), droplet formation (C)	70
Fig. 38	Total ion current (TIC) of direct infusion of 0.1 % phosphoric acid in 50:50 acetonitrile:water (v:v) at a flow rate of 0.30 $\mu\text{L min}^{-1}$ with the nano-ESI interface: the ion signal obtained with the syringe pump is pulsating compared to the signal obtained with pump B of the ASM	72
Fig. 39	Pictures of the fused silica nano-emitter obtained in the light microscope: new emitter (A), properly cut distal emitter end with conductive coating (B), irregular cut of distal end with damaged conductive coating (C), clogged emitter with visible black residue (D)	73
Fig. 40	Mounted standard electrospray interface with screw connection (left) and stainless steel capillary tip and sample cone tuned for operation at 4 $\mu\text{L min}^{-1}$ (right) (Picture: Johannes Deyerling)	73
Fig. 41	Extracted ion chromatograms with indicated data points of PFNA, PFOS and PFTrDA acquired in parallel MS functions due to coelution with 2 s scan time (limited separation due to nano-scale configuration and analyte trapping) . .	75
Fig. 42	Overlapping extracted ion chromatograms of mass labeled PFNA during injection of different calibration standards with nano-scale chromatography and direct injection	77
Fig. 43	Individual MS functions indicated as bars in single rows against the method time: (A) combined MS/MS method for the detection of PFCAs and PFAS, (B) PFCA-only MS/MS method for avoiding MS function overlap between PFAAs	78
Fig. 44	Centered MS spectra of atrazine: (A) predicted spectrum of MH^+ -ion, (B) spectrum during maximum intensity of 10 $\text{pg } \mu\text{L}^{-1}$ standard, (C) spectrum during maximum intensity of 80 $\text{pg } \mu\text{L}^{-1}$ standard	79
Fig. 45	Recoveries of positive ionizing pharmaceuticals and polar pesticides from spiked 1 mL water solutions; mean value of two measurements (n=2); carbamazepine was not included in the experiments	87

Fig. 46	Response deviation of syringe filtered standard solutions to unfiltered standard of native positive ionizing pharmaceuticals and polar pesticides (non-IS corrected, n=3)	89
Fig. 47	Response deviation of syringe filtered standard solutions to unfiltered standard of native positive ionizing pharmaceuticals and polar pesticides (non-IS corrected, n=3)	90
Fig. 48	Signal suppression and enhancement during extraction and cleanup of artificially spiked sampling cartridges; losses due to extraction and cleanup indicated as hatched column parts, matrix effects as plain column parts; SE:= Soxhlet extraction, CE:= cartridge elution	92
Fig. 49	Analyte partition between master and backup sampling cartridge for positive ionizing pharmaceuticals and polar pesticides observed while sampling 25 L artificially spiked distilled water; mean of three independent extraction tests; the signal intensity of naproxen in the extracts did not allow this calculation	94
Fig. 50	Signal suppression and enhancement determined with direct solid-phase extraction of artificially spiked water samples; losses due to extraction indicated as hatched column parts, matrix effects as plain column parts	95
Fig. 51	Partition of pharmaceuticals and polar pesticides between filter, master and backup sampling cartridge observed during sampling at the Three Gorges Dam (China); mean value of the measurements in 11, 31 and 50 m water depth	97
Fig. 52	Partition of perfluorinated alkyl acids (PFAAs) between filter, master and backup sampling cartridge observed during sampling at the Three Gorges Dam (China); mean value of the measurements in 11, 31 and 50 m water depth	98
Fig. 53	Depth profile of pharmaceuticals and polar pesticides determined in the Yangtze River upstream from the Three Gorges Dam in September 2013	99
Fig. 54	Depth profile of PFAAs determined in the Yangtze River upstream from the Three Gorges Dam in September 2013	100

List of Tables

4.1	List of PFCs contained within the native standard mixture and the mass labelled mixture	35
4.2	Dilution scheme for the preparation of PFAA standards used for calibration of the instrument in nano-scale configuration with direct injection	43
4.3	List of evaluated solid-phase extraction cartridges for laboratory cleanup	45
5.1	Retention time and resolution of adjacent peaks of pharmaceuticals and polar pesticides during initial gradient elution with trapping and nano-scale separation .	57
5.2	Retention time and resolution of critical peak pairs with optimized gradient shape and starting solvent B from 40 to 80 % achieved with trapping and nano-scale separation	58
5.3	Retention time and resolution of adjacent peaks during gradient elution of pharmaceuticals and polar pesticides achieved with nano-scale separation and direct injection	62
5.4	Peak area of internal standards (IS) determined in TOF-MS and MS/MS mode achieved by injecting 0.5 μ L of a calibration standard for pharmaceuticals and polar pesticides	76
5.5	List of parameters and results from system calibration obtained with nano-scale chromatography and direct injection; pharmaceuticals and polar pesticides were calibrated with single injections, PFAAs with triplicate measurements	81
5.6	List of parameters and results from system calibration obtained with micro-scale chromatography and direct injection with triplicate measurements for pharmaceuticals and polar pesticides and single measurements for PFAAs	84
5.7	List of possible suspects detected in extracted VO samplers from the river Selke in Saxony-Anhalt (Germany) and their corresponding verification level	103
5.8	List of possible suspects detected in extracted XAD sampling cartridge extracts from the Yangtze River (China), their verification level and abundance in the sampling cartridges	105

Bibliography

- [1] Georg Thieme Verlag, RÖMPP Online-Enzyklopädie, <http://www.roempp.com>, accessed: 2015-05-05.
- [2] OpenStreetMap, <http://www.openstreetmap.org>, accessed: 2015-05-01.
- [3] J. Zhang, Geochemistry of trace metals from chinese river/estuary systems: An overview, *Estuarine, Coastal and Shelf Science* 41 (6) (1995) 631–658. doi:10.1006/ecss.1995.0082.
- [4] A. Bergmann, Y. Bi, L. Chen, T. Floehr, B. Henkelmann, A. Holbach, H. Hollert, W. Hu, I. Kranzioch, E. Klumpp, S. Küppers, S. Norra, R. Ottermanns, G. Pfister, M. Roß-Nickoll, A. Schäffer, N. Schleicher, B. Schmidt, B. Scholz-Starke, K.-W. Schramm, G. Subklew, A. Tiehm, C. Temoka, J. Wang, B. Westrich, R.-D. Wilken, A. Wolf, X. Xiang, Y. Yuan, The Yangtze-Hydro Project: a Chinese-German environmental program, *Environmental Science and Pollution Research* 19 (4) (2012) 1341–1344. doi:10.1007/s11356-011-0645-7.
- [5] T. Floehr, H. Xiao, B. Scholz-Starke, L. Wu, J. Hou, D. Yin, X. Zhang, R. Ji, X. Yuan, R. Ottermanns, M. Roß-Nickoll, A. Schäffer, H. Hollert, Solution by dilution? - A review on the pollution status of the Yangtze River, *Environmental Science and Pollution Research* 20 (10) (2013) 6934–6971. doi:10.1007/s11356-013-1666-1.
- [6] China National Environmental Monitoring Center, Bulletin on the Ecological and Environmental Monitoring Results of the Three Gorges Project 2011, Tech. rep. (2011).
- [7] China National Environmental Monitoring Center, Bulletin on the Ecological and Environmental Monitoring Results of the Three Gorges Project 2009, Tech. rep. (2009).
- [8] China National Environmental Monitoring Center, Bulletin on the Ecological and Environmental Monitoring Results of the Three Gorges Project 2010, Tech. rep. (2010).
- [9] Greenpeace, Swimming in Poison - An Analysis of hazardous chemicals in Yangtze River fish, <http://www.greenpeace.org/eastasia/publications/reports/toxics/2010/swimming-in-poison-yangtze-fish/>, accessed: 2015-04-30 (2010).
- [10] China Internet Information Center, Wiki on Yangtze, <http://wiki.china.org.cn/wiki/index.php/Yangtze>, published under the auspices of the State Council Information Office and the China International Publishing Group, accessed: 2015-04-30.

- [11] AmbiWeb GmbH, Climate-Data.org - Klimadaten für Städte weltweit, <http://de.climate-data.org>, accessed: 2015-05-03.
- [12] T. Dorcey, A. Steiner, M. Acreman, B. Orlando (Eds.), *Large Dams: Learning from the Past, Looking at the Future. Workshop Proceedings.*, ICUN - The World Conservation Union and the World Bank Group, 1997.
- [13] A. Wolf, A. Bergmann, R.-D. Wilken, X. Gao, Y. Bi, H. Chen, C. Schüth, Occurrence and distribution of organic trace substances in waters from the Three Gorges Reservoir, China, *Environmental Science and Pollution Research* 20 (10) (2013) 7124–7139. doi: 10.1007/s11356-013-1929-x.
- [14] D. Deyerling, J. Wang, W. Hu, B. Westrich, C. Peng, Y. Bi, B. Henkelmann, K.-W. Schramm, PAH distribution and mass fluxes in the Three Gorges Reservoir after impoundment of the Three Gorges Dam, *Science of The Total Environment* 491-492 (0) (2014) 123–130. doi:10.1016/j.scitotenv.2014.03.076.
- [15] S. Jackson, A. Sleigh, Resettlement for China's Three Gorges Dam: socio-economic impact and institutional tensions, *Communist and Post-Communist Studies* 33 (2) (2000) 223–241. doi:10.1016/S0967-067X(00)00005-2.
- [16] G. Subklew, J. Ulrich, L. Fürst, A. Höltkemeier, Environmental impacts of the Yangtze Three Gorges project: An overview of the Chinese-German research cooperation, *Journal of Earth Science* 21 (6) (2010) 817–823. doi:10.1007/s12583-010-0133-x.
- [17] C. Wong, C. Williams, J. Pittock, U. Collier, U. Schelle, P. Schelle, World's top 10 rivers at risk, Tech. rep., WWF (2007).
URL <http://wwf.panda.org/?108620/Worlds-Top-10-Rivers-at-Risk>
- [18] B. Müller, M. Berg, Z. P. Yao, X. F. Zhang, D. Wang, A. Pfluger, How polluted is the Yangtze river? Water quality downstream from the Three Gorges Dam, *Science of The Total Environment* 402 (2-3) (2008) 232–247. doi:10.1016/j.scitotenv.2008.04.049.
- [19] F. Heeb, H. Singer, B. Pernet-Coudrier, W. Qi, H. Liu, P. Longrée, B. Müller, M. Berg, Organic Micropollutants in Rivers Downstream of the Megacity Beijing: Sources and Mass Fluxes in a Large-Scale Wastewater Irrigation System, *Environmental Science & Technology* 46 (16) (2012) 8680–8688. doi:10.1021/es301912q.

- [20] UNEP, Stockholm Convention at a glance, United Nations Environment Programme, 2015.
URL <http://chm.pops.int/Portals/0/download.aspx?d=UNEP-POPS-PAWA-OVERV-AtaGlance.En.pdf>
- [21] J. Weber, C. J. Halsall, D. Muir, C. Teixeira, J. Small, K. Solomon, M. Hermanson, H. Hung, T. Bidleman, Endosulfan, a global pesticide: A review of its fate in the environment and occurrence in the Arctic, *Science of The Total Environment* 408 (15) (2010) 2966–2984. doi:10.1016/j.scitotenv.2009.10.077.
- [22] EPA, Facts Sheet on Polycyclic Aromatic Hydrocarbons, United States Environmental Protection Agency, 2008.
- [23] A. M. Mastral, M. S. Callén, J. M. López, R. Murillo, T. Garcíá, M. V. Navarro, Critical review on atmospheric PAH. Assessment of reported data in the Mediterranean basin, *Fuel Processing Technology* 80 (2) (2003) 183–193.
URL <http://www.sciencedirect.com/science/article/pii/S0378382002002497>
- [24] J. Topinka, L. R. Schwarz, F. Kiefer, F. J. Wiebel, O. Gajdos, P. Vidová, L. Dobiás, M. Fried, R. J. Srám, T. Wolff, DNA adduct formation in mammalian cell cultures by polycyclic aromatic hydrocarbons (PAH) and nitro-PAH in coke oven emission extract, *Mutation Research/Genetic Toxicology and Environmental Mutagenesis* 419 (1-3) (1998) 91–105. doi:10.1016/S1383-5718(98)00127-2.
- [25] WHO, Air quality guidelines for Europe, 2nd Edition, World Health Organization, 2000.
URL http://www.euro.who.int/__data/assets/pdf_file/0005/74732/E71922.pdf?ua=1
- [26] C. Dasenbrock, L. Peters, O. Creutzenberg, U. Heinrich, The carcinogenic potency of carbon particles with and without PAH after repeated intratracheal administration in the rat, *Toxicology Letters* 88 (1-3) (1996) 15–21. doi:10.1016/0378-4274(96)03712-5.
- [27] B. D. Key, R. D. Howell, C. S. Criddle, Fluorinated Organics in the Biosphere, *Environmental Science & Technology* 31 (9) (1997) 2445–2454. doi:10.1021/es961007c.
- [28] J. P. Giesy, K. Kannan, Peer reviewed: Perfluorochemical surfactants in the environment, *Environmental Science & Technology* 36 (7) (2002) 146A–152A. doi:10.1021/es022253t.

- [29] J. H. Simons, W. J. Harland, Production of Fluorocarbons: III. From Hydrogen Fluoride-Soluble Organic Substances, *Journal of The Electrochemical Society* 95 (2) (1949) 55–59. doi:10.1149/1.2776735.
- [30] J. Simons, Electrochemical process of making fluorine-containing carbon compounds, US Patent 2,519,983 (1950).
- [31] W. Pearlson, The simons electrochemical fluorination process (commercial development at 3M), *Journal of Fluorine Chemistry* 32 (1) (1986) 29–40. doi:10.1016/S0022-1139(00)80505-9.
- [32] L. Conte, G. Gambaretto, Electrochemical fluorination: state of the art and future tendencies, *Journal of Fluorine Chemistry* 125 (2) (2004) 139 – 144. doi:10.1016/j.jfluchem.2003.07.002.
- [33] A. G. Paul, K. C. Jones, A. J. Sweetman, A First Global Production, Emission, And Environmental Inventory For Perfluorooctane Sulfonate, *Environmental Science & Technology* 43 (2) (2009) 386–392. doi:10.1021/es802216n.
- [34] American Chemical Society, Scifinder database, <https://scifinder.cas.org>, accessed: 2015-05-07.
- [35] N. Carmosini, L. S. Lee, Partitioning of Fluorotelomer Alcohols to Octanol and Different Sources of Dissolved Organic Carbon, *Environmental Science & Technology* 42 (17) (2008) 6559–6565. doi:10.1021/es800263t.
- [36] M. J. A. Dinglasan-Panlilio, S. A. Mabury, Significant Residual Fluorinated Alcohols Present in Various Fluorinated Materials, *Environmental Science & Technology* 40 (5) (2006) 1447–1453. doi:10.1021/es051619+.
- [37] M. Villagrasa, M. López de Alda, D. Barceló, Environmental analysis of fluorinated alkyl substances by liquid chromatography-(tandem) mass spectrometry: a review, *Analytical and Bioanalytical Chemistry* 386 (4) (2006) 953–972. doi:10.1007/s00216-006-0471-9.
- [38] E. Sinclair, S. K. Kim, H. B. Akinleye, K. Kannan, Quantitation of Gas-Phase Perfluoroalkyl Surfactants and Fluorotelomer Alcohols Released from Nonstick Cookware and Microwave Popcorn Bags, *Environmental Science & Technology* 41 (4) (2007) 1180–1185. doi:10.1021/es062377w.

- [39] A. A. Jensen, H. Leffers, Emerging endocrine disrupters: perfluoroalkylated substances, *International Journal of Andrology* 31 (2) (2008) 161–169. doi:10.1111/j.1365-2605.2008.00870.x.
- [40] K. Prevedouros, I. T. Cousins, R. C. Buck, S. H. Korzeniowski, Sources, Fate and Transport of Perfluorocarboxylates, *Environmental Science & Technology* 40 (1) (2006) 32–44. doi:10.1021/es0512475.
- [41] S. Taniyasu, K. Kannan, Y. Horii, N. Hanari, N. Yamashita, A Survey of Perfluorooctane Sulfonate and Related Perfluorinated Organic Compounds in Water, Fish, Birds, and Humans from Japan, *Environmental Science & Technology* 37 (12) (2003) 2634–2639. doi:10.1021/es0303440.
- [42] C. P. Higgins, J. A. Field, C. S. Criddle, R. G. Luthy, Quantitative Determination of Perfluorochemicals in Sediments and Domestic Sludge, *Environmental Science & Technology* 39 (11) (2005) 3946–3956. doi:10.1021/es048245p.
- [43] M. Smithwick, S. A. Mabury, K. R. Solomon, C. Sonne, J. W. Martin, E. W. Born, R. Dietz, A. E. Derocher, R. J. Letcher, T. J. Evans, G. W. Gabrielsen, J. Nagy, I. Stirling, M. K. Taylor, D. C. G. Muir, Circumpolar Study of Perfluoroalkyl Contaminants in Polar Bears (*Ursus maritimus*), *Environmental Science & Technology* 39 (15) (2005) 5517–5523. doi:10.1021/es048309w.
- [44] K. Kannan, J. C. Franson, W. W. Bowerman, K. J. Hansen, P. D. Jones, J. P. Giesy, Perfluorooctane Sulfonate in Fish-Eating Water Birds Including Bald Eagles and Albatrosses, *Environmental Science & Technology* 35 (15) (2001) 3065–3070. doi:10.1021/es001935i.
- [45] M. Shoeib, T. Harner, P. Vlahos, Perfluorinated chemicals in the arctic atmosphere, *Environmental Science & Technology* 40 (24) (2006) 7577–7583. doi:10.1021/es0618999.
- [46] S. Fiedler, Method development and determination of anthropogenic poly- and perfluorinated compounds in air, water, soil, house dust, and several consumer products, Ph.D. thesis, Technische Universität München (2010).
URL <http://nbn-resolving.de/urn/resolver.pl?urn:nbn:de:bvb:91-diss-20101213-978637-1-3>
- [47] Z. Xu, Fluorotelomer alcohols, perfluoroalkyl acids and semifluorinated alkanes in the house dust, air and sediment, Ph.D. thesis, Technische Universität München (2014).

URL <http://nbn-resolving.de/urn/resolver.pl?urn:nbn:de:bvb:91-diss-20140214-1182676-0-9>

- [48] L. W. Y. Yeung, S. J. Robinson, J. Koschorreck, S. A. Mabury, Part I. A Temporal Study of PFCAs and Their Precursors in Human Plasma from Two German Cities 1982-2009, *Environmental Science & Technology* 47 (8) (2013) 3865–3874. doi:10.1021/es303716k.
- [49] H. Fromme, O. Midasch, D. Twardella, J. Angerer, S. Boehmer, B. Liebl, Occurrence of perfluorinated substances in an adult german population in southern bavaria, *International Archives of Occupational and Environmental Health* 80 (4) (2007) 313–319. doi:10.1007/s00420-006-0136-1.
- [50] C. A. Moody, G. N. Hebert, S. H. Strauss, J. A. Field, Occurrence and persistence of perfluorooctanesulfonate and other perfluorinated surfactants in groundwater at a fire-training area at Wurtsmith Air Force Base, Michigan, USA, *Journal of Environmental Monitoring* 5 (2003) 341–345. doi:10.1039/B212497A.
- [51] E. Sinclair, K. Kannan, Mass Loading and Fate of Perfluoroalkyl Surfactants in Wastewater Treatment Plants, *Environmental Science & Technology* 40 (5) (2006) 1408–1414. doi:10.1021/es051798v.
- [52] H. F. Schröder, Determination of fluorinated surfactants and their metabolites in sewage sludge samples by liquid chromatography with mass spectrometry and tandem mass spectrometry after pressurised liquid extraction and separation on fluorine-modified reversed-phase sorbents, *Journal of Chromatography A* 1020 (1) (2003) 131–151. doi:10.1016/S0021-9673(03)00936-1.
- [53] German Federal Environment Agency, Do without Per- and Polyfluorinated Chemicals and Prevent their Discharge into the Environment, <http://www.umweltbundesamt.de/publikationen/do-without-per-polyfluorinated-chemicals-prevent>, accessed: 2015-05-04 (2009).
- [54] J. Hölzer, O. Midasch, K. Rauchfuss, M. Kraft, R. Reupert, J. Angerer, P. Kleeschulte, N. Marschall, M. Wilhelm, Biomonitoring of Perfluorinated Compounds in Children and Adults Exposed to Perfluorooctanoate-Contaminated Drinking Water, *Environmental Health Perspectives* 116 (5) (2008) 651–657. doi:10.1289/ehp.11064.
- [55] G. L. Kennedy, J. L. Butenhoff, G. W. Olsen, J. C. O'Connor, A. M. Seacat, R. G. Perkins, L. B. Biegel, S. R. Murphy, D. G. Farrar, The toxicology of perfluorooctanoate,

- Critical Reviews in Toxicology 34 (4) (2004) 351–384, pMID: 15328768. doi:10.1080/10408440490464705.
- [56] C. Fei, J. K. McLaughlin, L. Lipworth, J. Olsen, Maternal levels of perfluorinated chemicals and subfecundity, *Human Reproduction* 1 (1) (2009) 1–6. doi:10.1093/humrep/den490.
- [57] H.-J. Koch, C. v. Haaren, M. Faulstich, H. Foth, M. Jänicke, P. Michaelis, K. Ott, *Arzneimittel in der Umwelt - Stellungnahme*, Tech. rep., SRU - Sachverständigenrat für Umweltfragen (2007).
- [58] K. Nödler, T. Licha, K. Bester, M. Sauter, Development of a multi-residue analytical method, based on liquid chromatography-tandem mass spectrometry, for the simultaneous determination of 46 micro-contaminants in aqueous samples, *Journal Of Chromatography A* 1217 (42) (2010) 6511–6521. doi:10.1016/j.chroma.2010.08.048.
- [59] B. J. Vanderford, S. A. Snyder, Analysis of pharmaceuticals in water by isotope dilution liquid chromatography/tandem mass spectrometry, *Environmental Science & Technology* 40 (23) (2006) 7312–7320. doi:10.1021/es0613198.
- [60] A. Müller, W. Schulz, W. K. L. Ruck, W. H. Weber, A new approach to data evaluation in the non-target screening of organic trace substances in water analysis, *Chemosphere* 85 (8) (2011) 1211–1219. doi:10.1016/j.chemosphere.2011.07.009.
- [61] F. Wode, C. Reilich, P. van Baar, U. Dünnebier, M. Jekel, T. Reemtsma, Multiresidue analytical method for the simultaneous determination of 72 micropollutants in aqueous samples with ultra high performance liquid chromatography-high resolution mass spectrometry, *Journal of Chromatography A* 1270 (2012) 118–126. doi:10.1016/j.chroma.2012.10.054.
- [62] Q. Bu, B. Wang, J. Huang, S. Deng, G. Yu, Pharmaceuticals and personal care products in the aquatic environment in china: A review, *Journal of Hazardous Materials* 262 (2013) 189–211. doi:10.1016/j.jhazmat.2013.08.040.
- [63] J.-L. Liu, M.-H. Wong, Pharmaceuticals and personal care products (PPCPs): A review on environmental contamination in china, *Environment International* 59 (2013) 208–224. doi:10.1016/j.envint.2013.06.012.
- [64] German Federal Environment Agency, *Arzneimittel in der Umwelt - vermeiden, reduzieren, überwachen*, <http://www.umweltbundesamt.de/sites/default/files/>

medien/378/publikationen/01.08.2014_hintergrundpapier_arzneimittel_final_.pdf, accessed: 2015-05-07 (2014).

- [65] N. Banspach, Erstmals Zahlen über die Antibiotika-Abgabe in der Tiermedizin erfasst, http://www.bvl.bund.de/DE/08_PresseInfothek/01_FuerJournalisten/01_Presse_und_Hintergrundinformationen/05_Tierarzneimittel/2012/2012_abgabemengenregister/2012_09_11_pi_abgabemengenregister.html?nn=1461380, accessed: 2015-05-07 (2012).
- [66] Austrian Federal Environment Agency, Veterinärantibiotika in Wirtschaftsdünger und Boden, <http://www.umweltbundesamt.at/fileadmin/site/publikationen/BE272.pdf>, accessed: 2015-05-07 (2005).
- [67] A. Bergmann, R. Fohrmann, F.-A. Weber, Zusammenstellung von Monitoringdaten zu Umweltkonzentrationen von Arzneimitteln 2011, <http://www.uba.de/uba-info-medien/4188.html>, on behalf of the German Federal Environment Agency, accessed: 2015-05-07.
- [68] German Federal Statistical Office, Entsorgung und Verwertung von Klärschlämmen, <http://www.bmub.bund.de/themen/wasser-abfall-boden/abfallwirtschaft/statistiken/klaerschlam/>, accessed: 2015-05-08 (2012).
- [69] J. L. Oaks, M. Gilbert, M. Z. Virani, R. T. Watson, C. U. Meteyer, B. A. Rideout, H. L. Shivaprasad, S. Ahmed, M. J. Iqbal Chaudhry, M. Arshad, S. Mahmood, A. Ali, A. Ahmed Khan, Diclofenac residues as the cause of vulture population decline in Pakistan, *Nature* 427 (6975) (2004) 630–633. doi:10.1038/nature02317.
- [70] K. A. Kidd, P. J. Blanchfield, K. H. Mills, V. P. Palace, R. E. Evans, J. M. Lazorchak, R. W. Flick, Collapse of a fish population after exposure to a synthetic estrogen, *Proceedings of the National Academy of Sciences* 104 (21) (2007) 8897–8901. doi:10.1073/pnas.0609568104.
- [71] R. Länge, T. H. Hutchinson, C. P. Croudace, F. Siegmund, H. Schweinfurth, P. Hampe, G. H. Panter, J. P. Sumpter, Effects of the synthetic estrogen 17 β -ethinylestradiol on the life-cycle of the fathead minnow (*Pimephales promelas*), *Environmental Toxicology and Chemistry* 20 (6) (2001) 1216–1227. doi:10.1002/etc.5620200610.
- [72] R. Triebkorn, H. Casper, V. Scheil, J. Schwaiger, Ultrastructural effects of pharmaceuticals (carbamazepine, clofibrac acid, metoprolol, diclofenac) in rainbow trout (*On-*

- corhynchus mykiss*) and common carp (*Cyprinus carpio*), *Analytical and Bioanalytical Chemistry* 387 (4) (2007) 1405–1416. doi:10.1007/s00216-006-1033-x.
- [73] F. Liu, G.-G. Ying, R. Tao, J.-L. Zhao, J.-F. Yang, L.-F. Zhao, Effects of six selected antibiotics on plant growth and soil microbial and enzymatic activities, *Environmental Pollution* 157 (5) (2009) 1636 – 1642. doi:10.1016/j.envpol.2008.12.021.
- [74] L. Michelini, R. Reichel, W. Werner, R. Ghisi, S. Thiele-Bruhn, Sulfadiazine Uptake and Effects on *Salix fragilis* L. and *Zea mays* L. *Plants, Water, Air, & Soil Pollution* 223 (8) (2012) 5243–5257. doi:10.1007/s11270-012-1275-5.
- [75] M. Grote, C. Schwake-Anduschus, H. Stevens, R. Michel, T. Betsche, M. Freitag, Antibiotika-Aufnahme von Nutzpflanzen aus Gülle-gedüngten Böden - Ergebnisse eines Modellversuchs, *Journal für Verbraucherschutz und Lebensmittelsicherheit* 1 (1) (2006) 38–50. doi:10.1007/s00003-006-0008-3.
- [76] H. Heuer, Q. Solehati, U. Zimmerling, K. Kleineidam, M. Schloter, T. Müller, A. Focks, S. Thiele-Bruhn, K. Smalla, Accumulation of Sulfonamide Resistance Genes in Arable Soils Due to Repeated Application of Manure Containing Sulfadiazine, *Applied and Environmental Microbiology* 77 (7) (2011) 2527 – 2530. doi:10.1128/AEM.02577-10.
- [77] A. Schlüter, H. Heuer, R. Szczepanowski, L. J. Forney, C. M. Thomas, A. Pühler, E. M. Top, The 64 508 bp IncP-1 β antibiotic multiresistance plasmid pB10 isolated from a waste-water treatment plant provides evidence for recombination between members of different branches of the IncP-1 β group, *Microbiology* 149 (11) (2003) 3139–3153. doi:10.1099/mic.0.26570-0.
- [78] H. Heuer, R. Szczepanowski, S. Schneiker, A. Pühler, E. M. Top, A. Schlüter, The complete sequences of plasmids pB2 and pB3 provide evidence for a recent ancestor of the IncP-1 β group without any accessory genes, *Microbiology* 150 (11) (2004) 3591–3599. doi:10.1099/mic.0.27304-0.
- [79] K. G. Byrne-Bailey, W. H. Gaze, P. Kay, A. B. A. Boxall, P. M. Hawkey, E. M. H. Wellington, Prevalence of Sulfonamide Resistance Genes in Bacterial Isolates from Manured Agricultural Soils and Pig Slurry in the United Kingdom, *Antimicrobial Agents and Chemotherapy* 53 (2) (2009) 696–702. doi:10.1128/AAC.00652-07.
- [80] J. Y. M. Tang, F. Buseti, J. W. A. Charrois, B. I. Escher, Which chemicals drive biological effects in wastewater and recycled water?, *Water Research* 60 (0) (2014) 289–299. doi:10.1016/j.watres.2014.04.043.

- [81] J. Y. M. Tang, S. McCarty, E. Glenn, P. A. Neale, M. S. J. Warne, B. I. Escher, Mixture effects of organic micropollutants present in water: Towards the development of effect-based water quality trigger values for baseline toxicity, *Water Research* 47 (10) (2013) 3300–3314. doi:10.1016/j.watres.2013.03.011.
- [82] J. Wang, S. Bernhöft, G. Pfister, K.-W. Schramm, Water exposure assessment of aryl hydrocarbon receptor agonists in Three Gorges Reservoir, China using SPMD-based virtual organisms, *Science of The Total Environment* 496 (2014) 26–34. doi:10.1016/j.scitotenv.2014.07.015.
- [83] M. Mehrjouei, S. Müller, D. Möller, A review on photocatalytic ozonation used for the treatment of water and wastewater, *Chemical Engineering Journal* 263 (2015) 209–219. doi:10.1016/j.cej.2014.10.112.
- [84] X. Yang, R. C. Flowers, H. S. Weinberg, P. C. Singer, Occurrence and removal of pharmaceuticals and personal care products (PPCPs) in an advanced wastewater reclamation plant, *Water Research* 45 (16) (2011) 5218–5228. doi:10.1016/j.watres.2011.07.026.
- [85] T. Hillenband, F. Tettenborn, E. Menger-Krug, F. Marscheider-Weidemann, S. Fuchs, S. Toshovski, S. Kitthaus, S. Metzger, I. Tjoeng, P. Wermter, M. Kersting, C. Abegglen, Maßnahmen zur Verminderung des Eintrages von Mikroschadstoffen in die Gewässer, German Federal Office for Environment (Umweltbundesamt, UBA), 2014.
URL <http://www.umweltbundesamt.de/publikationen/massnahmen-zur-verminderung-des-eintrages-von>
- [86] EU, Directive 2000/60/EC of the European Parliament and of the Council establishing a framework for Community action in the field of water policy, The European Parliament and the Council of the European Union, 2000.
URL <http://eur-lex.europa.eu/legal-content/EN/TXT/PDF/?uri=CELEX:02000L0060-20140101&rid=2>
- [87] EU, Directive 2008/105/EC of the European Parliament and of the Council, The European Parliament and the Council of the European Union, 2008.
URL <http://eur-lex.europa.eu/legal-content/EN/TXT/PDF/?uri=CELEX:32008L0105&rid=2>
- [88] EU, Directive 2004/27/EC of the European Parliament and of the Council amending Directive 2001/83/EC on the Community code relating to medicinal products for human

use, The European Parliament and the Council of the European Union, 2004.

URL <http://eur-lex.europa.eu/legal-content/EN/TXT/PDF/?uri=CELEX:32004L0027&from=EN>

- [89] EU, Directive 2013/39/EU of the European Parliament and of the Council, The European Parliament and the Council of the European Union, 2013.

URL <http://eur-lex.europa.eu/legal-content/EN/TXT/PDF/?uri=CELEX:32013L0039&rid=1>

- [90] EU, Council Directive 80/778/EEC relating to the quality of water intended for human consumption, The Council of the European Union, 1980.

URL <http://eur-lex.europa.eu/legal-content/EN/TXT/PDF/?uri=CELEX:31980L0778&from=EN>

- [91] EU, Council Directive 98/83/EC on the quality of water intended for human consumption, The Council of the European Union, 1998.

URL <http://eur-lex.europa.eu/legal-content/EN/TXT/PDF/?uri=CELEX:01998L0083-20090807&rid=1>

- [92] WHO, Guidelines for Drinking-water Quality, 4th Edition, World Health Organization, 2011.

URL http://www.who.int/water_sanitation_health/publications/2011/dwq_guidelines/en/

- [93] BMJV, Trinkwasserverordnung - TrinkwV, Federal Ministry of Justice (Bundesministerium der Justiz und Verbraucherschutz, BMJV), 2001.

URL http://www.gesetze-im-internet.de/bundesrecht/trinkwv_2001/gesamt.pdf

- [94] BMJV, Trinkwasserverordnung - TrinkwV, Federal Ministry of Justice (Bundesministerium der Justiz und Verbraucherschutz, BMJV), 1975.

URL http://www.bgbl.de/banzxaver/bgbl/start.xav?startbk=Bundesanzeiger_BGBl&jumpTo=bgbl1175s0453.pdf

- [95] V. R. Meyer, Practical High-Performance Liquid Chromatography, Wiley VCH, 2010.

URL <http://www.myilibrary.com?ID=255055>

- [96] L. R. Snyder, Peer Reviewed: HPLC: Past and Present., *Anal. Chem.* 72 (11) (2000) 412 A-420 A. doi:10.1021/ac002846r.

- [97] M. Rodriguez-Aller, R. Gurny, J.-L. Veuthey, D. Guillarme, Coupling ultra high-pressure liquid chromatography with mass spectrometry: Constraints and possible applications, *Journal of Chromatography A* 1292 (0) (2013) 2–18. doi:10.1016/j.chroma.2012.09.061.
- [98] J. Nawrocki, The silanol group and its role in liquid chromatography, *Journal of Chromatography A* 779 (1-2) (1997) 29–71. doi:10.1016/S0021-9673(97)00479-2.
- [99] A. Vailaya, C. Horvath, Retention in reversed-phase chromatography: partition or adsorption?, *Journal of Chromatography A* 829 (1-2) (1998) 1–27. doi:10.1016/S0021-9673(98)00727-4.
- [100] H. Claessens, M. van Straten, Review on the chemical and thermal stability of stationary phases for reversed-phase liquid chromatography, *Journal of Chromatography A* 1060 (1-2) (2004) 23–41. doi:10.1016/j.chroma.2004.08.098.
- [101] L. Snyder, A. Maule, A. Heebsh, R. Cuellar, S. Paulson, J. Carrano, L. Wisley, C. Chan, N. Pearson, J. Dolan, J. Gilroy, A fast, convenient and rugged procedure for characterizing the selectivity of alkyl-silica columns, *Journal of Chromatography A* 1057 (1-2) (2004) 49–57. doi:10.1016/j.chroma.2004.09.063.
- [102] L. R. Snyder, J. W. Dolan, *High-Performance Gradient Elution: The Practical Application of the Linear-Solvent-Strength Model*, Wiley-VCH, 2007. doi:10.1002/0470055529.
- [103] E. Kováts, Gas-chromatographische Charakterisierung organischer Verbindungen. Teil 1: Retentionsindices aliphatischer Halogenide, Alkohole, Aldehyde und Ketone, *Helvetica Chimica Acta* 41 (7) (1958) 1915–1932. doi:10.1002/hlca.19580410703.
- [104] R. M. Smith, C. M. Burr, Retention prediction of analytes in reversed-phase high-performance liquid chromatography based on molecular structure : II. Long term reproducibility of capacity factors and retention indices, *Journal of Chromatography A* 475 (2) (1989) 75–83. doi:10.1016/S0021-9673(01)89664-3.
- [105] S. Yamauchi, Retention indices of phenols for internal standards in reversed-phase high-performance liquid chromatography: Application to retention prediction and selectivities of mobile phases and packing materials, *Journal of Chromatography A* 635 (1) (1993) 61–70. doi:10.1016/0021-9673(93)83114-8.

- [106] M. Marsin Sanagi, U. K. Ahmad, K. Hassan, G. Musa, Alkylbenzenes as a retention-index scale in reversed-phase high-performance liquid chromatography, *Journal of Chromatography A* 722 (1-2) (1996) 59–68. doi:10.1016/0021-9673(95)00453-X.
- [107] BMBF, RiSKWa: Risk Management of Emerging Compounds and Pathogens in the Water Cycle (2014).
URL <http://www.bmbf.riskwa.de/en/index.php>
- [108] BMBF, Risk-ident: Assessment of previously unknown anthropogenic trace contaminants and action strategies for risk management in aquatic systems. (2014).
URL <http://risk-ident.hswt.de/pages/en/home.php?lang=EN>
- [109] J. H. Gross, *Massenspektrometrie - Ein Lehrbuch*, Springer Spektrum, 2013. doi:10.1007/978-3-8274-2981-0.
- [110] I. Chernushevich, A. Loboda, B. A. Thomson, An introduction to quadrupole-time-of-flight mass spectrometry, *Journal of Mass Spectrometry* 36 (8) (2001) 849–865.
URL 10.1002/jms.207
- [111] M. Guilhaus, Special feature: Tutorial. Principles and instrumentation in time-of-flight mass spectrometry. Physical and instrumental concepts, *Journal of Mass Spectrometry* 30 (11) (1995) 1519–1532. doi:10.1002/jms.1190301102.
- [112] Waters-Micromass, *Q-ToF 2 User's Guide*, 2001.
- [113] L. Rayleigh, XX. On the equilibrium of liquid conducting masses charged with electricity, *Philosophical Magazine Series 5* 14 (87) (1882) 184–186. doi:10.1080/14786448208628425.
- [114] A. Gomez, K. Tang, Charge and fission of droplets in electrostatic sprays, *Physics of Fluids* (1994-present) 6 (1) (1994) 404–414. doi:10.1063/1.868037.
- [115] D. Duft, T. Achtzehn, R. Muller, B. A. Huber, T. Leisner, Coulomb fission: Rayleigh jets from levitated microdroplets, *Nature* 421 (6919) (2003) 128–128. doi:10.1038/421128a.
- [116] P. Kebarle, A brief overview of the present status of the mechanisms involved in electrospray mass spectrometry, *Journal of Mass Spectrometry* 35 (7) (2000) 804–817. doi:10.1002/1096-9888(200007)35:7<804::AID-JMS22>3.0.CO;2-Q.

- [117] M.-C. Hennion, Solid-phase extraction: method development, sorbents, and coupling with liquid chromatography, *Journal of Chromatography A* 856 (1-2) (1999) 3–54. doi: 10.1016/S0021-9673(99)00832-8.
- [118] SRC, PHYSPROP Database, <http://esc.syrres.com/fatepointer/search.asp>, accessed: 2015-05-02.
- [119] J. Bicker, A. Fortuna, G. Alves, A. F. ao, Liquid chromatographic methods for the quantification of catecholamines and their metabolites in several biological samples - A review, *Analytica Chimica Acta* 768 (2013) 12 – 34. doi:10.1016/j.aca.2012.12.030.
- [120] J. Lotharius, P. Brundin, Pathogenesis of parkinson's disease: dopamine, vesicles and [alpha]-synuclein, *Nature Reviews. Neuroscience* 3 (12) (2002) 932–942. doi:10.1038/nrn983.
- [121] S. H. Snyder, Catecholamines in schizophrenia, *Life Sciences* 13 (8) (1973) cxlviii – cxlix. doi:10.1016/0024-3205(73)90395-0.
- [122] J. Nagler, Method development for determination of monoamines in mice brain and investigation of neurotransmitter networks in wildtype and knockout mice, Master's thesis, Technische Universität München (2014).
- [123] M. A. Raggi, C. Sabbioni, G. Nicoletta, R. Mandrioli, G. Gerra, Analysis of plasma catecholamines by liquid chromatography with amperometric detection using a novel SPE ion-exchange procedure, *Journal of Separation Science* 26 (12-13) (2003) 1141–1146. doi:10.1002/jssc.200301486.
- [124] M. Tsunoda, C. Aoyama, H. Nomura, T. Toyoda, N. Matsuki, T. Funatsu, Simultaneous determination of dopamine and 3,4-dihydroxyphenylacetic acid in mouse striatum using mixed-mode reversed-phase and cation-exchange high-performance liquid chromatography, *Journal of Pharmaceutical and Biomedical Analysis* 51 (3) (2010) 712 – 715. doi:10.1016/j.jpba.2009.09.045.
- [125] M. M. Kushnir, F. M. Urry, E. L. Frank, W. L. Roberts, B. Shushan, Analysis of Catecholamines in Urine by Positive-Ion Electrospray Tandem Mass Spectrometry, *Clinical Chemistry* 48 (2) (2002) 323–331.
- [126] W. H. de Jong, E. G. de Vries, B. H. Wolffenbuttel, I. Kema, Automated mass spectrometric analysis of urinary free catecholamines using on-line solid phase extraction, *Journal*

- of Chromatography B 878 (19) (2010) 1506 – 1512. doi:10.1016/j.jchromb.2010.03.050.
- [127] E. C. Y. Chan, P. C. Ho, High-performance liquid chromatography/atmospheric pressure chemical ionization mass spectrometric method for the analysis of catecholamines and metanephrines in human urine, *Rapid Communications in Mass Spectrometry* 14 (21) (2000) 1959–1964. doi:10.1002/1097-0231(20001115)14:21<1959::AID-RCM117>3.0.CO;2-T.
- [128] X. He, M. Kozak, Development of a liquid chromatography-tandem mass spectrometry method for plasma-free metanephrines with ion-pairing turbulent flow online extraction, *Analytical and Bioanalytical Chemistry* 402 (9) (2012) 3003–3010. doi:10.1007/s00216-012-5768-2.
- [129] M. Gros, S. Rodríguez-Mozaz, D. Barceló, Fast and comprehensive multi-residue analysis of a broad range of human and veterinary pharmaceuticals and some of their metabolites in surface and treated waters by ultra-high-performance liquid chromatography coupled to quadrupole-linear ion trap tandem mass spectrometry, *Journal of Chromatography A* 1248 (0) (2012) 104–121. doi:10.1016/j.chroma.2012.05.084.
- [130] C. Wang, H. Shi, C. D. Adams, S. Gamagedara, I. Stayton, T. Timmons, Y. Ma, Investigation of pharmaceuticals in missouri natural and drinking water using high performance liquid chromatography-tandem mass spectrometry, *Water Research* 45 (4) (2011) 1818–1828. doi:10.1016/j.watres.2010.11.043.
- [131] N. A. Al-Odaini, M. P. Zakaria, M. I. Yaziz, S. Surif, Multi-residue analytical method for human pharmaceuticals and synthetic hormones in river water and sewage effluents by solid-phase extraction and liquid chromatography-tandem mass spectrometry, *Journal of Chromatography A* 1217 (44) (2010) 6791–6806. doi:10.1016/j.chroma.2010.08.033.
- [132] B. Kasprzyk-Hordern, R. M. Dinsdale, A. J. Guwy, Multi-residue method for the determination of basic/neutral pharmaceuticals and illicit drugs in surface water by solid-phase extraction and ultra performance liquid chromatography-positive electrospray ionisation tandem mass spectrometry, *Journal of Chromatography A* 1161 (1-2) (2007) 132–145. doi:10.1016/j.chroma.2007.05.074.
- [133] Y. Yoon, J. Ryu, J. Oh, B.-G. Choi, S. A. Snyder, Occurrence of endocrine disrupting compounds, pharmaceuticals, and personal care products in the Han River (Seoul, South

- Korea), *Science of The Total Environment* 408 (3) (2010) 636–643. doi:10.1016/j.scitotenv.2009.10.049.
- [134] G. Gervais, S. Brosillon, A. Laplanche, C. Helen, Ultra-pressure liquid chromatography-electrospray tandem mass spectrometry for multiresidue determination of pesticides in water, *Journal of Chromatography A* 1202 (2) (2008) 163–172. doi:10.1016/j.chroma.2008.07.006.
- [135] S. Ullah, T. Alsberg, U. Berger, Simultaneous determination of perfluoroalkyl phosphonates, carboxylates, and sulfonates in drinking water, *Journal Of Chromatography A* 1218 (37) (2011) 6388–6395. doi:10.1016/j.chroma.2011.07.005.
- [136] N. Theobald, W. Gerwinski, C. Caliebe, M. Haarich, Entwicklung und Validierung einer Methode zur Bestimmung von polyfluorierten organischen Substanzen in Meerwasser, Sedimenten und Biota; Untersuchungen zum Vorkommen dieser Schadstoffe in der Nord- und Ostsee (Texte 41/2007, Forschungsbericht 202 22 213), <http://www.umweltbundesamt.de/publikationen/entwicklung-validierung-einer-methode-zur>, German Federal Environment Agency (2007).
- [137] N. Theobald, C. Caliebe, W. Gerwinski, H. Hühnerfuss, P. Lepom, Occurrence of perfluorinated organic acids in the North and Baltic seas. Part 1: distribution in sea water, *Environmental Science and Pollution Research* 18 (7) (2011) 1057–1069. doi:10.1007/s11356-011-0451-2.
- [138] P. J. Taylor, Matrix effects: the achilles heel of quantitative high-performance liquid chromatography-electrospray-tandem mass spectrometry, *Clinical Biochemistry* 38 (4) (2005) 328–334. doi:10.1016/j.clinbiochem.2004.11.007.
- [139] M. Stüber, T. Reemtsma, Evaluation of three calibration methods to compensate matrix effects in environmental analysis with lc-esi-ms, *Analytical and Bioanalytical Chemistry* 378 (4) (2004) 910–916. doi:10.1007/s00216-003-2442-8.
- [140] A. Kloepper, J. B. Quintana, T. Reemtsma, Operational options to reduce matrix effects in liquid chromatography-electrospray ionisation-mass spectrometry analysis of aqueous environmental samples, *Journal of Chromatography A* 1067 (1-2) (2005) 153–160. doi:10.1016/j.chroma.2004.11.101.
- [141] F. Xie, R. D. Smith, Y. Shen, Advanced proteomic liquid chromatography, *Journal of Chromatography A* 1261 (2012) 78 – 90, high Speed and High Resolution Separations.

In Honour of Professor Milton Lee on the Occasion of his 65th Birthday. doi:10.1016/j.chroma.2012.06.098.

- [142] A. Murad, E. Rech, NanoUPLC-MSE proteomic data assessment of soybean seeds using the Uniprot database, *BMC Biotechnology* 12 (1) (2012) 82. doi:10.1186/1472-6750-12-82.
- [143] Y. Shi, R. Xiang, C. Horváth, J. A. Wilkins, The role of liquid chromatography in proteomics, *Journal of Chromatography A* 1053 (1-2) (2004) 27 – 36, *bioanalytical Chemistry: Perspectives and Recent Advances with Recognition of Barry L. Karger*. doi:10.1016/j.chroma.2004.07.044.
- [144] G. T. Gibson, S. M. Mugo, R. D. Oleschuk, Nanoelectrospray emitters: Trends and perspective, *Mass Spectrom. Rev.* 28 (6) (2009) 918–936. doi:10.1002/mas.20248.
- [145] M. del Mar Contreras, D. Arráez-Román, A. Fernández-Gutiérrez, A. Segura-Carretero, Nano-liquid chromatography coupled to time-of-flight mass spectrometry for phenolic profiling: A case study in cranberry syrups, *Talanta* 132 (2015) 929 – 938. doi:10.1016/j.talanta.2014.10.049.
- [146] K. Buonasera, G. D’Orazio, S. Fanali, P. Dugo, L. Mondello, Separation of organophosphorus pesticides by using nano-liquid chromatography, *Journal of Chromatography A* 1216 (18) (2009) 3970–3976. doi:10.1016/j.chroma.2009.03.005.
- [147] A. Schmidt, M. Karas, T. Dülcks, Effect of different solution flow rates on analyte ion signals in nano-esi ms, or: when does ESI turn into nano-ESI?, *Journal of the American Society for Mass Spectrometry* 14 (5) (2003) 492–500. doi:10.1016/S1044-0305(03)00128-4.
- [148] Waters Corporation, nanoAcquity UPLC System Operator’s Guide, 2006.
- [149] Sigma-Aldrich, Product Information Sheet: Amberlite XAD polymeric resin, 1998.
- [150] Y. Ye, J. Weiwei, L. Na, M. Mei, W. Donghong, W. Zijian, R. Kaifeng, Assessing of genotoxicity of 16 centralized source-waters in China by means of the SOS/umu assay and the micronucleus test: Initial identification of the potential genotoxicants by use of a GC/MS method and the QSAR Toolbox 3.0, *Mutation Research/Genetic Toxicology and Environmental Mutagenesis* 763 (0) (2014) 36–43. doi:10.1016/j.mrgentox.2013.11.003.